NASA TECHNICAL TRANSLATION NASA TT F 16,298

GRAPHICS OF SPACE MECHANICS [ANALYTICAL-GRAPHICAL METHODS IN SPACE NAVIGATION]

Georgiy Alekseyevich Yazvitskiy [Deceased]

(NASA-TT-F-16298) GRAPHICS OF SPACE MECHANICS [ANALYTICAL-GRAPHICAL METHODS IN SPACE NAVIGATION] (Kanner (Leo) Associates) 126 p HC $5.75 CSCL 22C
N75-23636
Unclas
G3/13 22159

Translation of "Kosmicheskaya grafomekhanika," Moscow, "Mashinostroyeniye," Press, 1975, 128 pp.

NATIONAL AERONAUTICS AND SPACE ADMINISTRATION
WASHINGTON, D.C. 20546 MAY 1975

STANDARD TITLE PAGE

1. Report No.	2. Government Accession No.	3. Recipient's Catalog No.
NASA TT F 16,298		

4. Title and Subtitle	5. Report Date
GRAPHICS OF SPACE MECHANICS [ANALYTICAL-GRAPHICAL METHODS IN SPACE NAVIGATION]	May 1975
	6. Performing Organization Code

7. Author(s)	8. Performing Organization Report No.
Yazvitskiy, Georgiy Alekseyevich [Deceased]	
	10. Work Unit No.
	11. Contract or Grant No. NASw-2481

9. Performing Organization Name and Address	13. Type of Report and Period Covered
Leo Kanner Associates, Redwood City, CA 94063	Translation
12. Sponsoring Agency Name and Address	14. Sponsoring Agency Code
National Aeronautics and Space Administration, Washington, D.C. 20546	

15. Supplementary Notes

Translation of "Kosmicheskaya grafomekhanika," Moscow, "Mashinostroyeniye," 1975, 128 pp.

16. Abstract

The book presents a set of geometrical methods of solving problems in space flight mechanics. These methods make it possible, without complicated mathematical equipment, to investigate space flight and to perform practical calculations with varying degrees of accuracy.

The book is written for design engineers, students at higher technical institutions of learning, and also for other readers interested in calculations of the trajectories of spacecraft flight. 7 tables, 96 illustrations, 13 references.

17. Key Words (Selected by Author(s))	18. Distribution Statement
	Unclassified-Unlimited

19. Security Classif. (of this report)	20. Security Classif. (of this page)	21. No. of Pages	22. Price
Unclassified	Unclassified	119	

NASA-HQ

Foreword

With the birth of astronautics, astronomy became an engineering science, and studies appearing in recent years evidence a new direction in applied mathematics -- methods of solving problems in space flight dynamics using graphical analysis. This graphical analysis consists above all in graphical methods of analyzing functional relationships that assist in space navigation in finding by the simplest method the physical meaning of complicated interrelationships in space-time and energy relations. Nomograms assist not only in making rapid calculations with an unlimited number of variations in initial data, but also penetrate to the physical meaning of the interrelationships of interest between the initial data and the end results of calculation. /3*

Analytical-graphical methods have maximum simplicity, graphical character, and operational accessibility. They yield the shortest approach to mastering the fundamental concepts without which well-informed designing is impossible, not to speak of the fact that in the predraft stage they serve as an irreplaceable tool of calculation. So the use of analytical-graphical methods of calculation and methods of investigation in astronomical problems for the purposes of space navigation is becoming inevitable. This is also furthered by the fact that in nomograms, to some extent, actual motions are simulated: the rotation of the Earth about its axis, the relative motion of the Sun, and the motion of planets and spacecraft in various coordinate systems.

The author aims to lay down the principles for the broad use of engineering analytical-graphical methods of calculation in astronautics with the example of developing elements of a universal computational complex for model problems. This book describes methods of using a system of calculation aids in solving practical problems in space navigation. In it the author endeavored to cover a broad range of problems, by laying down, first of all, as his basis, his leading principle /4 of the analytical-graphical approach to solving problems in space flight mechanics -- breaking down an overall problem into

three parts: space orientation, a plane orbital problem, and linking up the first two parts via vector constructions in the plane of the correcting impulse; and, secondly, developing analytical-graphical methods from the general theory of graphical constructions via nomograms to the computational devices.

The complex of computational devices proposed in this book can serve as a working tool in the hands of a design engineer.

The engineering orientation of the methods of calculation developed here lies in the fact that calculating specialist is able:

a) to see in searching for the optimal solution to a practical problem (for example, selecting a space flight trajectory) throughout the calculation on which factors and to what degree the end result of the calculation depends;

b) to monitor each step in the exact analytical calculation performed on electronic computers;

c) to find the most rational design dictated by specific astronomical factors (for example, the location of navigation and research instrumentation on a space object); and

d) to use simple means of analyzing flight test results.

The material of the book is divided into three parts. In Chapter 1 are presented background information from spherical astronomy. Chapter 2 explains the principles of constructing the simplest nomograms as means of preliminary analysis and calculation of energy and weight characteristics of rockets. The remaining three chapters contain solutions to general problems of orbital motion when passing from one orbit to another lying in a rotated plane.

In accordance with the overall scheme of the methods, the solutions to general problems in Chapter 3, 4 and 5 are presented thusly: solution to problems in space orientation, solution to the plane orbital problem, and solution to specific integrated problems in space navigation using universal computational devices that can implement the above-presented fundamental principle of the analytical-graphical approach to solving problems in space flight mechanics. The logical connection between these three tasks is shown schematically in Fig. 1. Adding specific details to the overall scheme subsequently leads to the construction of algorithm-flowcharts for solving model problems.

To enable the reader to himself construct several of the nomograms presented in the book in any scale and with any range of values for the parameters being calculated, the book presents

material from the theory of constructing the simplest nomograms. For broader familiarity with nomography, one can recommend the /5 handbook by B. A. Nevskiy [6].

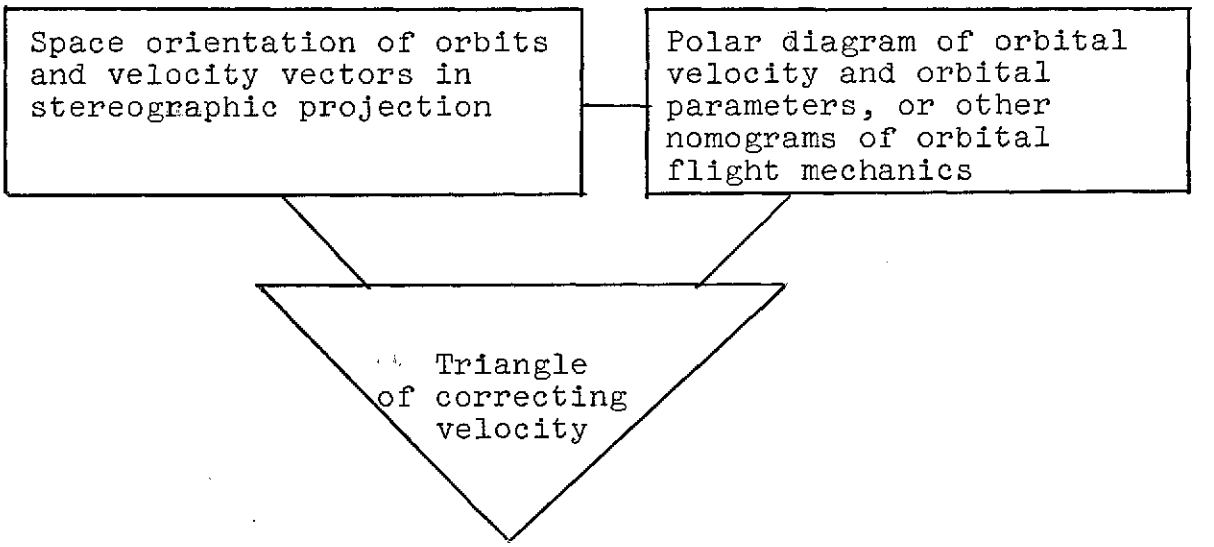
Space orientation of orbits and velocity vectors in stereographic projection
Polar diagram of orbital velocity and orbital parameters, or other nomograms of orbital flight mechanics
Triangle of correcting velocity

Fig. 1. Block diagram for solving space navigation problems (consolidated)

Sometimes the widespread judgement that graphical methods are supposedly fundamentally imprecise interferes with the rapid introduction of analytical-graphical methods into actual practice. For example, it is quite erroneous to consider as "approximate" the familiar method of constructing a graphical solution to the equation of the intersection of two curves, since the solution can be obtained with any, prespecified, accuracy [5]. It is another matter, when, for example, the elliptical orbit of Mars is replaced by an eccentric circle -- here there is plainly an approximation that places certain constraint on the accuracy of the solution to the problem. It is not difficult to give examples of approximately analytical methods of calculation that have gained acceptance, which the method of replacing an infinite series by its first terms is well-known. Approximate methods, above all, are characterized by the presence of a specific approximation, and only from this standpoint should one approach an estimation of their applicability. So it is not the type of method ("analytical" or "graphical") that defines the concept "exact" or "approximate" but the presence or absence of an approximation in the proposed scheme for the solution to a problem.

The potentialities of analytical-graphical methods are boundless. Engineering practice brings up more and more new problems that require formulating new algorithms. Systematizing these algorithms and developing methods of their construction, possibly even as algorithms, which will determine the procedure /6 of screening and performing operations on a universal computational instrument by the transparent nomogram technique, open up a broad approach to developing a new direction in applied mathematics that is necessary in practice.

Engineer K.A. Merenblyum was very active in developing the "invariant nomographic scale" method proposed in the book for determining a launch date. Much work in constructing the nomograms included in the book was done by engineer G. S. Zolotarenko.

The publisher is grateful Doctor of Physics and Mathematics Sciences, Professor V. A. Yegorov for his careful examination of the manuscript and for several valuable comments, which were taken into account in the final readying of the manuscript.

TABLE OF CONTENTS

		Page
Foreword		i
Chapter 1.	Fundamentals of Spherical Astronomy	1
1.1.	Stellar sky	1
1.2.	Spherical coordinates	1
1.3.	Time reckoning	5
1.4.	Use of the relation between astronomical and geographical coordinates in navigation	8
1.5.	General principles of constructing block diagrams for solving problems in space navigation by analytical-graphical methods	10
Chapter 2.	Constructing Simplest Nomograms and Preliminary Energy Calculations	12
2.1.	Nomograms of equated points	13
2.2.	Preliminary calculations in energetics	15
Chapter 3.	Space Orientation	29
3.1.	Fundamentals	30
3.2.	Fundamental elementary construction procedures	35
3.3.	Orientation of orbits and velocity vectors	37
Chapter 4.	Orbital Flight	
4.1.	Characteristics of a gravity field	42
4.2.	Orbital parameters	45
4.3.	Types of orbits	49
4.4.	Energy balance of an orbit	50
4.5.	Flight time	52
4.6.	Polar diagram	54
4.7.	Podera as a hodograph of orbital velocity	57
4.8.	Nomograms of orbital flight	61
4.9.	Disc nomograms	68
4.10.	Nomograms of Kepler's equation	72
4.11.	Network nomograms	75
Chapter 5.	Space Navigation	81
5.1.	Universal computational tool	84
5.2.	Transfer to other orbits	93
5.3.	Determination of optimal transit orbits and launch date	97
5.4.	Invariant nomographic scale	105
5.5.	Determination of space orientation of transit orbit and launch time	108
5.6.	Example of construction of operational device in space navigation	112
References		118

GRAPHICS OF SPACE MECHANICS [ANALYTICAL-GRAPHICAL METHODS IN SPACE NAVIGATION

Georgiy Alekseyevich Yazvitskiy [Deceased]

CHAPTER 1

FUNDAMENTALS OF SPHERICAL ASTRONOMY

1.1. Stellar sky

Upon first acquaintance with the night sky, a person initially /7* begins to recognize celestial bodies by their brightness. Therefore, in astronomy it is customary to characterize the brightness of stars by the so-called "stellar magnitude." Table 1 presents a correspondence between integral stellar magnitudes and the magnitudes of visible brightness.

TABLE 1

Stellar magnitude	1	2	3	4	5	6
Visible brightness n	100	39,8	15,8	6,3	2,5	1
$\lg n$	2,0	1,6	1,2	0,8	0,4	0

With the unaided eye stars can be seen up to the sixth stellar magnitude. The ratio of visible brightnesses of stars with adjoining integral stellar magnitudes is 2.512. Simultaneously, above the horizon the unaided eye can distinguish up to 3000 stars. In practical astronomy and navigation, use is made of the brightest stars, which number up to 20 in both hemispheres. Table 2 presents the brightest navigation stars and their main characteristics. The brightest star, Sirius has a stellar magnitude of 1.58.

1.2. Spherical coordinates

To construct spherical coordinates, in astronomy use is made of the concept of the celestial sphere -- a sphere of arbitrary radius with its center at the point of observation. Actually, it is very convenient to the observer to conceive of the heavens in the form of a large hollow sphere on the surface of which are projected all the celestial bodies. Due to enormous /8 distances from the center of observation (Earth) to the stars, they appear to be at the same distance, that is, on the sphere.

---

* Numbers in the margin indicate pagination in the foreign text.

Thus, the celestial sphere maps the visible stellar sky and is used in solving astronomical problems in which allowance for linear distances to the celestial bodies is not required, and only the angular coordinates are necessary. The rotation of the Earth, occurring counterclockwise, if viewed from the North Pole, leads to the visible motion of the stellar sky in the opposite direction.

TABLE 2

Name of star		Right ascension	Inclination	Visible stellar magnitude	Distance (in light years)
Latin	Russian				
α Canis Majoris	α Bol'shoy Pyos (Sirius)	6^h43^m	−16°40′	1.58	8.7
α Lyrae	α Lira (Vega)	18^h36^m	38°45′	0.14	27
α Aurigae	α Voznichiy (Capella)	5^h14^m	45°58′	0.21	46
α Bootis	αVolopas (Arktur)	14^h14^m	19°22′	0.24	37
β Orionis	β Orion (Rigel')	5^h13^m	−8°15′	0.34	540
α Carinae	αKil' (Kanopus)	6^h23^m	−52°41′	0.86	230

Remark. A light year is the distance that light travels in one tropical year. A light year is $9.46 \cdot 10^{12}$ km.

In solving various problems in space navigation, it is convenient to introduce, when determining the angles of rotation, a reference sphere, by selecting its center and radius in accordance with the requirements of the problem, and by representing the projections of the space objects on its external side.

A great circle on the celestial sphere is a basic element in the construction of spherical (curvilinear) coordinates. In contrast to the small circle this is a circle whose plane extends through the center of the sphere and, thus, its center coincides with the center of the celestial sphere. The arc

of a great circle is the shortest distance between two points on the celestial sphere. The angular distance between two points on the celestial sphere is measured by the arc of the great circle lying between these points. The great circle of a celestial sphere at an equal distance from the poles is called the celestial equator. The poles of the celestial sphere are determined as follows: if one extends the axis of rotation of the Earth in both directions, it will pass through the celestial sphere at two points, called the celestial poles. The northern pole of the celestial sphere is designated so that, in observations on the Earth, the diurnal rotation of the stars around it will seem to be visible counterclockwise. /9

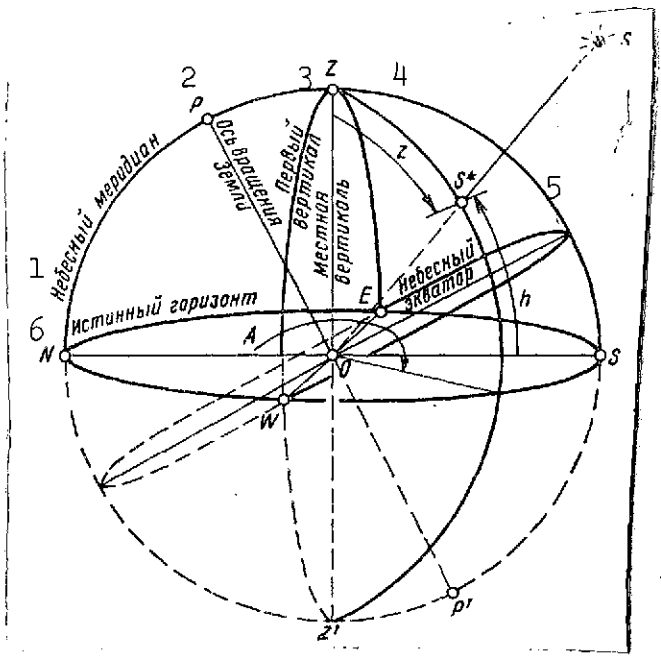

Fig. 2. Fundamental circles on the celestial sphere

Key: 1. Celestial meridian
2. Axis of rotation of the Earth
3. First vertical
4. Local vertical
5. Celestial equator

The main points and the great circles on the celestial sphere shown in Figs. 2 and 3 will be elements of subsequent graphical constructions, therefore they must be examined in greater detail. The points denoted by the italicized Latin letters are formed by the intersection of the sphere by lines extending from the center of sphere O, or else they are the points of intersection of two great circles. A great circle is formed by the intersection of the celestial sphere by a plane extending through the center of observation. Let us present several notations and definitions (see Figs. 2 and 3): P and P' are the celestial poles; PP' is the celestial axis; Z is the zenith, the point at which the celestial sphere is intersected by a plumb line extended upward at the point of observation; Z' is the nadir; N and S are the north and south points respectively; E and W are the east and west points, respectively; and ZZ' is the local vertical;

the celestial meridian is a vertical circle extending over the celestial sphere through the north point and south point and lying in the observer's plane; /10

the first vertical is a vertical circle at a right angle to the celestial meridian;

the true horizon is the line at which the celestial sphere is intersected by a plane equidistant from points C and C' (zenith point and nadir point);

the ecliptic is a great circle that is the line along which the plane of the Earth's rotation around the sun intersects the celestial sphere; S' is the point observed;

the inclination of the ecliptic is the angle by which the ecliptic intersects the celestial equator;

the point of vernal equinox is the point at which the ecliptic intersects the celestial equator in the south-north direction; and

the point of autumnal equinox is the point at which the ecliptic intersects the celestial equator in the north-south direction.

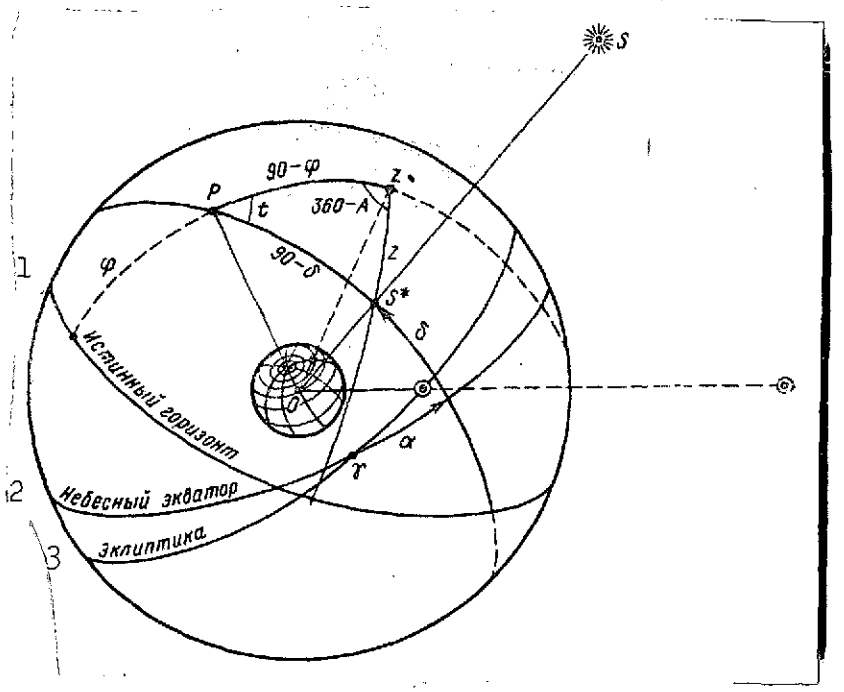

Fig. 3. Parallactic triangle

Key: 1. True horizon
2. Celestial equator
3. Ecliptic

ORIGINAL PAGE IS
OF POOR QUALITY

the position of a point in the celestial sphere is conveniently determined by the spherical coordinates, which consist of the polar distance (latitude) and longitude. The system of spherical coordinates is determined by the position /11 of its pole P and, therefore, the equator. The polar distance measured along the meridian from pole P to S* is called the local meridian.

Longitude is the angular distance measured along the equator from the local meridian to the zero meridian established for the given coordinate system.

Curvilinear celestial spherical coordinates, depending on the position of the origin or coordinates of this system, are divided into heliocentric, geocentric, topocentric, barycentric, planetocentric, and selenocentric (see Chapter 2 and see reference [7] for more details).

1.3. Time reckoning

The rotation of the Earth about its axis is a periodic process occurring continuously and uniformly. The life and activities of man were always intimately associated with the change of night and day, therefore the fact that underlying the measurement of time since antiquity has been the visible diurnal rotation of the celestial sphere is not fortuitous. The passage of a cellestial body across the celestial meridian as the result of the visible diurnal rotation of the celestial sphere around the Earth's axis of rotation is called culmination.

During a day a celestial body culminates twice: at the point of upper culmination when its elevation above the horizon is the greatest, and at the point of low culmination, when its elevation is the smallest. Time is measured by the hour angle of some point, the time interval between two successive culminations, which defines the unit of time -- the day. The hour angle (we denoted by the letter t) is the angle between the celestial meridian and the hour circle drawn across the star. The hour circle is reckoned from the meridian in the direction of diurnal rotation of the stellar sky, that is, along the equator along the West, and is measured in hours with a limit of values from 0 to 24 hours.

The moment of the upper culmination corresponds to the beginning of the astronomical day, and the moment of the lower culmination (solar mean) denotes the beginning of civil days. Depending on the choice of the point for the reckoning of time, there are the following systems of measuring time: sidereal, true solar and mean solar. Characteristics of these systems are given in Table 3.

Sidereal time is the time reckoned from the moment of the upper culmination of the point of vernal equinox to any other position of the point, and it is expressed in fractions of a sidereal day.

True solar time is the time reckoned from the moment of the lower culmination of the true Sun to any other of its positions, and it is expressed in fractions of a true solar day.

Mean solar time is the time elapsing from the moment of the lower culmination of the mean equatorial Sun to any other of its positions, and it is expressed in fractions of a mean solar day. /12

TABLE 3

Time of system of reckoning	Point at which time is determined	Advantages	Disadvantages
Sidereal	Point of vernal equinox	Constancy of unit of measurement	Unsatisfactory to use by persons in daily, Sun-related life
True solar	Center of true Sun	Simplicity of measurement	Inconstancy of unit of measurement
Mean solar	Center of mean equatorial Sun	Constancy of unit of measurement	--

The relationship between sidereal time s and the equatorial coordinate of a star (t_* and α_*) is expressed by the formula

$$s = t_* + \alpha_*$$

At the moment of culmination $t_* = 0$, whence $s = \alpha_*$.

The mean ecliptic Sun is the imaginary point in the celestial sphere moving uniformly along the ecliptic and encountering the true Sun at the perihelion and aphelion. [1]

[1] The perihelion is the point closest to the Sun in the orbit of a celestial body moving around the Sun.
Aphelion is the point furthest from the Sun in the orbit of a celestial body revolving around the Sun.

TABLE 4

Name of year	How determined	Mean duration
Tropical	Passage of Sun across the vernal equinox	365.242199 days or 365 days, 5 hr 48 min 46 sec (shortened by 5 sec per millenium)
Sidereal	Passage of Sun across the same location in the stellar background	365.25636 days or 365 days 6 hr 9 min 9.6 sec
Anomalistic	Passage of Sun across the perihelion	365.25964 days
Julian	--	365.25 days

The mean equatorial Sun is the imaginary point of a celestial sphere moving uniformly along the celestial equator so that at each instance of time its right ascension is equal to the mean longitude of the true Sun. The right ascension of the mean equatorial Sun is always equal to the longitude of the mean ecliptic Sun.

The equation of time is the difference between the hour angles of the true Sun and the mean equatorial Sun (correction to the true solar time in order to obtain the mean solar time).

Zone time is the local mean solar time of the principal geographic meridian of the hour zone in which a given station is located.

Legal time is the time established by a decree of the USSR Sovnarkom [Council of People's Comissariats], dated 16 June, 1930. /13 Under this decree, all clocks were shifted forward 1 hour relative to zone time. Thus, the mean noonday in Moscow will be 12 h 30 min, Moscow time.

Universal time is the local mean solar time at the Greenwich meridian.

Ephemeris time is the time that passes entirely uniformly. For practical purposes, this time differs little from universal time.[2]

A year is the interval of time between two successive passages of the Sun or the Earth across a specific point.

Table 4 gives the characteristics of the systems of reckoning large intervals of time.

1.4 Use of the relation between astronomical and geographical coordinates in navigation.

Navigation is the science of the rules and procedures of piloting ships. Reference points are needed in navigation. Observation of the Earth's surface from on board an aircraft or a vessel, owing to the sphericity of the Earth, is limited to the visible horizon. This makes it possible to scan a negligible part of the global surface, while the stellar sky overhead enables one to see at once half of the heavens. Advances in extended navigation, that is, navigation far from coastlines beyond the limits of their visibility, has since remote antiquity led to the development of methods of orientation by the stars. The relationships of astronomical coordinates of the stars (declination and right ascension) with geographical coordinates of the observation of the positions of stars in the sky make it possible to determine the location of objects on the globe.

Declination is the angular distance of a celestial body from the equator (arc of the great circle from the equator to the celestial body). Declination is positive in the direction of the North Pole and negative in the direction of the South Pole.

Right ascension is the angular distance of the circle of declination from the vernal equinox. The right ascension is reckoned from the vernal equinox along the equator from 0^h to 24^h in a direction opposite to the diurnal rotation of the celestial sphere.

The geographical position of a celestial body -- the point of the projection of the celestial body onto the Earth's surface --

---

[2] The difference between ephemeris time and universal time in 1960 was adopted as +34 sec. Replacement of the concept of "universal time" by "ephemeris time" in the ephemerides of the Sun, planets and stars does not introduce any changes. But in the ephemerides of the Moon this replacement leads to a 1 sec change in the right ascensions of the Moon, and up to 0.1 sec change in the lunar orbital inclinations (Astronomicheskiy kalendar' VAGO za 1960 g. [Astronomical Calendar of the All-Union Astronomical and Geodetic Society for 1960]).

is denoted by S_0 (Fig. 4). The celestial body is at the zenith (Z = 0) for this point on the Earth at the given instant of time.

The positional circle, with the circle of equal elevations, is the locus of points on the Earth where the given star has a given zenith distance Z. The diameter of the positional circle will be the chord of the arc of a straight circle whose midpoint is at the geographical position of the celestial body S_0. Half of this arc has an angular value equal to the zenith distance Z, and expresses the distance to the geographical position of the star measured along the great-circle course[3] expressed in degrees.

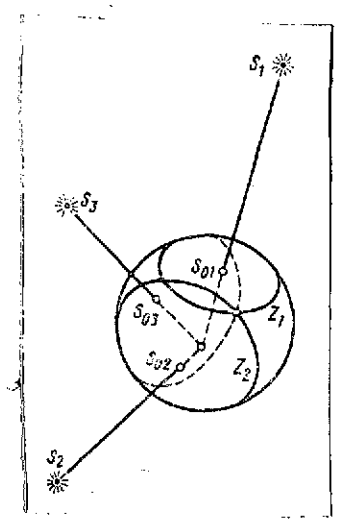

Fig. 4. Somner's method

Determining the location on the globe for measuring the zenith distances of two stars (so-called Somner's method) is a method long used in navigational and aviation astronomy. The desired position is determined from the intersection of the positional circles of these stars corresponding to the measured zenith distances Z_1 and Z_2 (see Fig. 4). To avoid ambiguity, a third star with zenith distance Z_3 can be measured. Knowing the geographical position of the star at the given instant of time, one can determine its horizontal coordinates for any point on the globe. Hence it follows that from the measured coordinates of a star one can determine its position. The position of the zenith of point A (Fig. 5) in the equatorial coordinates δ_Z and α_Z defines the position of the object by the formula

$$\varphi = \delta_z; \quad \lambda = \alpha_z - G,$$

where ϕ is the geographical latitude; λ is the geographical longitude, δ_Z is the declination of the zenith; α_Z is the right ascension of the zenith, or local sidereal time; and G is Greenwich sidereal time.

---

[3] The great-circle course is the shortest line between two points on the surface of the Earth.

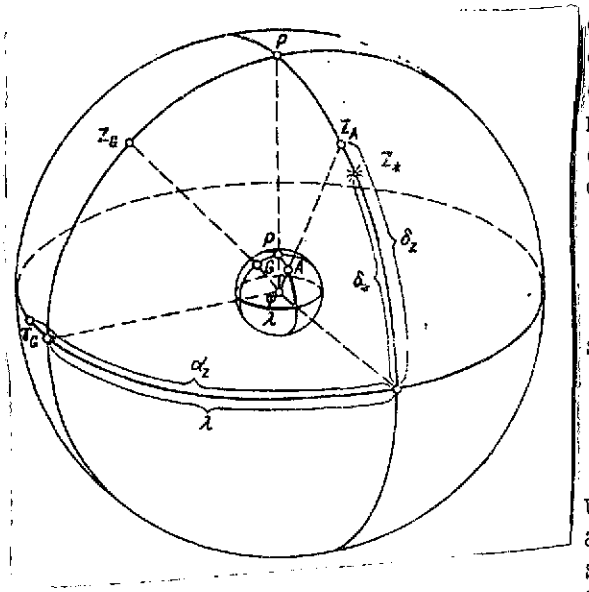

Fig. 5. Relationship of astronomical and geographical coordinates

The coordinates of the observation point ϕ and λ, based on the measured zenith distance of the celestial body Z_* at the moment of its culmination, as can be seen from Fig. 5, are determined with the formulas

$$\varphi = \delta_* + Z_*; \quad \lambda = \alpha_* - G,$$

since

$$\delta_z = \delta_* + Z_* \quad \text{and} \quad \alpha_z = \alpha_*,$$

where α_* and δ_* are the right ascension and declination of the star, respectively; and G is the Greenwich sidereal moment of culmination.

It is not difficult to note that the latitude of the observation point is equal to the elevation of the pole above the horizon.

1.5. General principles of constructing block diagrams for solving problems in space navigation by analytical-graphical methods.

The general principle of the analytical-graphical approach to investigating orbital flight (or computing it) can be explained with an example in which the parameters of an orbit are determined for a given SC (spacecraft), the velocity at a given point in space. The analytical solution of this problem starts, as we know, from the assigned values of the coordinates of this point X, Y and Z, the derivatives of $\dot{X}$, $\dot{Y}$ and $\dot{Z}$, and the time t, which /16 are the starting conditions for integrating the differential equations of motion of the SC. But under the analytical-graphical method, any problem in determining orbital parameters can be broken down into the following two problems.

1. Determine the orbital parameters as a plane curve by solving the plane problem in celestial mechanics employing appropriate nomograms and graphs.

2. Determine the orientation of the orbit in space and the space orientation of the vectors by solving problems in

spherical astronomy, using transparent nomograms and special constructions thereon, whose basis is the stereographic projection of the spherical coordinates (Wulf's grid).

The history of the use of Wulf's grid is as follows. More than 70 years ago, Professor Wulf, in using the stereographic grid in crystallography, took note of the similarlity between the formulations of problems in measuring angles in crystals and in astronomy. He proposed using his method of solution that he developed for crystals, for problems in spherical astronomy. Wulf's work was complete in 1904, and in 1909 it was published as a booklet [3]. In the 1930's Wulf's grid found use in aviation astronomy under the name "Azimuthal Grid," since it served principally in determining azimuths.

Later, tables of elevations and azimuths (TEA) of the Sun, Moon and planets came to be used, and gradually Wulf's grid was forgotten. The demands of operational calculations in astronautics gave new life to Wulf's grid, which has unusually great universality [13]. The field of use of the grid in our computational device is being immeasurably expanded compared with its descriptions, which differ little from the 1909 accounts, confining its use to problems in coordinate transformations. Expanding the field of use of the stereographic grid required the author to suitably rework the material in the literature. The description of the use made of Wulf's grid made in this book was formulated to generalize the method of solving the largest possible number of problems.

We also note that the stereographic projection used in determining the orientation of an orbit in space is a grid of orthogonal circles and is constructed by drawing only straight lines and circles. In this respect, the structure of the polar diagram is analogous -- the hodograph of orbital velocity used in determining orbital elements in the plane of the orbital velocity, since it also is constructed with a compass and straight-edge.

CHAPTER 2

CONSTRUCTING SIMPLEST NOMOGRAMS AND PRELIMINARY ENERGY CALCULATIONS

Symbols

$a = dv/dt$	is the acceleration of the spacecraft /17
c	is the escape velocity of gases from engine nozzle
D	is the range of spacecraft flight
g	is the acceleration due to gravity
$K = R_x/P$	is the drag coefficient
K_{av}	is the average (velocity-wise) value of the drag coefficient
M_{sc}	is the mass of the spacecraft structure
m	is the instantaneous mass of the spacecraft
$\dot{m} = dm/dt$	is the mass flow of the [reaction] mass
$m_0 = q + m_{sc} + m_F$	is the initial mass of the spacecraft
m_F	is the mass of the expanded fuel in time t
m_{TE}	is the terminal mass of the launch vehicle
n	is the number of launch vehicle stages
P	is the spacecraft engine thrust
$P_{sp} = P/\dot{m}g$	is the specific thrust of the spacecraft engine used as the engine characteristic, it is defined as the ratio of thrust P to the mass flow of fuel
P^*	is the thrust-to-height ratio
$p = m_0/q$	is the relative initial mass
q	is the payload mass
R_x	is the [bow] aerodynamic drag
$S = M_{SC} + m_F/M_{SC}$	is the coefficient of the design efficiency of the launch vehicle
T	is the total spacecraft flight time /18
t	is the instantaneous time
v	is the spacecraft velocity
v_0	is the spacecraft velocity calculated by Tsiolkovskiy's formula
$v_{rel} = v/c$	is the relative spacecraft velocity
v_{ab}	is the mean spacecraft velocity over the trajectory section
v^*_{av}	is the main spacecraft velocity in dimensionless terms
v_{max}	is the maximum velocity at the end of the powered trajectory section
$y = m_0/m_0 - mt$	is a constant
$z = m_0/m_F$	is Tsiolkovskiy's number
θ^*	is the instantaneous angle of inclination of the velocity vector $\bar{v}$ to the local horizon

θ^*_{av} is the mean (time-wise) angle of inclination of the trajectory

$\mu = m_f/m_0$ is the relative fuel mass

τ is the time required to consume the entire rocket mass (if it were entirely made of fuel).

2.1. Nomograms of equated points

A nomogram of equated points is the term given to a nomogram in which the scales of the variables lie in a plane in such a way that all points corresponding to the particular values of the variables related by the functional dependence lie along the same straight line.

From the definition of this kind of nomogram follows a simple method of their use, which as we know is based on seeking the point of intersection of two lines -- the scale of the desired variable and line connecting the points of the two scales of the given variables. Let us subsequently agree to refer to the sighting line as the line connecting the two given points corresponding to the values on the different scales.

The simplest nomograms of equated points are nomograms with three parallel rectilinear functional scales, expressing the relationship between the functions of three variables x, y and z associated by the relation

$$f_3(z) = f_1(x) + f_2(y).$$

These nomograms are called the additive nomograms. The /19
scale divisions on these nomograms are marked with the values of the variables; the positions of the divisions are determined by the values of the ordinates equal to the corresponding values of the functions. Thus, the equations of scales for this type of nomogram can be represented in the form

$$y_1 = \lambda_1 f_1(x);\ y_2 = \lambda_2 f_2(y);\ y_3 = \lambda_3 f_3(z),$$

where λ_1, λ_2, and λ_3 are the unit scale divisions.

When one uses the logarithmic scale, an additive nomogram is transformed into a multiplicative nomogram:

$$\varphi_3(z) = \varphi_1(x)\,\varphi_2(y), \qquad (2.1)$$

since for this case we have

$$f_1(x)=\lg\varphi_1(x);\ f_2(y)=\lg\varphi_2(y);\ f_3(z)=\lg\varphi_3(z). \tag{2.2}$$

Fig. 6 shows the construction of this nomogram. It is not difficult to obtain the relations for the scales λ_1, λ_2, and λ_3 and the distances between the scales h_1 and h_2:

$$\frac{h_1}{h_2}=\frac{\lambda_1}{\lambda_2};\quad \lambda_3=\frac{\lambda_1\lambda_2}{\lambda_1+\lambda_2}. \tag{2.3}$$

In the particular case when $\lambda_1 = \lambda_2 = \lambda$; $h_1 = h_2$, the third scale will be found in the middle, and its unit scale division will be $\lambda/2$.

In constructing a nomogram or a functional relation of the type

$$Z^k = AX^mY^n \tag{2.4}$$

by X, Y and Z here and in the following we will mean not only the variables, but also their functions. The unit scale divisions (moduli) of the logarithmic scales will increase by k, m, and n times, respectively. Negative values of k, m or n indicate the reverse direction of increase in scale values. The origin of reference of each scale in this nomogram is determined from the data of one arbitrary calculation (analytical).

Now let us proceed to examining more complicated -- movable -- nomograms. We will call nomograms with which calculation is carried out by changing the position of one of several scales -- moving nomograms. The logarithmic scale is the simplest and most common kind of sliding nomogram. The main feature of this class of nomograms is the constant difference of the values of the two linear (uniform) scales beneath a cursor when they are secured in one position, and the constant ratio of the values of the two logarithmic scales beneath a cursor when they are also secured in one position. Thus, using two logarithmic scales sliding one relative to the other, one can express the functions of four variables associated by equations of the type /20

$$\frac{X}{Y}=\frac{Z}{W} \tag{2.5}$$

when there are identical unit scale divisions, and one can express functions of four variables associated by equations of the type

$$\frac{X^m}{Y^n}=\frac{Z^k}{W^u}$$

when the unit scale divisions are chosen appropriately to the exponents of the functions. The manner in which these nomograms are used is shown in Fig. 7. Using these nomograms, from any three quantities one can find a fourth. As to design, these nomograms are made in the form of slide rules or concentric discs secured with fasteners at their common center. The arbitrarily selected mutual position of two scales in one part of a nomogram instrument (sliding relative to the other) uniquely determines the mutual position of the two other scales in the other part. This position is determined by means of a single analytical calculation, which is best performed with an example that has initial data most convenient for the computation. /21

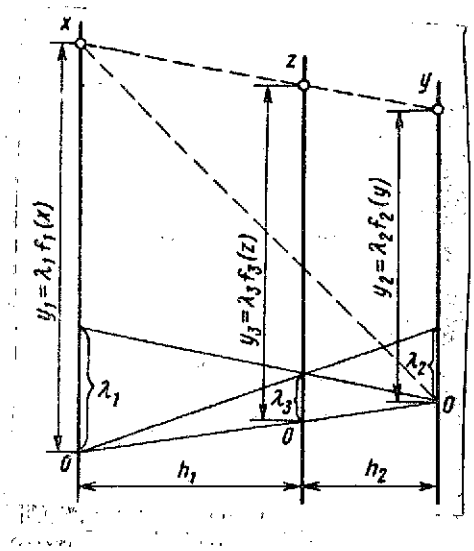

Fig. 6. Nomogram with parallel scales

2.2. Preliminary calculations in energetics

Meshcherskiy's equation, defining the motion of a rocket with a variable mass m when aerodynamic drag is present and with the component of the gravitational force mg sin θ* in a projection onto the longitudinal axis of the velocity coordinate system will be

$$m\frac{dv}{dt}=-c\frac{dm}{dt}-R_x-mg\sin\theta^*. \qquad (2.6)$$

When $R_x = 0$ and $g = 0$, we get an equation that does not depend on t:

$$dv=-c\frac{dm}{m}, \qquad (2.7)$$

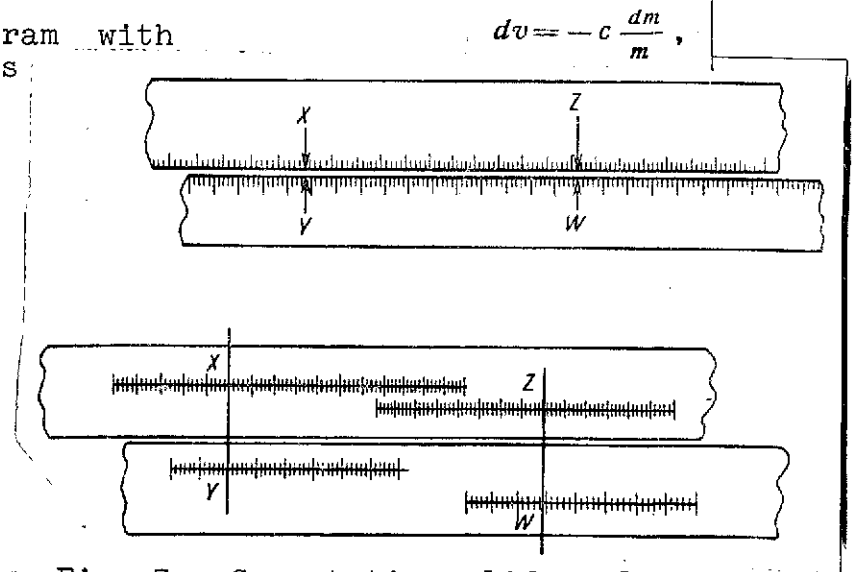

Fig. 7. Computation slide rules

ORIGINAL PAGE IS OF POOR QUALITY

whose solution is the familiar Tsiolkovskiy's formula:

$$v = c \ln z. \tag{2.8}$$

Tsiolkovskiy's formula gives the magnitude of the velocity in free space devoid of a gravitational field and a resistive medium. By introducing the specific thrust P_{sp} and expressing the fuel mass m_f in terms of the relative quantity μ, we get

$$P_{sp} = c/g \tag{2.9}$$

$$\mu = m_F/m_0 \tag{2.10}$$

Referring to Eqs. (2.9) and (2.10), we reduce Eq. (2.8) to the form

$$v = gP_{sp} \ln z = -gP_{sp} \ln (1 - \mu). \tag{2.11}$$

The nomogram in Fig. 8 was constructed for this working formula analogously to Eq. (2.4), which was discussed in the previous section. By comparing Eqs. (2.4) and (2.11) in our case we get

$$\left.\begin{aligned} Z = v;\ A = g = 9.81\ \text{m/sec}^2 \\ X = P_{sp};\ Y = \ln z;\ k = m = n = 1. \end{aligned}\right\}$$

Since there are no negative values, all three scales in the nomogram have the same direction. The values of P_{sp} and v are inscribed on the logarithmic scales, and the scale for z values is constructed from the values of the natural logarithms of these quantities in the same logarithmic scale. The unit scale division of the middle scale is half as small, therefore the equations for the scales in this nomogram will be of the form /22

$$y_1 = \lambda \lg P_{sp};\quad y_2 = \lambda \lg \ln z;\quad y_3 = \frac{\lambda}{2} \lg v,$$

where λ is the scale factor determining the size of the nomogram (chosen according to the required accuracy of the calculation). An 11-scale logarithmic slide rule (GOST [State Standard] 5161-57) can serve as the sliding nomogram in performing calculations based on Tsiolkovskiy's formula, since with this slide rule, besides the ordinary logarithmic scale, there is also the scale lg ln X. In Fig. 9, the upper part shows the manner in which this slide rule is used, while the lower part ensures its application /23

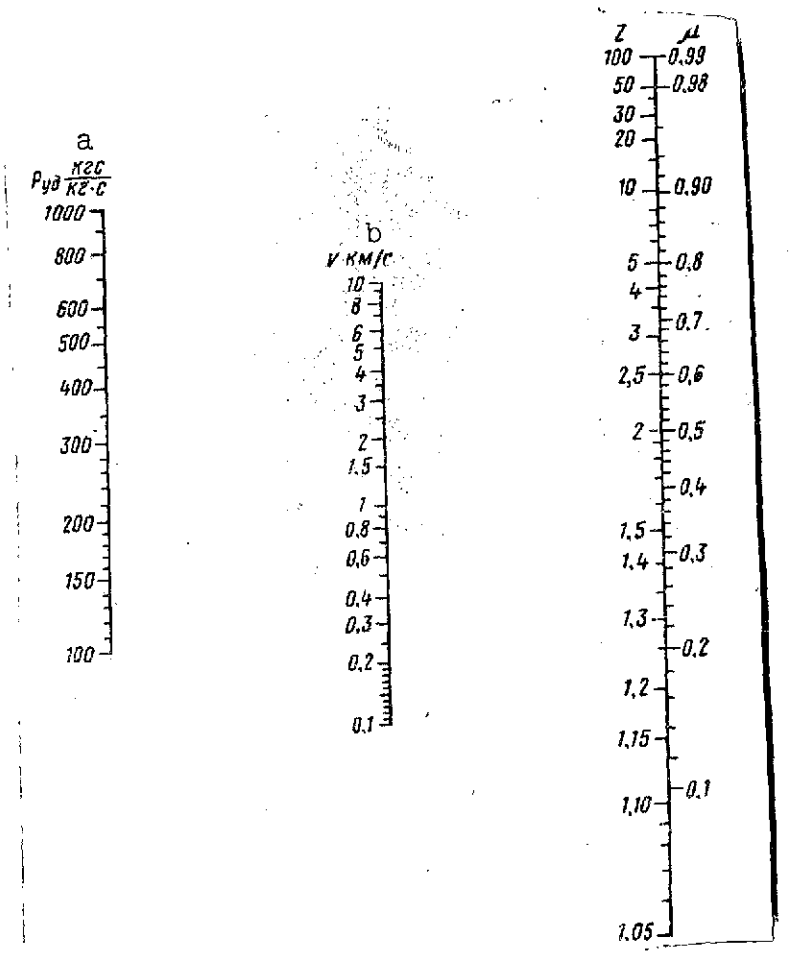

Fig. 8. Nomogram of Tsiolkovskiy's formula: $v = gP_{sp}\ln Z = -gP_{sp}\ln(1-\mu)$

Key: a. P_{sp}, kg/kg·sec
b. v, km/sec

in calculations based on Tsiolkovskiy's formula. This method of use is derived from representing Eq. (2.11) in the form of Eq. (2.5)

$$\frac{P_{sp}}{\frac{1}{g}} = \frac{v}{\ln z}.$$

ORIGINAL PAGE IS
OF POOR QUALITY

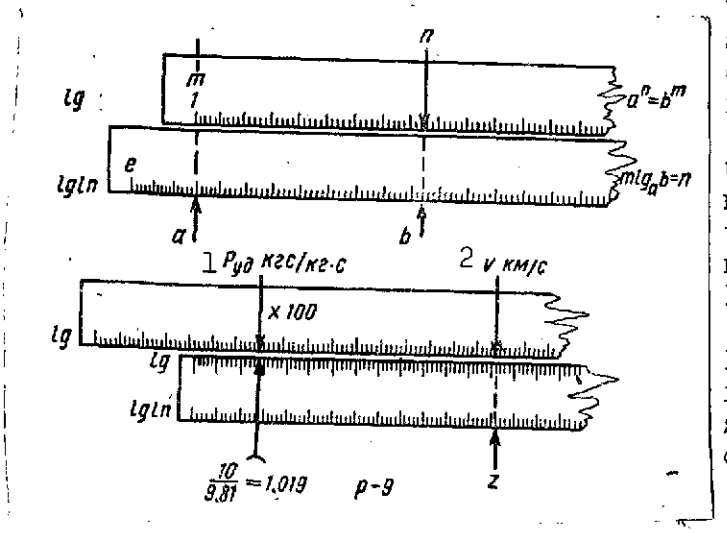

Fig. 9. Calculation using Tsiolkovskiy's formula and an ll-scale slide rule

Key: 1. P_{sp}, kg/kg·sec
2. v, km/sec

Now, if we place a mark on the lower logarithmic scale of the slide rule equal to the quantity 10/9.81 = 1.019, then the following rules of scale positioning and procedures in making readings from them will be in effect:

P_{sp} is read off from the upper logarithmic scale multiplied by 100, and this value is set opposite the mark placed on the lower logarithmic scale.

z is read off from the ln ln X scale, and opposite it on the upper logarithmic scale the velocity is read off in km/sec.

Thus, from two of the three quantities v, z and P_{sp} we can determine the third.

We can obtain Tsiolkovskiy's formula in dimensionless terms if we write /24

$$v_{rel} = v/c$$

then

$$v_{rel} = -\ln(1-\mu) \qquad (2.12)$$

Fig. 10 shows a plot of this formula in a semilogarithmic coordinate grid in the form of a straight line. Laid out along the Y axis is v_{rel}, and along the X axis -- ln (1 - μ), with the scale scribed with the corresponding μ values. The μ scale was constructed in the positive direction of the axis, therefore the logarithmic grid in the plot received the reverse direction. To draw a straight line we find the coordinate of point 2: μ = 0.95 and v_{rel} = 2.996 ≈ 3; and the coordinates of the point 1: μ = 0 and v_{rel} = 0, at which we will find the origin of coordinates.

The velocity of a multistage rocket consisting of n stages can be expressed thusly:

$$v = c_1 \ln z_1 + c_2 \ln z_2 + \ldots + c_n \ln z_n.$$

For the same exhaust velocity from all stages, that is, when $c_1 = c_2 = \ldots = c_n = c$

$$v = c \ln \prod_{k=1}^{k=n} z = -c \ln \prod_{k=1}^{k=n} (1-\mu).$$

When the z values are equal and when the μ values are equal for all stages of the multistage rocket, we will have:

$$\begin{aligned} z_1 &= z_2 = \ldots = z_n = z; \\ \mu_1 &= \mu_2 = \ldots = \mu_n = \mu; \\ v &= c \ln z^n = -c \ln (1-\mu)^n. \end{aligned}$$

In this case, we can use Tsiolkovskiy's formula, by substituting into it the value of the common parameter z, which is related by the function with the parameter for one stage as follows:

$$\begin{aligned} z_0 &= z^n; \\ z &= \sqrt[n]{z_0}; \\ \mu_0 &= 1-(1-\mu)^n; \\ \mu &= 1-\sqrt[n]{1-\mu_0}. \end{aligned} \qquad (2.13)$$

Now let us substitute these values into the relative velocity formula:

$$v_{rel} = -\ln (1 - \mu)^n.$$

Based on this function, in the upper part of the graph shown in Fig. 10 are plotted the scales of the μ values for two-, three-, and four-stage rockets (for identical exhaust velocities and identical parameters z) by increasing the unit scale division two, three and four times, respectively. /25

The change in velocity with time when c is kept constant can yield the same Tsiolkovskiy's formula, since μ is the relative flight time:

$$T/t, \text{ where } \tau = m_0/\dot{m}$$

Actually, we have

$$\mu = \frac{m_t}{m_0} = \frac{\dot{m}T}{m_0} = \frac{T}{\frac{m_0}{\dot{m}}} = \frac{T}{\tau}.$$

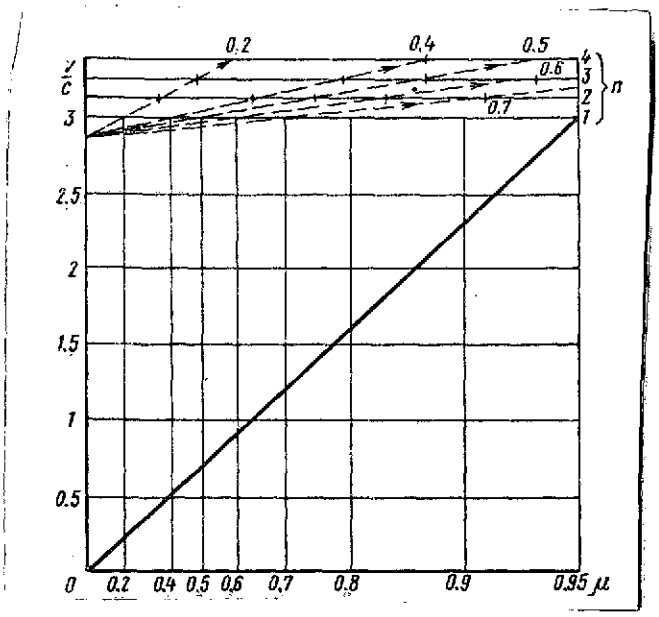

Fig. 10. Plot of dimensionless velocity

The gravity field and the aerodynamic drag in preliminary calculations can allowed for by a simple method if we have the requisite statistical data. Let us look at the idea of the method and its substantiation.

According to Eq. (2.7) /26 we have

$$-c\frac{dm}{m}=dv_0. \qquad (2.14)$$

Knowing that $-c\frac{dm}{dt}=P$, we can reduce Eq. (2.6) to the form

$$dv=-c\frac{dm}{m}(1-R_x)-g\sin\theta^*\,dt.$$

But referring to Eq. (2.14), we can write

$$dv=dv_0-\frac{R_x}{P}dv_0-g\sin\theta^*dt.$$

By integrating, we get

$$v=v_0-\int\frac{R_x}{P}dv_0-g\int\sin\theta^*dt+C. \qquad (2.15)$$

It is not difficult to show that the arbitrary constant C is equal to zero. At the initial point when t = 0, we have v = 0, v_0 = 0 and R_x = 0. Here the third term in the right-hand side of Eq. (2.15), having the dimension of velocity, is also equal to zero. Thus, Eq. (2.15) can be represented as

$$v=v_0-v_0\frac{\int_0^{v_0}\frac{R_x}{P}dv_0}{v_0}-gt\frac{\int_0^t\sin\theta^*dt}{t},$$

or for comparison with Tsiolkovskiy's formula, we can write

$$v+gt\sin\theta^*_{av}=\left[1-\left(\frac{R_x}{P}\right)_{av}\right]gP_{av}\ln z, \qquad (2.16)$$

ORIGINAL PAGE IS
OF POOR QUALITY

where $(R_x/P)_{av} = K_{av}$.

This representation of Eq. (2.15) indicates the possibility of using the same nomogram that we used when solving Tsiolkovskiy's formula. Only now we will lay out the quantity $P_{sp}(1 - K_{av})$ along the P_{sp} scale, and the quantity $v' = v + gt \sin \theta^*_{av}$.

The statistical treatment of the calculation data of existing rocket designs, depending both on rocket type and trajectory type, must serve as the source from which the coefficients K_{av} are obtained.

The formulas of the slant range of powered flight in the absence of external forces can be obtained by integrating Tsiolkovskiy's formula. Let us write out Tsiolkovskiy's formula in the following form:

$$v = c \ln \frac{m_0}{m_0 - \dot{m}t}.$$

Then the flight range at constant exhaust velocity will be determined by the expression /27

$$D = c \int_0^T \ln \frac{m_0}{m_0 - \dot{m}t} dt, \qquad (2.17)$$

where the time of flight T referring to Eq. (2.10), is associated with z thusly,

$$T = \frac{m_T}{\dot{m}} = \frac{m_0 \mu}{\dot{m} z} = \frac{m_0 (z-1)}{\dot{m} z}.$$

We denote:

$$\frac{m_0}{m_0 - \dot{m}t} = y, \text{ then } t = \frac{m_0 (y-1)}{\dot{m} y},$$

whence we have

$$\frac{dt}{dy} = \frac{\dot{m} y m_0 - m_0 (y-1) \dot{m}}{\dot{m}^2 y^2} = \frac{m_0}{\dot{m} y^2}.$$

Since $y = 1$ when $t = 0$ and $y = z$ when $t = T$, in the new notation Eq. (2.17) becomes

$$D = \frac{c m_0}{\dot{m}} \int_1^z \frac{1}{y^2} \ln y dy. \qquad (2.18)$$

By integrating using the "integration by parts" technique, after uncomplicated transformations, we get

$$D = cT\left(1 - \frac{\ln z}{z-1}\right). \tag{2.19}$$

From this we derive the expression for the mean velocity

$$v_{av} = \frac{D}{T} = c\left(1 - \frac{\ln z}{z-1}\right) = c - \frac{v_{max}}{z-1}. \tag{2.20}$$

The expression of the mean velocity in dimensionless values will be

$$v^*_{av} = 1 - \frac{\ln z}{z-1} = 1 + \frac{1-\mu}{\mu}\ln(1-\mu). \tag{2.21}$$

From the plot of this function shown in Fig. 11, it is clear that the mean velocity is always smaller than the exhaust velocity. If μ tends to unity, the mean velocity approaches the exhaust velocity. We get another form of the range formula from the expression for the specific thrust:

$$P_{sp} = \frac{Pt}{gm_F}.$$

Dividing the numerator and denominator by the initial weight gm_0 and introducing the thrust-to-weight ratio P^*, we get /28

$$P^* = \frac{P}{gm_0}; \tag{2.22}$$

$$P_{sp} = \frac{P^* t}{\mu}. \tag{2.23}$$

According to Eqs. (2.20) and (2.21), we can write out the expression for the range:

$$D = ctv^*_{av} = gP_{sp}tv^*_{av}$$

By here substituting P_{sp} from Eq. (2.23) and v_{av} from Eq. (2.21), we get

$$D = \frac{gP^*t^2}{\frac{\mu}{v_{av}}} = \frac{gP^*t^2}{\frac{\mu}{1 + \frac{1-\mu}{\mu}\ln(1-\mu)}}.$$

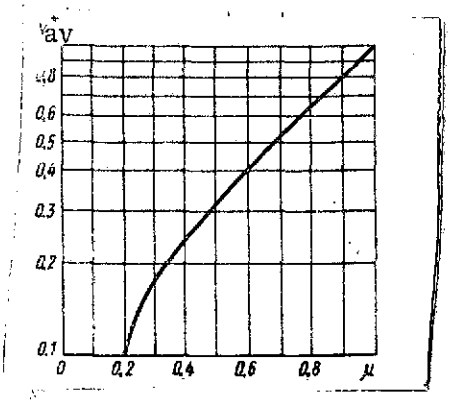

Fig. 11. Plot of mean velocity

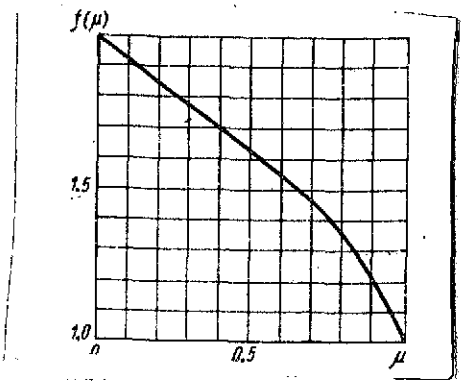

Fig. 12. Plot of coefficient f(μ)

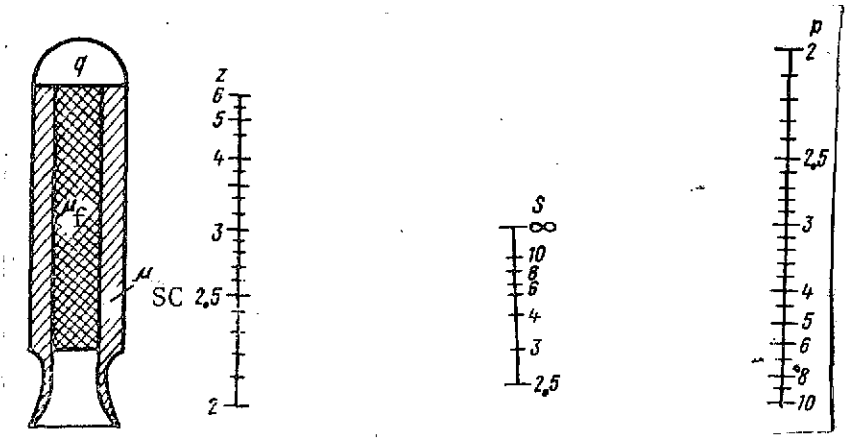

Fig. 13. Nomogram of mass characteristics

By denoting

$$f(\mu) = \frac{\mu}{1 + \frac{1-\mu}{\mu}\ln(1-\mu)}, \qquad (2.24)$$

we finally get

$$D = \frac{gP^*t^2}{f(\mu)}. \qquad (2.25)$$

ORIGINAL PAGE IS
OF POOR QUALITY

This range formula has a clear physical meaning. Thus, for example, at the limiting case when there is no mass flow of fuel, that is, when $\mu = 0$, the formula transforms into the well- /29 known elementary formula of equi-accelerated motion, since $f(\mu) = 2$, and gP^* is the acceleration a of the spacecraft. Here

$$D = \frac{at}{2}.$$

This situation is possible only when we use "ideal fuel," that is, fuel imparting a thrust to the spacecraft without decrease in mass. See Fig. 12 for the plot of function $f(\mu)$.

Mass and design characteristics of rockets are illustrated by the scheme of mass distribution by spacecraft components shown in Fig. 13.[1] This scheme yields the determination of the following parameters: S, p, m_0 and μ (see notation to this chapter). The relation between these parameters can be expressed by the equation

$$\mu = \frac{z-1}{z} = \frac{S-1}{S}\,\frac{p-1}{p}. \qquad (2.26)$$

Fig. 13 shows the nomogram of this equation. By knowing any two parameters, from this nomogram we can rapidly determine the third (by placing a transparent straightedge along the sighting line).

Calculation of the energetics and the mass and design characteristics of the spacecraft is considerably simplified by constructing a specialized computational slide rule. This slide rule was designed by the author by employing two nomograms (see Figs. 8 and 13) and by combining them into a single computational /30 device shown in Fig. 14. The equation solved by means of this device, when reduced to an expression of the type (2.5), is of the form

$$\frac{gP_{sp}}{v'} = \frac{[\ln(1-\mu)]^{-1}}{1-\left(\frac{R_c}{P}\right)_{av}}.$$

The slide rule has six scales designed for the above-considered six parameters. Plotted along the top of the fixed part is the scale of the terminal velocity v and P_{sp} values. The same scale serves for both parameters since their values differ uniformly by two orders. For a given position of the v and P_{sp} scale, it is not difficult to calculate the position of the origin of reference

---

[1] The schematic diagram is taken from [12].

of the K_{av} scale, which as a result will correspond to $\mu = 0.64$. Below is the p and S scale. The following are inscribed on the cursor: two scales for μ along the edges and the K_{av} scale in the middle. The functional relationship between the scales is as follows: if one places opposite a P_{sp} value the K_{av} value, the position of the v scale relative to the upper μ scale will give the mutual correspondence between these parameters for the given P_{sp}. If the arrow "S" on the cursor is placed opposite a given S on the lower scale, then between the lower μ scale and the parameter p a mutual correspondence is established for a given S. Use of the slide rule can be explained with the example of determining total rocket mass. The sequence of operations in solving this problem is as follows:

1. By setting a K_{av} value opposite a P_{sp} value, we get the value of μ opposite the required velocity v.

2. By placing the cursor with arrow "S" at the S value lying opposite the μ value obtained in step 1 (along the lower scale), we get the relative rocket mass p. Next, the product pq gives us the value of the total mass m_0, and the product $m_0\mu$ gives us the fuel mass m_F. This computational aid is convenient to use also when processing statistical material to find the values of the coefficient K_{av} (see above). /32

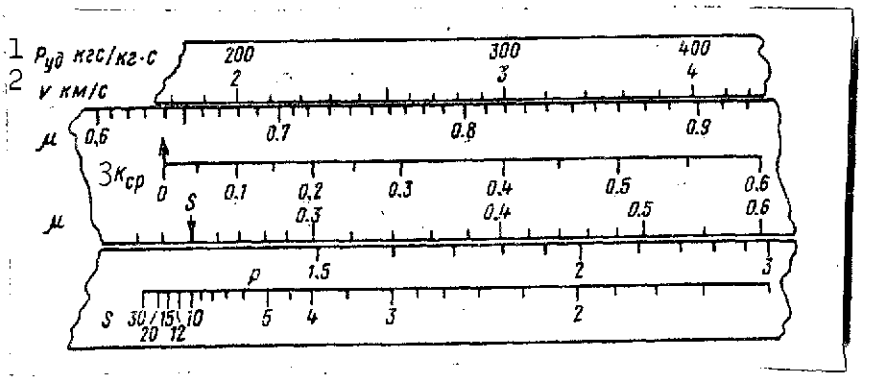

Fig. 14. Computational slide rule of spacecraft energetics

Key: 1. P_{sp}, kg/kg·sec
2. v, km/sec
3. K_{av}

ORIGINAL PAGE IS
OF POOR QUALITY

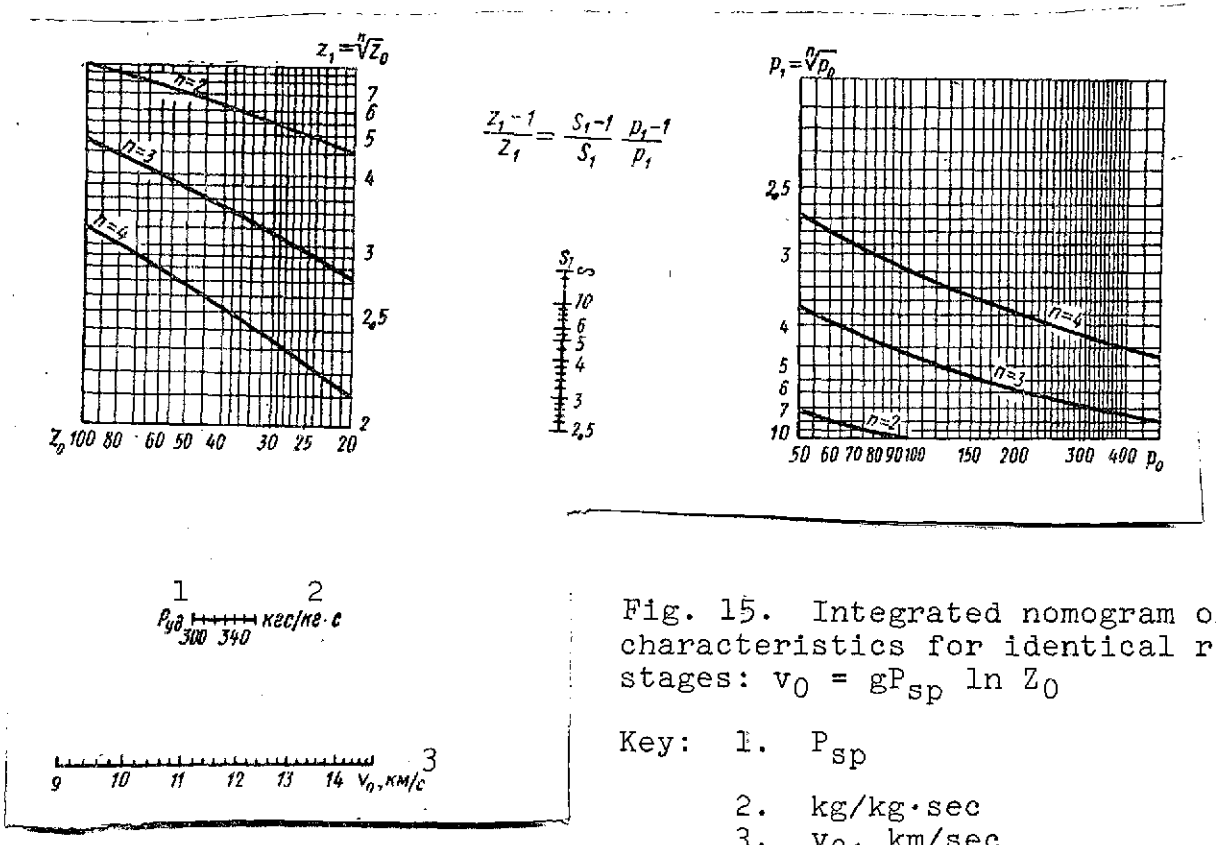

Fig. 15. Integrated nomogram of mass characteristics for identical rocket stages: $v_0 = gP_{sp} \ln Z_0$

Key: 1. P_{sp}

2. kg/kg·sec
3. v_0, km/sec

Let us examine the solution to this problem using the example of the German V-2 rocket (see [8]). The terminal true rocket velocity v = 1500 m/sec. Starting from the flight time T = 64 sec, let us determine the velocity losses associated with the presence of the gravitational field $\Delta v \approx 640$ m/sec. As a result, we get $v' = 1500 + 640 = 2140$ m/sec. For a launch weight or mass $m_0 = 13000$ kg and fuel weight or mass $m_F = 9000$ kg, we get $\mu = m_F/m_0 \approx 0.7$. By setting the cursor with the value $\mu = 0.7$ opposite $v' = 2141$ m/sec, we get $K_{av} \approx 0.1$ opposite the value $P_{sp} = 200$.

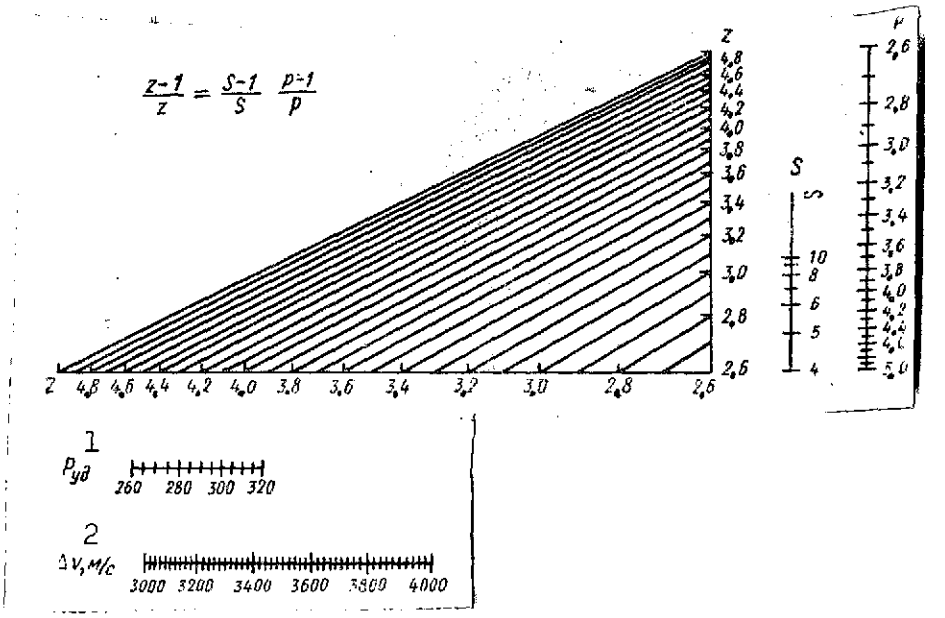

Fig. 16. Integrated nomogram for mass characteristics for different rocket stages:

$$\Delta v_0 = g P_{sp} \ln z$$

Key: 1. P_{sp}
2. Δv, m/sec

The nomograms shown in Fig. 15 also reflects the relation between the six principal mass and energy characteristics of the rocket: v, P_{sp}, z, n, S and p. This nomogram graphically reveals the full interrelationship among the parameters and can be employed in approximate calculations carried out in various directions.

Let us examine the device and the employment of the nomogram with the example of calculating the relative initial mass p. The first part of the nomogram gives us the relation between z_0, v and P_{sp}, where z_0 is Tsiolkovskiy's number calculated as a function of the parameters v and P_{sp}. Essentially the first part is the nomogram shown in Fig. 8. In the second part, we

ORIGINAL PAGE IS
OF POOR QUALITY

convert z_0 into z for each stage of the spacecraft (and vice versa), depending on the number of stages n (see Eqs. (2.13)). In this part we will select the number of stages to get the realistic value z. The third part of the nomogram associates p and z with parameter S' (see nomogram in Fig. 13). S' can be specified from statistical data of a study of modern spacecraft design. In other cases it can be the unknown for purposes of assigning specifications for a spacecraft design under development. The fourth part is used in reconverting p into m_0. By multiplying p by q, we get the launch weight or mass of the rocket. Within the limits of the assumptions of equal c, z and μ for all rocket stages, calculation based on this nomogram is approximate in nature. For more exact calculations with reference to difference P_{sp} and z for different stages, the calculation has to be conducted for each stage separately. For this purpose we use the nomograms shown in Fig. 16. /33

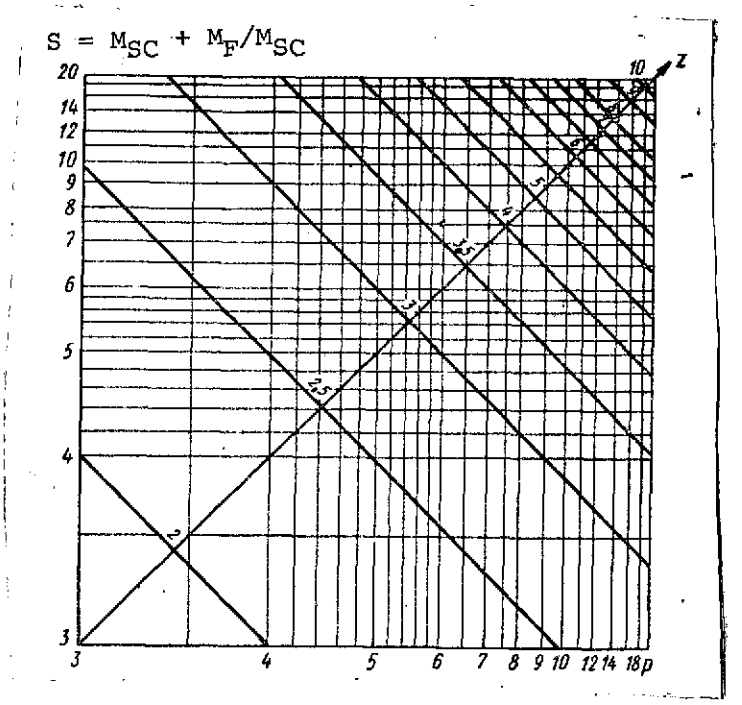

Fig. 17. Grid of mass characteristics

The grid of the review nomogram (Fig. 17) is intended for constructing a graphical review diagram of various rocket series. The grid of lines of constant z, p and S serves as the basis for this nomogram. With this grid and any two values, acting as coordinates, one can find its (rocket's) location.

ORIGINAL PAGE IS
OF POOR QUALITY

CHAPTER 3

SPACE ORIENTATION

Symbols /34

i	is the angle of inclination of orbit (orbital inclination)
h	is the length of the scale segment from the projection center in the stereographic projection
P	is the parallactic angle (this is the angle at which the distance between the centers of two spheres is seen if the observer's eye is at the rocket mass center)
$\bar{v}$	is the spacecraft velocity
$\bar{v}$	is the spacecraft velocity vector
$\Delta\bar{v}$	is the correcting spacecraft velocity vector
r	is the radius of the meridian of the sphere in the stereographic projection
r_0	is the distance between the centers of the two spheres
r_S	is the instantaneous distance from the center of the Earth to the rocket mass center
Z	is the angular radius in the stereographic projection
α	is the arc of the equator
θ	is the angle of inclination of velocity vector $\bar{v}$ to the Ox axis of the launch coordinate system, or the so-called trajectory angle
λ_S, ϕ_S	are the angular coordinates of the rocket relative to the center of the Earth in the polar system of coordinates
ϕ	is the latitude of the sphere in the stereographic projection
Ω	is the position of the ascending angle of the orbit (longitude) -- reckoned from the vernal equinox
ω	is the angular distance of the orbital pericenter from its ascending angle
γ	is the sign of the vernal equinox

The plane extending through the center of attraction and vector $\Delta\bar{v}$ is called the plane of the correcting velocity vector.

3.1. Fundamentals

By determining the instantaneous division of objects moving in space (Fig. 18) in the polar coordinate system by the position vector O_1S_1, we will have the polar coordinates r_S, λ_S, ϕ_S. By considering that in all problems of space orientation it is desirable to consider the angular coordinates λ_S and ϕ_S separately, we will single them out for solving problems in a spherical coordinate system. We will use coordinate r_S for solving plane problems. In solving problems in orientation we will use the equatorial stereographic projection of the grid of spherical coordinates as the universal transparent nomogram for solving the spherical triangles (see below). In contrast to observational astronomy, it is convenient for us to use predominantly not the internal, but the external surface of the globe. /35

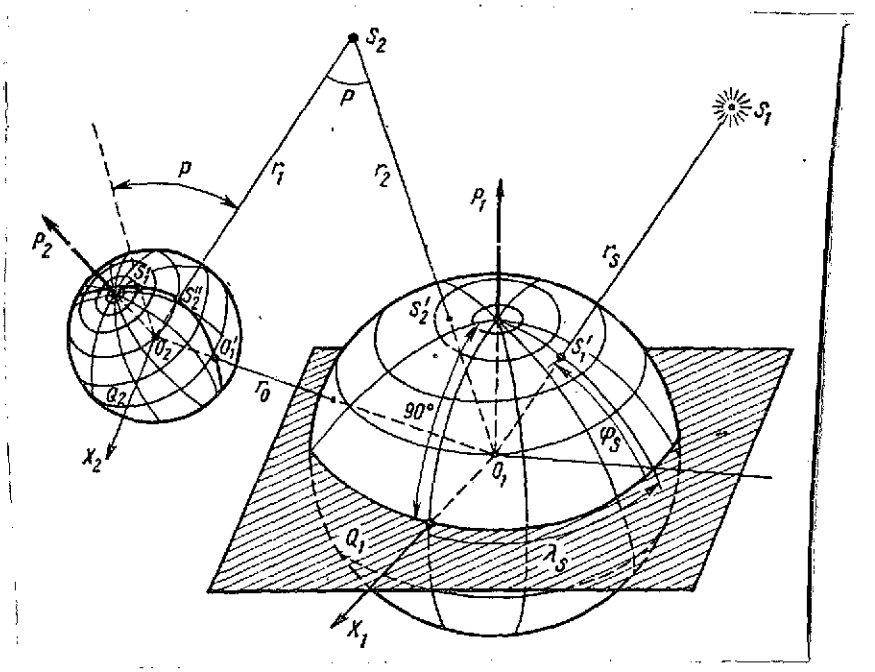

ORIGINAL PAGE IS
OF POOR QUALITY

Fig. 18. Relationship between polar coordinates when another sphere is present

Recall that circles on a sphere are defined by two parameters: the position of the center and of the angular radius. The transition from sphere Q_1 to Q_2 is carried out by the appropriate rotation of the spherical coordinate axes O_1P_1 and O_1X_1 and by allowance for the paralactic angle P by solving the plane triangle

$O_1O_2S_2$. It is not difficult to see that converting from topocentric coordinates to planetocentric coordinates is a particular case of this transformation when the center of the second sphere is situated on the surface of the first. By passing from sphere Q_1 to Q_2, the projection of the object S_2, that is, the point S_2', will move along the arc of a great circle connecting point S_2' with the point of the projection of the center of sphere of Q_1 onto the sphere Q_2 (point Q_1'), by the angle P. /36

When $r_1 >> r_0 << r_2$, $P \simeq 0$, which will always obtain for stars and can be regarded as among the particular cases when the assumption $r_1 >> r_0 << r_2$ falls within the limits of calculation accuracy.

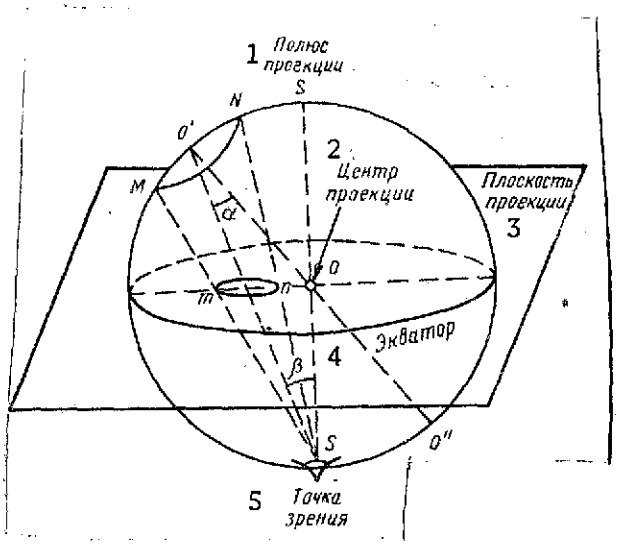

Fig. 19. Stereographic projection

Key: 1. Pole of projection
2. Center of projection
3. Equator
4. Plane of projection
5. Observer's point

To represent the grid of spherical coordinates on a plane, it is convenient to select the stereographic projection. In this projection any circle on a sphere represents also a circle. The stereographic projection is one of the forms of perspective projection, which are subdivided into central, stereographic, external and orthographic. They differ by the position of the observer's station along the normal to the plane of the projection with respect to the sphere. The projection of the surface of a globe (sphere) onto a plane (Fig. 19) is called a stereographic projection, when the observer's point is on the sphere at the end of a diameter normal to the plane of the projection. Table 5 shows the types of stereographic projections and their characteristics.

Let us prove the assumption which influenced the choice of the stereographic projection, namely that any circle of the sphere projected onto it will also be in the form of the circle. Let us take the arbitrary circle MN on the sphere (see Fig. 19). The projection of this circle MN onto the plane passing through the center of the sphere, as we can see from the drawing, will be the section of a circular oblique cone. The bisector of the angle MSN is the axis of the projection cone, that is, the line OO' connecting the center of

the circle on the sphere to the point O'. The diameter O'O" will be the normal to the plane of the circle MN, and the diameter SS' will be the normal to the plane of the circle MN. /37

TABLE 5

Stereographic projections	Position of point of tendency of sphere biplane parallel to the plane of the projection	Particular case of plane of the projection (plane extending through the center of this sphere)
Polar (Fig. 21)	At the pole	Equatorial
Equatorial (see Fig. 22)	At the equator	Meridional
Horizontal (see Fig. 23)	On the sphere	Plane of great circle

It is not diffuclt to prove the equality of the angles α and β as angles measured by halves of the equal arcs SO" and O'S' or the angles of the equilateral triangle O'SO. From the property of a circular oblique cone it follows that if the cone base (MN) is a circle and if the plane of the cone section (MN) is parallel to the plane of the base, this section will also be a circle. From Fig. 19 it is not clear that the plane MN is parallel to mn, but if the plane of the section MN together with the points of the section itself are rotated 180° around the cone axis, this plane will become parallel to the base (on the condition of the equality of angles α and β), where all points in section MN will coincide with the surface of the cone.

Another important property of the stereographic projection is its symmetry with respect to the center. By virtue of this, rotating this projection by some angle about the axis extending through the center of the section perpendicular to the projection plane will correspond to rotating the sphere about the same axis by the same angle. The principal element in the grid of spherical coordinates in the stereographic projection is the scale of degree divisions of the great circle projected onto the diameter of the circle, as shown in Fig. 20. Thus, for example, for the meridional scale of latitudes in the polar projection, we will have

$$h = r \operatorname{tg} \frac{90° - \varphi}{2} = r \operatorname{tg} \left(45° - \frac{\varphi}{2}\right),$$

from whence we get h = 0 for $\phi = +90°$, h = r for $\phi = 0°$ and h = ∞ for $\phi = -90°$.

The functional scale $h = f(\phi)$ is the basis on which all stereographic projections are constructed. In the polar projection (Fig. 21) it yields the law of distribution of parallels. Here the meridians are straight lines situated along a uniform degree scale of longitude. In the equatorial projection (Fig. 22), the functional scale yields the law of degree scales of the grid equator and the grid axis.

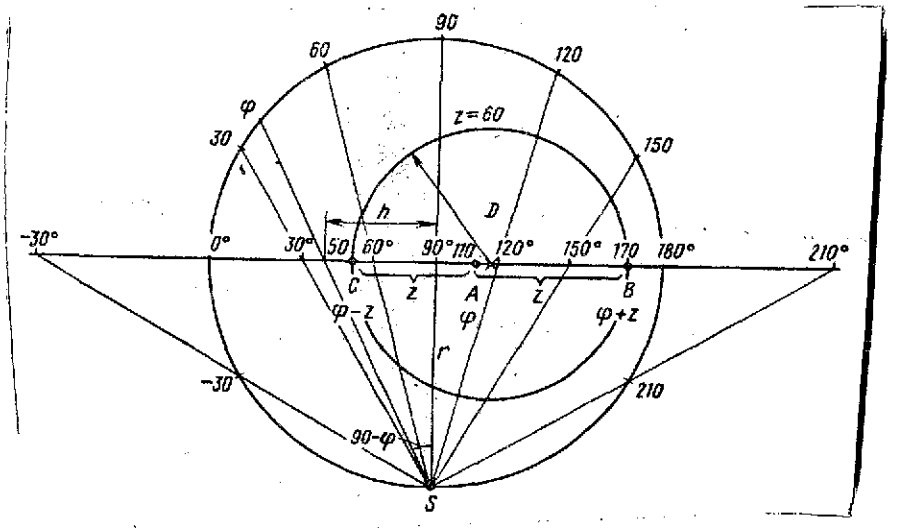

ORIGINAL PAGE IS
OF POOR QUALITY

Fig. 20. Construction of circle with given radius

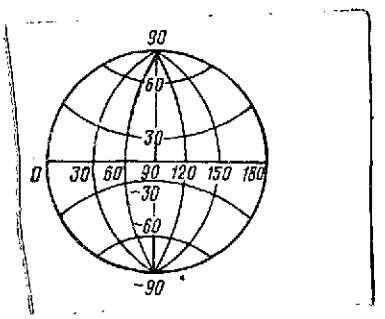

Fig. 21. Polar grid

The polar stereographic projection with its center at the pole is convenient in compiling maps of the surface hemispheres of planets, their satellites and maps of the celestial hemispheres. It makes it possible to simulate the rotation of a planet or a satellite about its axis. However, owing to the large distortions in the southern hemisphere in constructing the maps one must be restricted to the latitude -30°. The equatorial projection (Wulf's grid) is used as a universl tool for constructing all projections, since it contains all great-circle arcs.

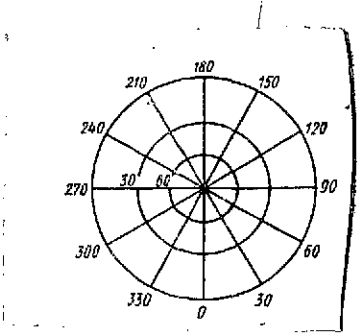

Equatorial Fig. 22. Equatorial grid

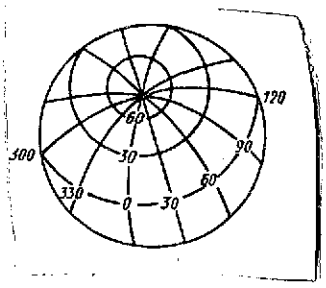

ORIGINAL PAGE IS
OF POOR QUALITY

Oblique Fig. 23. Oblique grid

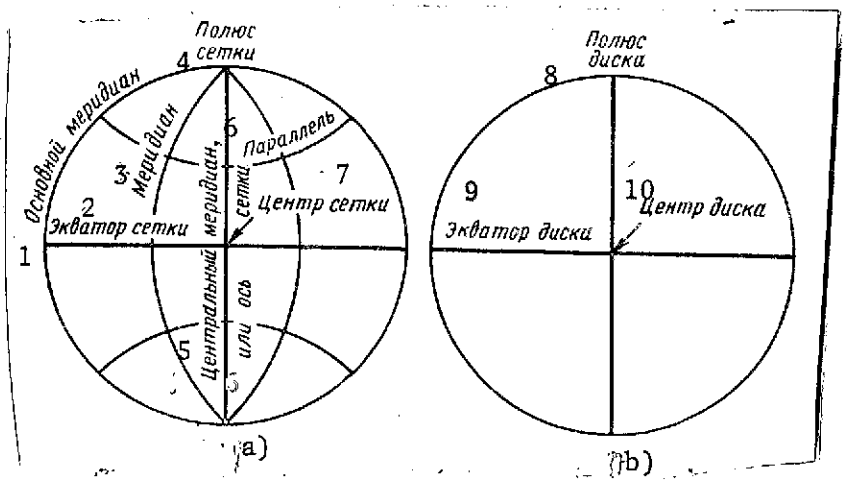

Fig. 24. "Grid" (a) "disc" (b)

Key:
1. Principal meridian
2. Grid equator
3. Meridian
4. Grid pole
5. Central meridian or grid axis
6. Parallel
7. Grid center
8. Disc pole
9. Disc equator
10. Disc center

The horizontal or oblique projections (Fig. 23), which is the general case of the stereographic projection, according to the methods of construction described here below, can be carried out also by using the equatorial grid. /39

Thus, what then is the equatorial grid or Wulf's grid? Wulf's grid is an equatorial, or transverse stereographic projection (Fig. 21) of meridians and parallels onto the plane of one of the meridians. In this projection the central meridian and equator are mapped by straight lines bearing the degree scales for latitudes and longitudes, respectively. Wulf's grid, when rotated by the center, enables us to find the great-circle course between any two points on the sphere.

In this book, Wulf's grid is a constituent part of a universal computational aid used in solving orientation problems (see below in Chapter 3). In solving problems using the grid, it is convenient to perform all projections on transparent paper. We will call this sheet the "disc" and in the following we will refer to the plane on which Wulf's grid is plotted as the "grid" (Fig. 24). To carry out the construction steps, it is necessary to draw on the "disc" a circle with radius equal to the radius of the "grid," and to draw two mutually perpendicular diameters. Further, it is useful for the disc and grid to be seated on the same axis extending through the center of the circles, with the provision of mutual rotation.

The solutions of the all the numerous astronomical and navigational problems, employing the device thus designed are based on only the three following procedures: /40

a) constructing a great circle (great-circle course);

b) constructing a small circle -- the positional circle of equal distances from a given point; and

c) constructing and measuring spherical angles.

3.2. Fundamental elementary construction procedures

Constructing the arc of a great circle (great-circle course) extending through two given points A and B and measuring the distances between them are carried out as follows (Fig. 25):

1. The positions of points A and B are entered on to the disc.

2, By rotating the disc one finds the position at which one of the grid meridians passes simultaneously through points A and B. This meridian will be the desired great circle.

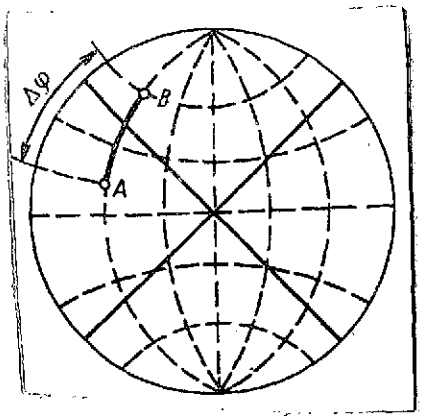

Fig. 25. Great-circle course.

3. By the difference between the latitudes of points A and B one determines their angular distance $\Delta\phi$ (for the globe the angular distance is converted into a linear distance from the fact that 1° ≈ 111 km, while for the moon -- 1° ≈ 32 km).

Constructing a circle with given angular radius Z around a given point A proceeds as follows (see Fig. 20):

1. The position of point A is plotted on to the disc.

2. By rotating the disc, one aligns point A with the equator and from it determines its coordinate ϕ.

3. Two points B and C with coordinates, respectively, of $\phi + Z$ and $\phi - Z$ are read from the disc along the grid equator.

4. The distance between points B and C is halved, and from the point D thus obtained, as from a center, a circle extending through both marks B and C is traced. /41

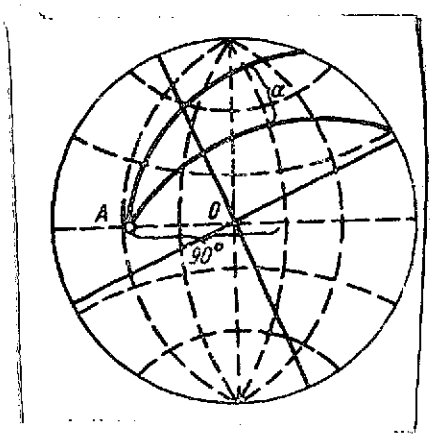

Fig. 26. Spherical angle.

Construction in the use of spherical angles is based on the fact that the spherical angle is determined by an equatorial arc, if the vertex of the angle is taken as the pole. By rotating on the disc the position of the vertex of angle A (Fig. 20) until it coincides with the grid equator, along it we measure off the angle 90° from the vertex and we find the necessary equator to measure the angles, as the corresponding grid meridian. To construct the angle α, along the equator thus found, we lay out the required arc from the given side of the angle. Then, through the point obtained and the vertex of the angle we draw the arc of a great circle as was explained in the construction of a great-circle course (see above). By measuring the angle, one determines the equatorial arc α enclosed between its sides.

The line of azimuths is drawn through the given point of a sphere as follows:

1. By rotating a disc one places the given point on the grid equator and as in the construction of the spherical angles, finds for it, as for a pole, the corresponding equator, which in this case maps the horizon.

2. The lines of azimuths (great circles) are constructed by connecting with great-circle arcs the divisions of the grid meridian mapping the horizon with the given point, as in the construction of a great-circle course.

The grid of horizontal coordinates is constructed for any point on a sphere, which corresponds to the general case of constructing a stereographic projection (see Fig. 23), by combining the methods outlined above used in constructing a circle with given angular radius and drawing a line of azimuths through a given point on the sphere.

A great circle perpendicular to the arc of a given great circle at a given point A is constructed as follows:

1. The given great-circle arc is aligned with the grid meridian and on its equator is found the pole of this circle P.

2. A circle passing through points A and P is constructed, as the arc of a great circle.

Spherical coordinates are transformed as follows: since spherical coordinates differ from each other by the displacement of the pole by some angle in the plane of some meridian, this meridian is taken as the principal meridian, being the great circle in which both poles are situated (in both coordinate systems).

1. The position of the point in the launch coordinate system when its pole is at the grid pole is entered onto the disc.

2. By turning the disc one finds the position at which the /42
pole occupies its position in the new coordinate system.

3. Now the new coordinates are read off from the grid.

3.3. Orientation of orbits and velocity vectors

To orient an orbit in space we will use the projection of the orbit onto a sphere with its center at the focus of the orbit (the center of attraction), as shown in Fig. 27. Obviously, the orbit of any contour -- because it is a plane curve -- will be mapped onto the sphere by a great circle obtained by the intersection of the sphere by the orbital plane. The orbital plane will

intersect the plane of the equator of our spherical coordinate system along the nodal line connecting points ρ and η, where ρ is the ascending node and η is the descending node. The position of the point in space is defined by the following orbital elements: Ω, i, ω. To orient the velocity vectors of space objects (planets, planetary satellites, and spacecraft) we will use the same sphere, by aligning the origin of vectors at the sphere center O. It is not difficult to see that the projection of the velocity hodograph coincides with the orbital projection; the point v* corresponding to the arrival at the target sphere of the instantaneous instantaneous velocity vector $\bar{v}$ is separated from the satellite position N* by the angle 90° + θ in the direction of its motion along the orbit. Here by θ we will mean the angle between the normal to the radius position vector of the satellite $\bar{r}_s$ and its velocity vector $\bar{v}$. Therefore, in solving the problem of transferring from one orbit to another, the projection onto the celestial sphere of velocities v_1 and v_2 at the transfer point will define the position of the plane of the correcting velocity vector $\Delta\bar{v}$ by the great-circle arc extending through v^*_1 and v^*_2 as shown in Fig. 28.

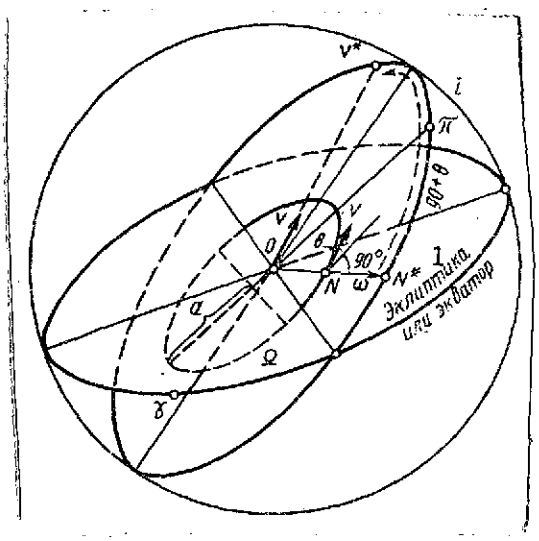

Fig. 27. Orientation of orbits and the velocities: case of motion from apocenter to pericenter ("falling"), when θ is negative.

Key: 1. ecliptic or equator

The above-described principles of construction using Wulff's grid provide the key to a rapid and graphic solution of all problems associated with spherical coordinates and the determination of time in problems of spacecraft orientation, determining the possibility of spacecraft visibility and determining the conditions of spacecraft navigation. Here is a list of the fundamental problems solved by the above-described methods:

-- converting solar time to sidereal time and vice versa;

-- orientation of a spacecraft relative to celestial bodies;

-- determining elements of the space orientation of orbits;

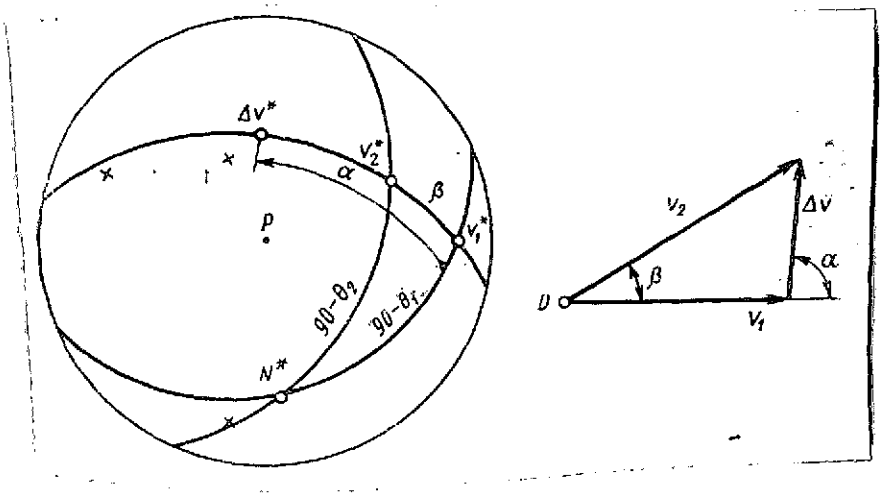

Fig. 28. Orientation of orbit in stereographic projection

-- determining spacecraft launch time;

-- determining coordinates of spacecraft location;

-- determining navigational parameters;

-- determining angles of entry and angles of departure of spacecraft from planetary atmospheres;

-- determining conditions of illumination and photography of planets; and

-- determining conditions of radio communications and antenna pointing.

CHAPTER 4

ORBITAL FLIGHT

Symbols /44

a	the orbital semimajor axis
b	is the orbital semiminor axis
c	is the constant of the integral of areas (the magnitude of the kinetic moment vector) -- the distance from orbital focus to orbital center
C	is the projection of the orbital velocity vector onto the normal to the radius-vector
E	is the eccentric anomaly
e	is the eccentricity of a second-order curve
F	is the force of attraction between masses of material points -- gravitational force
f	is the gravitational constant (force of attraction of unit masses per unit distance)
g	is the gravitational acceleration -- acceleration due to gravity
H	is an auxiliary variable corresponding to E in hyperbolic motion
h	is the constant of the integral of energy -- the energy level
K_1	is the degree of inversion
k	is the coefficient of orbital escape velocity -- the ratio of the instantaneous orbital velocity via the spacecraft to the first escape velocity at the initial trajectory point v_{01}
k_1	is the instantaneous value of a dimensionless coefficient -- the ratio of the magnitude of the instantaneous orbital velocity of the spacecraft to the first escape velocity
k_0	is the initial value of the coefficient of orbital velocity -- the ratio of the initial spacecraft or velocity to the first escape velocity at the initial trajectory point.
ℓ	is the distance between the u and v scales in the Kepler equation nomograms
M	is the mass of an arbitrarily large celestial body (the principal central celestial body)
M_0	is the mean epoch anomaly -- the angle that a radius-vector would describe if it were uniformly rotated
m	is the instantaneous mass of the spacecraft or any other celestial body

n_1 and n_2	are the scale factors (moduli) of the scales
p	is the focal parameter of second-order curves (orbit)
$\bar{R}$	is the projection of the orbital velocity vector onto the normal to the line of apsides.
r	is the distance from the attracting center to the spacecraft
$\bar{r}$	is the radius-vector from the attracting center to the spacecraft
r_π	is the distance of the pericenter -- the minimum value of the radius-vector
r_α	is the distance of the apocenter -- the maximum value of the radius-vector
r_0	is the initial value of the radius-vector
$\bar{r}_1$ and $\bar{r}_2$	are the radii-position vectors (initial and terminal, respectively)
$\bar{r}_i$ and $\bar{r}_j$	are the mutually inverted vectors
$\bar{r}_n$	is the radius-vector normal to the orbital diameter
S	is the length of the chord between the points of the initial and terminal spacecraft positions
T	is the period of revolution of the spacecraft
t	is time
U	is the gravitational potential (the potential of the force of attraction for a spherical Earth model) -- the work done in bringing unit mass from a given point to infinity
U_{SC}	is the potential of the centrifugal force -- the kinetic energy of the spacecraft
v	is the instantaneous spacecraft velocity
$\bar{v} = \dot{\bar{x}}_p$	is the orbital velocity vector
v_0	is the initial spacecraft velocity
v_n and v_r	are the normal and radial components of the spacecraft velocity
v_π and v_α	are the spacecraft velocities at the orbital pericenter and apocenter, respectively
v_1	is the first local escape velocity of the spacecraft
v_2	is the second escape velocity of the spacecraft
v_{01}	is the first escape velocity of the spacecraft at the initial trajectory point /46
$W = U + U_{SC}$	is the gravitational potential -- the total energy of motion of the spacecraft
x and y	are the abscissa and ordinate in a rectangular Cartesian coordinate system
x_p	is the segment of the podera chord
θ	is the angle of inclination of velocity $\bar{v}$ to the Ox axis of the launch coordinate system or, the so-called, trajectory angle

ϑ	is the true anomaly -- the angle corresponding to polar angle ϕ in astronomy
λ_1 and λ_2	are the angular coordinates of the spacecraft relative to the Earth's center in the polar coordinate system, corresponding to the initial and terminal radius-vector -- $\bar{r}_1$ and r_2
ρ and ϕ	are the polar coordinates
μ	is the gravitational parameter of the given body -- the coefficient equal to the product of the gravitational constant by the mass of the central body; $\mu = Mf$.

The line of apsides is a line connecting the pericenter and the apocenter. A hodograph is a circular vector diagram.

A hodograph of orbital velocity is the locus of points of the ends of velocity vectors along an orbit intersecting the origin of coordinates with their origin.

A projective transformation is a method of obtaining a new scale for a given direction by projecting points of the initial scale with the aid of a given center. For more details on projective transformations, see [4].

4.1. Characteristics of a gravity field

In spite of all the complexity of celestial mechanics, understanding the physical principles of space flight is quite simple. This becomes possible because various formal mathematical methods, which are effective means of a profound theoretical investigation (we have in mind the equations of Lagrange and Hamilton), add nothing to our physical concepts based on elementary principles of mechanics, which underlie the well-known laws of Newton. Space flight mechanics provides an exceptional opportunity, starting with the simplest cases, of proceeding gradually from the simple to the complex not only in understanding physical phenomena, but also in the algorithmization of the problems formulated, with which calculations can be performed in the order of successive approximation.

Astronomy deals not only with large quantities, but also with large ranges of their variation, with problems in which one quantity can be negligibly small compared to another. For example, /47 the mass of the satellite (often even an artificial satellite) is negligibly small compared with the mass of the central body attracting it. The distance from Earth to Moon is also negligibly small compared with the distance to the Sun, and so on. This

circumstance makes easier our examination of numerous problems, enabling us often to make significant simplifications without appreciable error. So the elementary problem of the motion of two bodies will serve as the basis for solving a large variety of problems.

The starting point for examining the mechanics of space flight and for penetrating into the area of problems solved in this present work is Newton's law of universal gravity. We will call forces of gravity gravitational forces. The examination of gravitational forces leads to the concept of a gravity field -- a space where the action of these forces can be detected. Thus, by Newton's law the following function is valid for the magnitude of the gravitational force:

$$F=\frac{m_1 m_2}{r^2} f, \tag{4.1}$$

where $f = 6.67 \cdot 10^{-11}$ N·m^2/kg^2. Here, by using Newton's second law of mechanics, we define acceleration, then we get

$$g_1=\frac{F}{m_1};\quad g_2=\frac{F}{m_2};\quad g_1=\frac{m_2}{r^2} f;\quad g_2=\frac{m_1}{r^2} f. \tag{4.2}$$

This simple, but interesting result shows that the acceleration of a body in a gravity field depends on the mass of the attracting body and does not depend on the mass of the attracted body. Here we should note that a body in the gravity field of another body, that is, the body considered in the given specific instance, must be regarded as an attracted body. Thus, the gravity field at any point of the body can be characterized by the magnitude of the acceleration caused by it. The so-called gravitational potential -- the work done in moving unit mass of a body from a given point to infinity -- serves as another characteristic of the gravity field:

$$U=\int_r^{\infty} \frac{dM}{r^2} dr = \frac{fM}{r}. \tag{4.3}$$

Two bodies acted on only by forces of mutual attraction will move about their common center of attraction. However, when one of them has a virtually small mass compared to the mass of the other body, we can assume that the body with mass M to be fixed, and we can regard the other body as its satellite moving in a specific orbit relative to the central body. The quantity fM is called the gravitational parameter of the central body, which then determines its gravity field.

By confining ourselves to the motion around one central body (planet or the Sun), in the following we will consider the so-called central gravity field in which the lines of action of the gravitational force will diverge radially from the center of the arbitrarily large body. The line of action of the gravitational force at each point in the field defines the local vertical for it. We will agree to call the direction along this line toward the attracting center the direction of action "downward," while the direction along this line from the attracting center we will agree to call the direction of action "upward." We will call motion toward the center of gravity "descent," while motion in the opposite direction we will call "ascent." We will further agree to name the plane normal to the local vertical the plane of the local horizon. /48

Now let us pay special attention to the fact that by examining orbital motion in a central gravity field, we are dealing only with one external force -- the gravitational force causing gravitational acceleration. This acceleration, by changing its magnitude inversely proportional to the square of the distance to the central body and being always directed toward it, changes the velocity, thereby being responsible for the nature of orbital motion, and the broad possibilities in selecting the dependence of the change in the spacecraft acceleration with time during its ascent provides all the diversity of orbital types.

Let us introduce yet another important quantity, which also characterizes the gravity field at any point in space. The magnitude of the velocity determining the circular orbit, if it is applied to a spacecraft in the horizontal direction (at a right angle to the line of action of a gravitational force) is called the first local escape (or circular) velocity. In order to be inserted into a circular orbit, in the horizontal direction one must build up a velocity v_1 at which the centrifugal acceleration v_1^2/r would be equal to the gravitational acceleration:

$$\frac{v_1^2}{r}=\frac{fM}{r^2}.$$

Hence we have

$$v_1=\sqrt{\frac{fM}{r}} \quad \text{or} \quad v_1^2=\frac{fM}{r}. \tag{4.4}$$

4.2. Orbital parameters

The equations of motion at the point with mass M in a central gravity field are usually set up in a polar coordinate system with the pole at the center of attraction M (Fig. 29), starting from the magnitude of the initial velocity v_0 at the initial point. Differential equations of motion are formulated based on the energy balance or the equilibrium of forces leading to the equation of acceleration. Here omitting all the operations in setting up and solving these equations, which can be found in [9], we note only which physical laws and corollaries thereof form the basis for setting up the differential equations. /49

Further let us show to which results solving these equations leads, by dwelling in detail on the geometric interpretation of the solution. From the equality of the change in kinetic energy to the change in potential energy we get

$$h = v^2 - \frac{2fM}{r} = v^2 - 2v_1^2, \tag{4.5}$$

and from the constancy of the angular momentum, which is the momentum of the horizontal component of the orbital velocity, we have

$$c = rv_n = rv\cos\theta. \tag{4.6}$$

The solution of equations of motion in the central gravity field can be reduced to the form /50

$$r = \frac{\frac{c^2}{fM}}{1 + \sqrt{\frac{c^2}{f^2M^2}h + 1}\cos\theta}. \tag{4.7}$$

If we compare this solution with the equation of conic sections in polar coordinates

$$\varrho = \frac{p}{1 + e\cos\varphi}, \tag{4.8}$$

we can conclude that one of the conic sections as follows will be the orbit of this motion: circle, ellipse, parabola or hyperbola. The central attracting body will be at the one of the foci of the section (see Fig. 29). Eqs. (4.7) and (4.8) are written in the polar coordinate system with Ox axis directed along the axis of the conic section from the center of attraction O to the

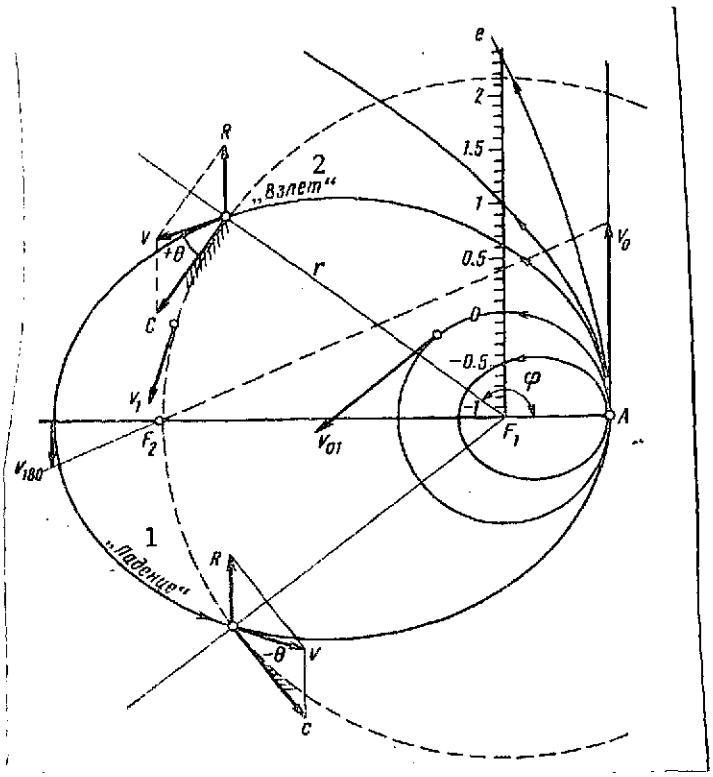

Fig. 29. Orbits originating from the same point

Key: 1. "Descent"
2. "Ascent"

to the initial orbital point. We take as the initial point (it is marked by the letter A in Fig. 29) the orbital point where the orbital velocity is directed at a right angle to the radius-vector, that is, has a horizontal direction. A plane normal to the line along which the gravitational force acts must be taken as the horizontal plane. In this case θ = 0.

The following are the principal elements defining the dimensions and shape of the orbit: a, e and c. A comparison of Eqs. (4.7) and (4.8) gives us the following starting relation for determining the orbital parameters:

$$p = r_{90^\circ} = \frac{c^2}{fM} \tag{4.9}$$

$$e = \sqrt{\frac{c^2}{f^2M^2}h + 1}. \tag{4.10}$$

ORIGINAL PAGE IS
OF POOR QUALITY

Noting that

$$a=\frac{r_\pi}{1-e}=\frac{r_a}{1+e}=\frac{r_\pi+r_a}{2}=\frac{r_0}{1-e}=\frac{p}{1-e^2}, \tag{4.11}$$

we get the formula for determining the orbital semimajor axis:

$$a=-\frac{fM}{h}. \tag{4.12}$$

Hence it is clear that the semimajor axis a does not depend on the direction of the velocity $\mathbf{v}$, since the expression for the constant of the energy integral h (see Eq. (4.5)) does not contain θ, and the energy level of the orbit is defined only by a and M. /56 For convenience in calculation, it is desirable to introduce the concepts of orbital velocity coefficients -- dimensionless coefficients defined in terms of v_1 and v_{01} (see Eq. (4.4)) thusly:

$$k_1=\frac{v}{v_1}; \tag{4.13}$$

$$k=\frac{v}{v_{01}}; \quad k_0=\frac{v_0}{v_{01}}. \tag{4.14}$$

Since

$$v_1^2=\frac{fM}{r} \quad \text{and} \quad v_{01}^2=\frac{fM}{r_0}, \tag{4.15}$$

then

$$\frac{v_1^2}{v_0^2}=\frac{r_0}{r} \quad \text{and} \quad \frac{k_1^2}{k^2}=\frac{r}{r_0}.$$

Because $fM = v_1^2 r = v_{01}^2 r_0$, follows from Eq. (4.4), the *Eq.* orbital parameters will be expressed by the formulas

$$h=v^2-2v_1^2; \tag{4.16}$$

$$c=rv\cos\theta=r_0v_0; \tag{4.17}$$

$$p=r_{90^\circ}=\frac{c^2}{fM}=r_0k_0^2; \tag{4.18}$$

$$e=\sqrt{\frac{c^2}{f^2M^2}h+1}=\sqrt{1-\cos^2\theta\left(2k_1^2-k_1^4\right)}, \tag{4.19}$$

where when θ = 0 we get

$$e = k^2 - 1; \tag{4.20}$$

$$a = -\frac{fM}{h} = \frac{r}{2 - k_1^2}. \tag{4.21}$$

From Eqs. (4.21), (4.11) and (4.15) we can readily obtain the formulas defining the dimensionless coefficients k or k_1 (we will call them dimensionless velocities) at any point on the orbit as a function of the dimensionless distance from the attracting center, equal to r/r_0 or r/a.

Hence we have

$$k_1 = \sqrt{2 - \frac{r}{a}} = \sqrt{2 - \frac{r}{r_0}(1 - e)}; \tag{4.22}$$

$$k = \sqrt{\frac{2}{r/r_0} + e - 1} = \frac{k_1}{\sqrt{r/r_0}}. \tag{4.23}$$

To obtain the dimensional magnitude of velocity, we must multiply the resulting coefficient k or k_1 by the magnitude of the corresponding first escape velocity. /52

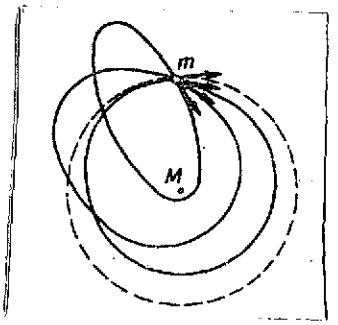

Fig. 30. Dependence of orbital shape on initial angle

Any orbit is characterized by two parameters: a and e. Parameter e for an elliptical orbit indicates the degree of its elongation, and for a hyperbolic orbit -- the degree of its rectifiability (e = 0 for a circle). The semimajor axis of an orbit a depends only on the magnitude of the velocity (for a fixed center of attraction and a constant initial distance from it) and does not depend on its direction (see Eq. (4.2)). As for eccentricity, it depends both on the magnitude of the initial velocity and on the direction of the velocity (see Eq. (4.19)).

Fig. 30 shows the change in the shape of an orbit resulting from changing just the direction of the initial velocity. To determine the eccentricity, let us use these expressions:

$$e = \frac{r_a - r_\pi}{r_a + r_\pi}. \tag{4.24}$$

4.3. Types of orbits

As was noted, any spacecraft orbit in a central gravity field is one of the lines of the conic section at one of whose foci the central attracting body is situated. Let us examine more closely the change in the shape of an orbit with a gradual increase in the initial horizontal velocity from a plot of orbits originating from the same point A (see Fig.29). For zero initial velocity v_0 a vertical descent takes place along a straight line (the maximum compressed ellipse). Further, with increase in velocity, the situation changes. If the initial velocity is smaller than the first escape velocity, the spacecraft will continue its motion thusly: first on losing altitude, it begins to describe an ellipse situated within the circular orbit (if it were able to move along it), from the apocenter to the pericenter, thus executing first a descent with increase in velocity, and after reaching the pericenter, as ascent with decrease in velocity. In the absence of an atmosphere the ascent will occur with arrival at the former altitude. In this case, point A will be the apocenter.

When the initial velocity is increased to the value v_{01}, the second focus F_2 will be displaced in our figure toward the left, that is, closer to F_1, and when /53

$$\frac{v_0}{v_{01}} = k_0 = 1$$

it will merge with it into a single point, which now will be the center of the circular orbit. At a still higher velocity the spacecraft will initially begin to gain altitude, moving along an elliptical orbit that is physically a periodic ascent (with decrease in velocity) and descent (with gain in velocity). When there is no atmosphere, the spacecraft even in this instance will make a descent [sic] to its former altitude. Here the point A will be the pericenter. With a further increase in velocity from v_{01} to $\sqrt{2}v_{01}$, the second focus F_2 will continue to shift further leftward, departing toward infinity ($+\infty$).

Thus, when $v_0 = \sqrt{2}v_{01}$ and $k_0 = \sqrt{2}$, the motion will occur along a parabolic orbit. An infinitely elongated ellipse transforms into a parabola with e = 1 carrying the spacecraft virtually beyond the limits of the sphere of action of the central body, where it will have zero velocity at an infinitely distant point.

The velocity $v_2 = \sqrt{2}v_1$, determining the parabolic orbit for a spacecraft is called the second escape velocity. It is also customary to call this velocity the escape velocity [a Russian synonym of the phrase in the previous sentence], or the separation velocity, since it can overcome all the energy of the gravity field. At a velocity greater v_2, the spacecraft will move in

a hyperbolic orbit, departing toward infinity with a residual velocity -- the velocity that is virtually the same as the velocity at the boundary of the sphere of action. By the sphere of action we will mean the region of space within which in practice we can calculate the motion of a spacecraft as being under the influence of the gravitational force of just the given central body. The radii of the spheres of action for the Earth, Moon and planets are incomparably large compared to their own radii.

Hyperbolic orbits have a negative pole a and a second focus, arriving from $-\infty$ (if the motion occurs to the left in Fig. 29, then this must be understood as motion as $+\infty$). At an infinitely large initial velocity we obtain an orbit that is degenerate from both hyperbola branches into a single straight line coincident with the vector $\bar{v}_0$ in direction.

We must direct the reader's attention to the fact that for the eccentricity e, which is the ratio of the distance between foci to the magnitude of the major axis, it is useful to introduce the sign [sense] of the direction in orbital mechanics, since orbital foci are not equivalent to the foci of the curves of the conic sections in analytic geometry. This nonequivalence arises because an orbit has its center at one focus, while the other focus is "empty." Therefore, the so-called internal ellipses (ellipses lying within the circular orbitals) must have a negative eccentricity and then the functions derived earlier will be valid for all orbits originating from the same point (including here also the straight line of plumb descent, for which e = -1). /54

4.4. Energy balance of an orbit

The potential energy of a spacecraft per unit mass can be expressed by the gravitational potential (4.3)

$$U = -\frac{fM}{r} = -v_1^2, \tag{4.25}$$

and the kinetic energy -- the energy of motion of the spacecraft per unit mass -- will be

$$U_{SC} = \frac{mv^2}{2m} = \frac{1}{2}v^2, \tag{4.26}$$

and the total energy will be of the form

$$W = U + U_{SC} = \frac{1}{2}v^2 - v_1^2. \tag{4.27}$$

Let us trace further how the potential and kinetic energies will change as the spacecraft moves in its orbit. For this purpose we will consider the quantities

$$\frac{U}{fM} \text{ and } \frac{U_{SC}}{fM}.$$

From Eq. (4.25), we get

$$\frac{U_{SC}}{fM} = -\frac{1}{r}, \tag{4.28}$$

and using Eqs. (4.26), (4.22), (4.13) and (4.4) we find

$$\frac{U_{SC}}{fM} = -\frac{1}{2a} + \frac{1}{r}; \tag{4.29}$$

$$\frac{W}{fM} = -\frac{1}{2a}. \tag{4.30}$$

From Eqs. (4.8) and (4.11) it follows that

$$r = \frac{a(1-e^2)}{1+e\cos\vartheta}. \tag{4.31}$$

Substituting this value of r into Eqs. (4.28) and (4.29), we get /55

$$\left.\begin{aligned} \frac{U}{fM} &= -\frac{1}{a(1-e^2)} - \frac{e}{a(1-e^2)}\cos\vartheta; \\ \frac{U_{SC}}{fM} &= \frac{1}{a(1-e^2)} + \frac{e}{a(1-e^2)}\cos\vartheta - \frac{1}{2a}. \end{aligned}\right\} \tag{4.32}$$

From this it is clear that the energy change as a function of the angle ϑ obeys a oscillatory (harmonic) law with the same amplitude $\frac{e}{a(1-e^2)}$ and Eqs. (4.32) are with respect to each other the mirror reflections relative to the energy level

$$-\frac{1}{2}\frac{W}{fM}.$$

Let us sum up our main results:

1. The energy level of an orbit h = 2W is defined as the different between the squares of the orbital velocity and the escape velocity for a given point, remaining constant for the entire orbit, that is,

$$h = v^2 - v_2^2.$$

In order to obtain this, it is sufficient to use Eqs. (4.24) and (4.27). For a given mass of the central body the energy level uniquely defines the semimajor axis of the orbit (see Eq. (4.12)).

Knowing the distance to the central body, its mass and the magnitude of the velocity at a given point, it is not difficult to determine the semimajor axis of the orbit of the spacecraft.

2. To determine the eccentricity of an orbit we must, besides knowing the magnitude of the velocity, also know the angle of ascension of the vector velocity above the local horizon θ.

3. We can construct the spacecraft orbit from the value of the semimajor axis and the eccentricity. To totally define an orbit in space it remains to find its further space orientation.

4.5. Flight time

Even before Newton established the law of universal gravity the great German scientist Johannes Kepler discovered the following highly important laws of the kinematics of motion of celestial bodies, which have not lost their significance to the present time and which are convenient for some of our computational operations:

1. The orbit of each planet is an ellipse at one of whose foci is situated the Sun. /56

2. The radius-vector of a planet sweeps out equal areas in equal time intervals.

3. The squares of the periods of revolution of each planet are proportional to the cubes of its mean distances to the Sun. From Kepler's second law it follows that the ratio of the velocity at the pericenter to the velocity at the apocenter is equal to the reciprocal of the corresponding distances to the center of attraction. Kepler's third law enables us to determine the masses of planets from observational data of the revolution of satellites. The relationship between the mass of a planet M, period of revolution of satellite T and the mean distance r from the center of the planet to the satellite can be expressed by the formula

$$M = \frac{4\pi^2}{f}\frac{r^3}{T^2}. \qquad (4.33)$$

Kep Kepler's equation serves in calculating the position of a celestial body in its elliptical orbit. It enables us to derive the relationship between E and M_0:

$$M_0 = E - e \sin E. \tag{4.34}$$

By assigning the time t, let us determine the value M_0 from the formula

$$M_0 = \frac{2\pi}{T} t, \tag{4.35}$$

where T is uniquely defined by the semimajor axis of the ellipse a based on the formula

$$T = \frac{2\pi}{\sqrt{fM}} a^{3/2}. \tag{4.36}$$

Here we must note that from the geometrical point of view E is the angle used in the familiar method of geometrical construction of an ellipse based on the points between two concentric circles whose radii are equal to b and a respectively (Fig. 31). The following relation obtains between E and ϑ

$$\operatorname{tg} \frac{\vartheta}{2} = \frac{\sqrt{1+e}}{\sqrt{1-e}} \operatorname{tg} \frac{E}{2}; \tag{4.37}$$

on the basis of which the nomogram shown in Fig. 57 was constructed.

Kepler's equation for hyperbolic orbits (see [2]) is of the form

$$M_0 = e \operatorname{sh} H - H. \tag{4.38}$$

The geometrical significance of H can be made clearer from Fig. 32. A simple method of the graphical solution of Kepler's equations is based on representing them in the form

$$57.3 \sin E = E - M/e \text{ (for elliptical orbits);} \tag{4.39}$$

$$57.3 \operatorname{sh} H = M + H/e \text{ (for hyperbolic orbits)} \tag{4.40}$$

and in seeking the point of intersection of the sinusoids is described with a straight line that has a slope 1/e, as shown in Figs. 33 and 34. Nonetheless, it is very convenient to use Lambert's method [2] for hyperbolic orbits. Lambert's theorem enables us to determine the flight time in terms of four scalar quantities: a, r_1, r_2 and S. The working formulas are these (Fig. 35):

$$R=r_1+r_2; \tag{4.41}$$

$$\operatorname{ch}\lambda_1=1+\frac{R+S}{2a}; \tag{4.42}$$

$$\operatorname{ch}\lambda_2=1+\frac{R-S}{2a}. \tag{4.43}$$

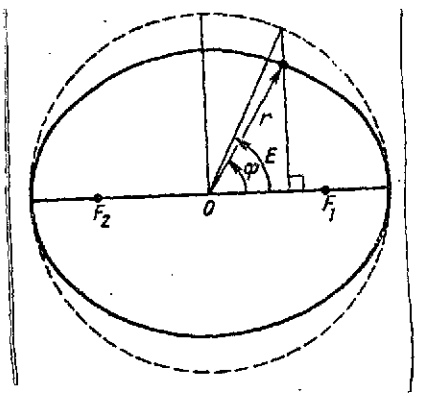

Fig. 31. Eccentric anomaly

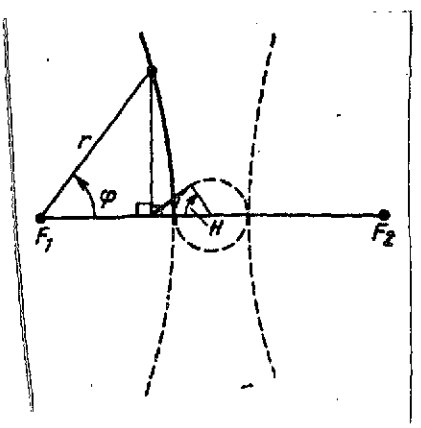

Fig. 32. Eccentric anomaly for hyperbolas

Denoting further

$$\left.\begin{aligned}\operatorname{sh}\lambda_1-\lambda_1&=M_{01};\\ \operatorname{sh}\lambda_2-\lambda_2&=M_{02},\end{aligned}\right\} \tag{4.44}$$

we finally get

$$M_0=M_{01}-M_{02}. \tag{4.45}$$

The graph shown in Fig. 36 /58 is used in practical calculations, where from two quantities obtained from Eqs. (4.42 and (4.43) we seek two others: M_{01} and M_{02}. Further, we find their difference by Eq. (4.45), that is, M_0, from which we can readily find the flight time.

4.6. Polar diagram

The geometrical interpretation of orbital parameters leads to a universal construction that combines the polar diagram of the orbit and the hodograph of the orbital velocity (see [9]). Let us show /59 how this is done. Eq. (4.8) can

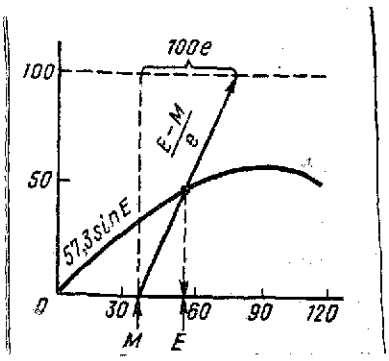

Fig. 33. Graphical solution of Kepler's equation for an ellipse

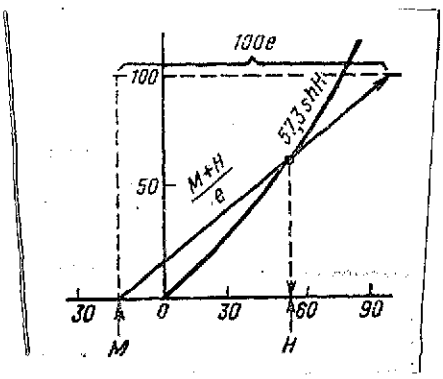

Fig. 34. Graphical solution of Kepler's equation for a hyperbola

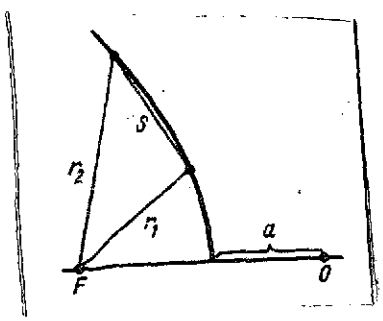

Fig. 35. Explanation of functions in Lambert's theorem

be written thusly:

$$\frac{\frac{l}{\varrho}}{p} = 1 + e\cos\varphi. \qquad (4.46)$$

Hence follows the geometrical construction shown in Fig. 37, where the coordinate X of point N mapping the position of the spacecraft in its orbit is the reciprocal of the radius-vector r when the quantity $p = r_{90°}$ is taken as the unit of measurement. From Eq.(4.19) that relates eccentricity to velocity v (in terms of k_1) and to θ, we get

$$e^2 = \cos^2\theta \cdot k_1^4 - 2\cos^2\theta \cdot k_1^2 + 1. \qquad (4.47)$$

from Eq. (4.15) we have

$$k_1^2 = k^2 \frac{r}{r_0}, \qquad (4.48)$$

and from Eq. (4.6) we get

$$rv\cos\theta = r_0 v_0, \quad \text{or} \quad \frac{r}{r_0} = \frac{v_0}{k}. \qquad (4.49)$$

Recalling Eq. (4.14), we can write

$$\frac{v_0}{v} = \frac{k_0}{v\cos\theta}. \qquad (4.50)$$

Further, substituting the value of (4.50) into Eq. (4.49) and (4.49) into (4.48), we get

$$k_1^2 = \frac{kk_0}{\cos\theta}. \qquad (4.51)$$

ORIGINAL PAGE IS
OF POOR QUALITY

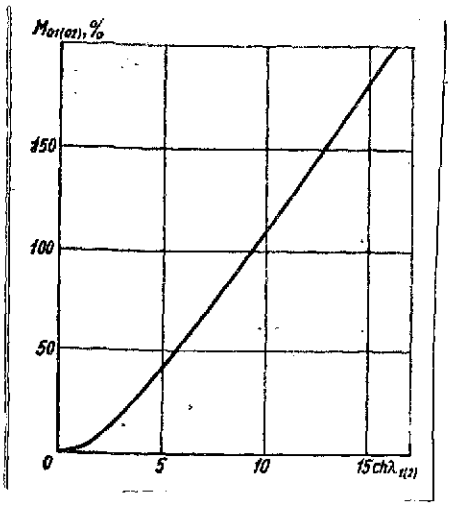

Fig. 36. Plot of the determination of $M_{01(02)}$

Finally, substituting k_1 we have found into Eq. (4.47), let us derive the final formula

$$e^2 = k^2 k_0^2 - 2kk_0 \cos\theta + 1, \tag{4.52}$$

expressing the "theorem of cosines" for the triangle ONM (see Fig. 37), where the side "e" lies opposite the angle θ. The segment GN, when OM is equal to unity, will be

/60

$$kk_0 = v\frac{v_0}{v_{01}^2}, \tag{4.53}$$

and, thus, enables us to determine the magnitude (dimensionless) of the velocity in the orbit. And the magnitude of the velocity itself can be defined thusly:

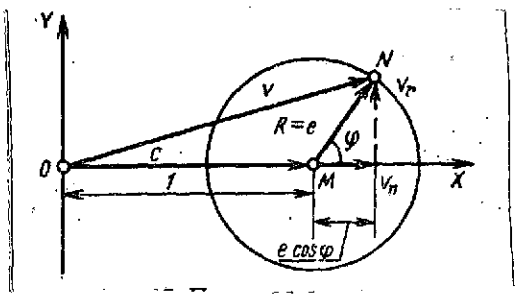

Fig. 37. Polar diagram

$$v = ON\frac{v_{01}^2}{v_0} = ON\frac{v_{01}}{k_0}. \tag{4.54}$$

The scale coefficient of velocity can be expressed in terms of gravitational parameter μ and the constant of the integral of areas c as follows:

$$\frac{v_0}{v_{01}^2} = \frac{v_0 r_0}{fM} = \frac{c}{fM}. \tag{4.55}$$

Since the angle at point O was found to be equal to the angle θ, it is not difficult to see that the drawing in Fig. 37 is the hodograph of the orbital velocity (see list of symbols to Chapter 4) in a rotating velocity coordinate system, where the OX axis is the horizontal axis, and the Oy axis is the vertical axis, and the decomposition of the velocity vector onto the axes yields the components v_n and v_r. Using the velocity hodograph as a vector diagram where all the vectors are proportional to the magnitude of the orbital velocity with identical scale

coefficent, we can take any of the vectors as unity and obtain in this case the dimensionless magnitude of the velocity.

It is obvious that it would be most convenient to take as unity the vector velocity at the initial point, that is, at the pericenter. Let us denote this by $\overline{OF}$. Then the vector $\overline{OM}$ will express the value of v/v_0. From the velocity hodograph we can also get the absolute values of the orbital velocity v if the vector $\overline{OF}$ in the same scale maps the initial velocity v_0. Fig. 37 illustrates a quite interesting conclusion, stating that the vector of the orbital velocity, on the one hand, is the sum of two nonorthogonal vectors $\overline{C}$ and $\overline{R}$ constant in magnitude, which is the result of decomposition of the orbital velocity vector in two directions -- the normal to the radius-vector and the normal to the line of apsides as shown in Fig. 38. The magnitude of these invariants can be defined by the relations:

$$\overline{R}=\frac{v_\pi - v_a}{2}; \quad \overline{C}=\frac{v_\pi + v_a}{2}. \tag{4.56}$$

The hodograph is constructed as follows: of the two vectors $\overline{R}$ and $\overline{C}$, one is assumed to be fixed and the other is rotated at its end, forming the hodograph. Depending in which coordinate system the hodograph will be constructed, one chooses the fixed vector. In the polar rotating coordinate system one selects the vector $\overline{C}$, while in the inertial Cartesian one selects the vector $\overline{R}$ (see Fig. 38).

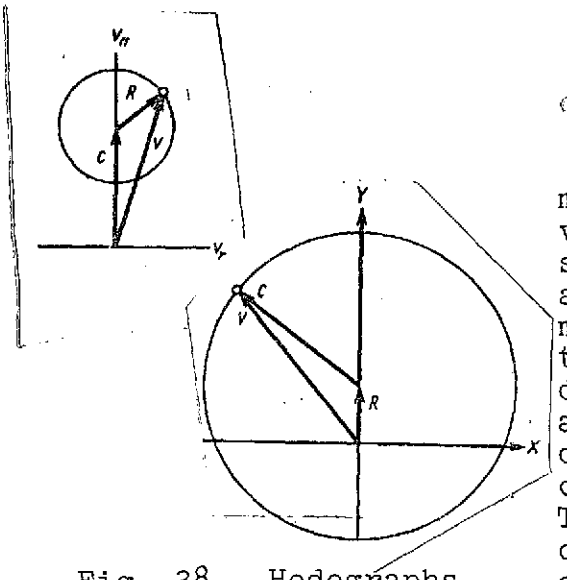

Fig. 38. Hodographs

4.7. Podera as a hodograph of orbital velocity

Let us examine yet another geometrical interpretation of orbital velocity -- the interpretation as a segment of the chord of the podera of a conic section. For this purpose we must present the basic principles from the theory of geometrical constructions defining the podera of a conic section and inversion. The locus of projections of a focus onto a sliding tangent is called the podera of the conic section. The podera of a conic section is a circle constructed on the major axis of the conic section as on a diameter (Fig. 39). Two vectors drawn from the same point F, whose product is equal to the constant K_i are called mutually reciprocal, or inversion vectors, and the method of finding the reciprocal vectors is called inversion. The point F is called

the pole or the center of inversion, and the number K_i is called the degree of inversion. It is then difficult to show that chords drawn through point A lying within the circle with its center O (Fig. 40) are divided at this point into two segments, which are the inversion vectors r_i and r_j. Actually, by drawing a chord normal to the diameter extending through the points O and F, we get two equal vectors r_n. Further, by connecting the ends of the vectors shown as shown in Fig. 40 with the lines BD and CE we get two congruent triangles FBD and FCE. Denoting the magnitude of the equal vectors by r_n, we can write $r_1/r_n = r_n/r_j$ or $r_i r_j = r^2_n = b^2$, where $r^2_n = b^2 = K_i$.

It is also not difficult to show the inversion of vectors of a circular hodograph for the external position of the point of origin of the vectors -- the inversion pole. From the congruence of the triangles FBD and FCE (see Fig. 40), we get $r_i/r_a = r_b/r_j$ or $r_i r_j = r_a r_b$ where $r_a r_b = K_i$.

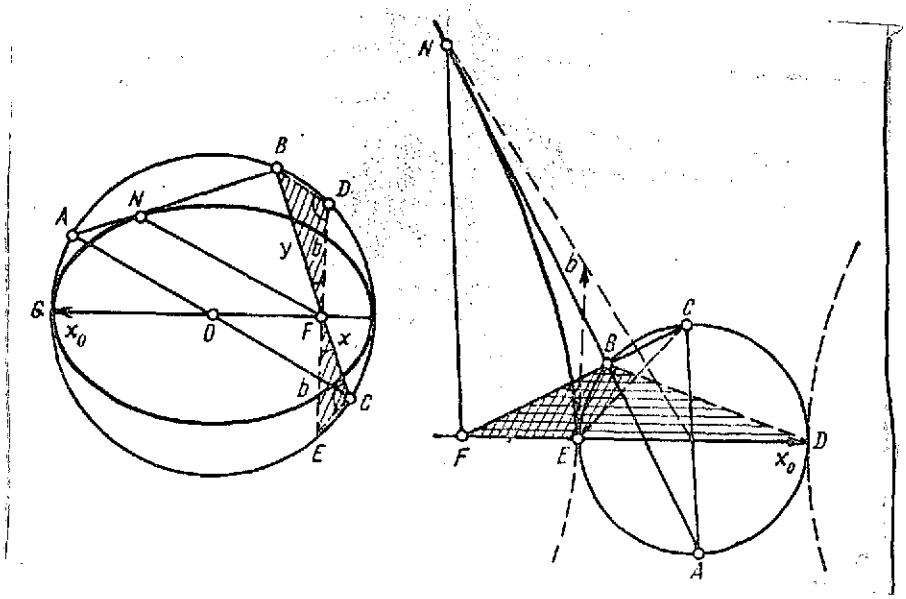

Fig. 39. Poderas

Based on the foregoing, we can proceed to the inverse curves and, in particular, show that the curve of the inverse line is the circle extending through the origin of vectors with its center lying on the perpendicular to the line. The combination of inversion and scale transformations affords broad possibilities in nomography for the geometrical interpretation of orbital velocities.

ORIGINAL PAGE IS
OF POOR QUALITY

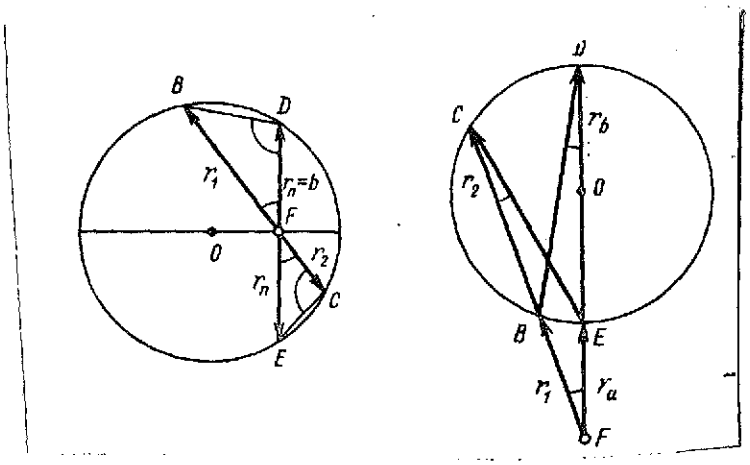

ORIGINAL PAGE IS
OF POOR QUALITY

Fig. 40. Proof of the invertibility of circular-hodograph vectors

Let us turn to Fig. 39. The chord of the podera BC, coincident within normal dropped down from focus F to the sliding tangent AB, is divided at the focus into the two segments BF and FC, whose lengths become the reciprocals if we take as the unit of measurement the length of the semiminor axis (see the above definition of inversion).

Besides these geometrical constructions, it is also known that the diameter of a podera AC on which the angle formed by the tangent AB and the normal BC extending through focus F is taken is parallel to the radius-vector $\overline{FN}$ drawn through the point of tangent N. From the congruence of triangles ABC and NBF, by denoting the length of the segment FC by x_p, and the segment FB by y_p, we can write /63

$$\frac{AC}{FN}=\frac{2a}{r}=\frac{x_p+y_p}{y_p}.$$

Further, considering that $\overline{FD}=\overline{FE}=b$ and $x_p y_p = b^2$, we get

$$\frac{2a}{r}=\frac{x_p^2}{b^2}+1, \quad \text{whence} \quad x_p^2=b^2\frac{a}{r}\left(2-\frac{r}{a}\right).$$

By comparing this function with Eq. (4.22), here we introduce k_1 according to the notations in Eqs. (4.13) and (4.14)

$$x_p^2=b^2\frac{a}{r}k_1^2=b^2\frac{a}{r_n}k^2,$$

whence

$$k^2=\left(\frac{v}{v_{01}}\right)^2=\frac{x_p^2 r_n}{b^2 a}.$$

On the other hand, according to Eq. (4.20) we have

$$k_0^2=\left(\frac{v_0}{v_{01}}\right)^2=1+e.$$

Dividing the expression for k^2 by k_0^2, we obtain

$$\left(\frac{v}{v_0}\right)^2=\frac{x_p^2}{\frac{b^2 a(1+e)}{r_n}}.$$

Since $r_n = p/1 + e$ and $p = b^2.a$, $r_n = b^2/a(1 + e)$. By substituting r_n into the formula for $(v/v_0)^2$, we get

$$\left(\frac{v}{v_0}\right)^2=\frac{x_n^2}{a^2(1+e)^2}, \text{ or } \frac{v}{v_0}=\frac{x_n}{a(1+e)}; \text{ since } a=\frac{r_n}{1-e}, \; 1+e=\frac{2a-r_n}{a}.$$

Hence we finally get

$$\frac{v}{v_0}=\frac{x_n}{2a-r_n}=\frac{x_n}{x_0}$$

This expression defines the magnitude of the scale vector $\bar{x}_0$ equal to the segment FG: . For the hyperbola the major axis is negative and expression for x_0 becomes . In accordance with these relations, in Fig. 39 are shown the scale vectors $\bar{x}_0$ for the two types of orbits.

Thus, summing up, we can note that the segment of the chord of the podera FC denoted by x is the vector of the orbital velocity, and the podera itself is the hodograph of the orbital velocity in the Cartesian inertial coordinate system rotated 90° in the direction of the spacecraft motion, since the chord of the podera is perpendicular to the tangent, that is, to the direction of motion. The direct vertical descent AF is a degenerate internal ellipse for which e = -1. It will have a podera in the form of a circle constructed on r_n as on a diameter. Determining the velocity vectors in this limiting case by means of the podera, owing to the fusion of the infinitely "thin" ellipse with the line OF, leads to an indeterminacy of the form $v/v_0 = 0/0$. However, this problem can be resolved very simply if we use Eqs. (4.22) and (4.23), by substituting the value e = -1 in them. As a result

$$k_1=\frac{v}{v_1}=\sqrt{2}\sqrt{1-\frac{r}{r_0}}; \qquad (4.57)$$

$$k=\frac{v_1}{v_{01}}=\sqrt{2}\sqrt{\frac{r_0}{r}-1}. \qquad (4.58)$$

The plot shown in Fig. 41 was constructed on the basis of these functions. As we can see, when in a vertical descent, a spacecraft acquires the second escape velocity with respect to the initial point at half the path from the point to the center of attraction, and the first escape velocity -- at 1/3 of the path. We only note that the local magnitude of the first escape velocity will also be attained at half-path. /65

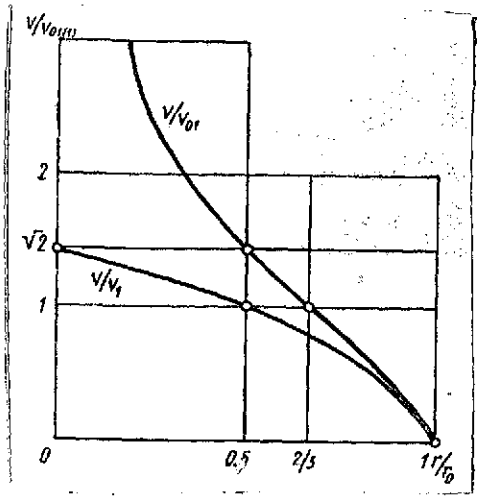

Fig. 41. Plot of K_1 for vertical descent

4.8. Nomograms of orbital flight.

Nomograms of initial data of orbital flight are intended mainly to determine the dimensional magnitudes of velocity and the time relative to the corresponding dimensionless coefficients obtained by calculations using the nomograms and the computational devices. Nomograms of this type determine the values of g, v_1 or v_2 and T as functions of M and r:

$$g=fMr^{-2}; \qquad (4.59)$$

$$v_1^2=fMr^{-1};\ v_2=2v_1^2; \qquad (4.60)$$

$$T^{-2}=\frac{1}{4\pi^2}fMr^{-3}. \qquad (4.61)$$

Simple relations between the variables lead to the simplest nomogram of equated points with parallel rectilinear scales (Fig. 42). The nomogram thus constructed enables us, if we know any of the two variables indicated as the initial data, to find all the remaining variables by applying the cursor in the plane of the nomogram so that it intersects the two corresponding scales at the desired values. In most practical problems M and r are the given variables, therefore it is useful to place their scales at the edges of the nomogram, as was done in Figs. 43 and 44 for higher calculation accuracy.

It became possible to construct this nomogram due to the fact that each of the three variables g, v_1 or v_2 and T can be separately expressed in terms of two variables M and R by using a formula of the (2.4) type. For higher accuracy, the nomograms were constructed in a narrower data range than is sometimes required. The nomogram shown in Fig. 44 was intended for near-planetary orbits, while the one shown in Fig. 44 was intended for near-solar orbits. Scales of M and r comprise a group of three scales corresponding to Eq. (4.59), and their unit scale divisions are identical, therefore the modulus of the logarithmic scale for r is twice as large, since r in Eq. (4.59) is to the -2 power. The position and scale of the unit scale division for v_1 were determined as follows. For the position of the M and r scales given in the previous construction, the position of the v_1 scale was determined. Further, by virtue of the quadratic formula (4.60) the modulus of the v_1 is doubled. Similarly, the T scale was constructed in accordance with Eq. (4.61). It bears noting once again that the negative exponent requires a change in the direction of scale over the one it is placed, by the reciprocal.

The nomogram for determining orbital parameters by the velocity vector (Fig. 45) was constructed analogously to the preceding nomogram. It determines the orbital elements a and e from the velocity given by the vector at any given point in space, that is, by the quantities v, θ and r for different central attracting bodies with mass M. The following relations were used in constructing the nomogram:

$$\frac{a}{r} = \frac{1}{2-\left(\frac{v}{v_1}\right)^2}; \tag{4.62}$$

$$e^2 - 1 = \cos^2\theta\left[\left(\frac{v}{v_1}\right)^4 - 2\left(\frac{v}{v_1}\right)^2\right]. \tag{4.63}$$

This nomogram is shown in Fig. 45 for elliptical orbits, and in Fig. 46 -- for hyperbolic orbits. Let us trace the operations in solving this problem of determining the parameters using these nomograms. First, we determine the magnitude of the first local escape velocity using the nomogram (see Figs. 42, 43 and 44) in terms of M and r. Let us find the dimensionless magnitude of the velocity as the ratio v/v_1 on the left scale of the nomogram. On this same line using the scale at the right, to this value will correspond the desired semimajor axis in the dimensionless form -a/r, whence it is not difficult to obtain a. By further connecting with a straight line the point found with the point of the given angle θ in the central scale, on the right scale we get the eccentricity.

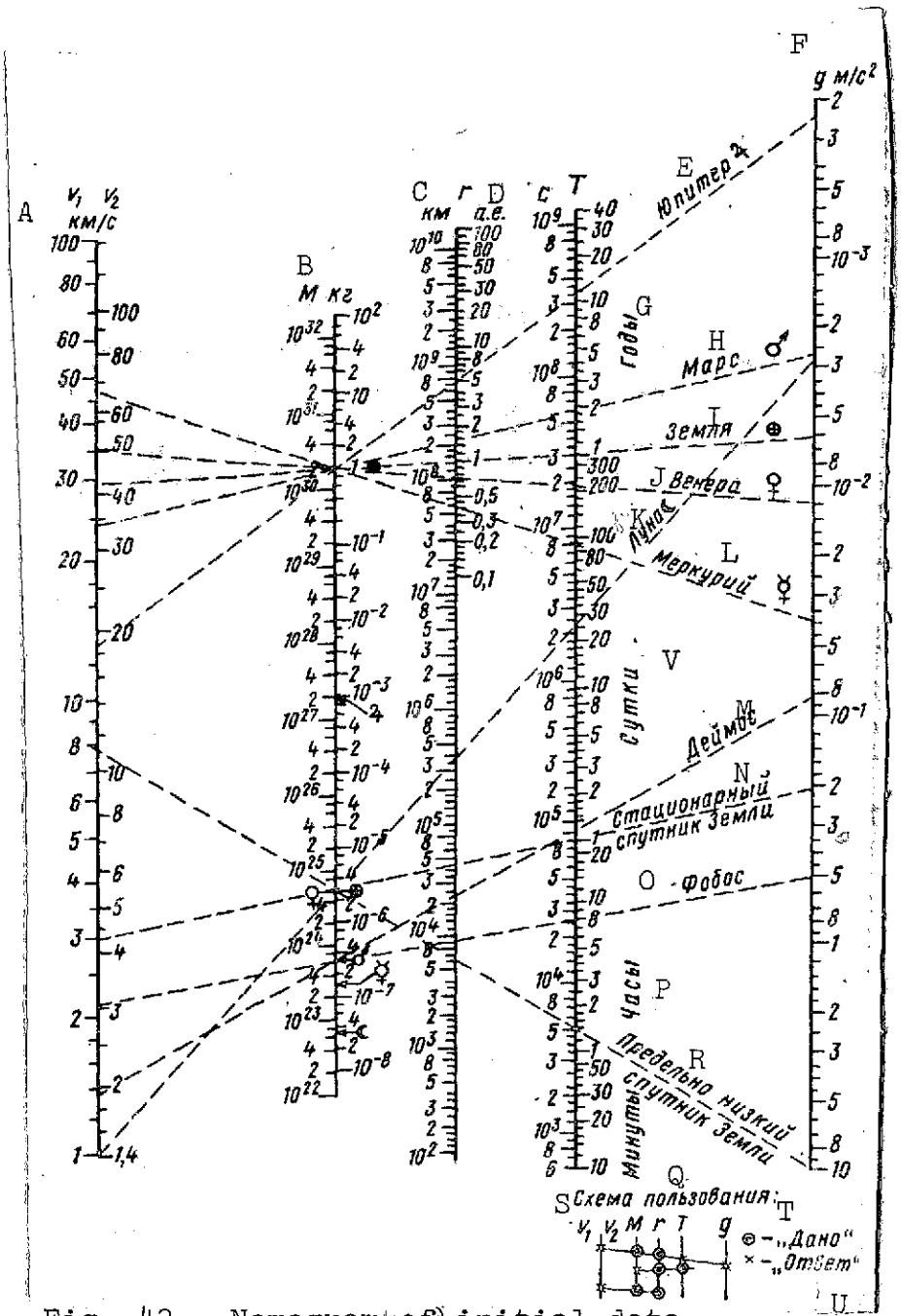

Fig. 42. Nomogram of initial data

Key:
A. km/sec
B. kg
C. km
D. Astronomical unit
E. Jupiter
F. m/sec^2
G. Years
H. Mars
I. Earth
J. Venus
K. Moon
L. Mercury
M. Deimos
N. Stationary Earth satellite
O. Phobos
P. Hours
Q. Minutes
R. Lowest possible Earth satellite
S. Scheme of use
T. "Given"
U. "Answer"
V. Days

ORIGINAL PAGE IS
OF POOR QUALITY

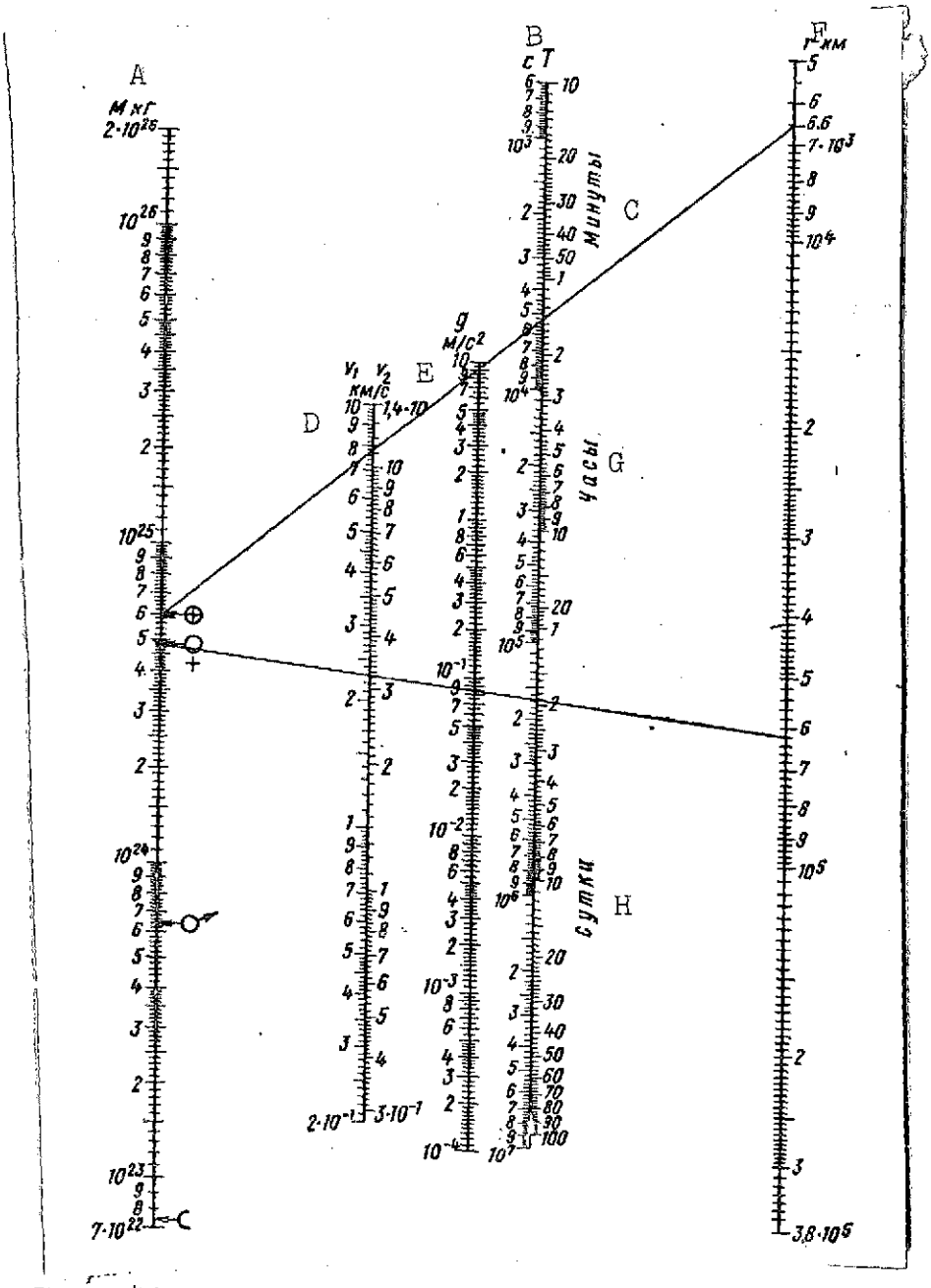

Fig. 43. Nomogram for near-planetary orbits

Key:
A. M, kg
B. sec, T
C. Minutes
D. km/sec
E. m/sec^2
F. r, km
G. Hours
H. Days

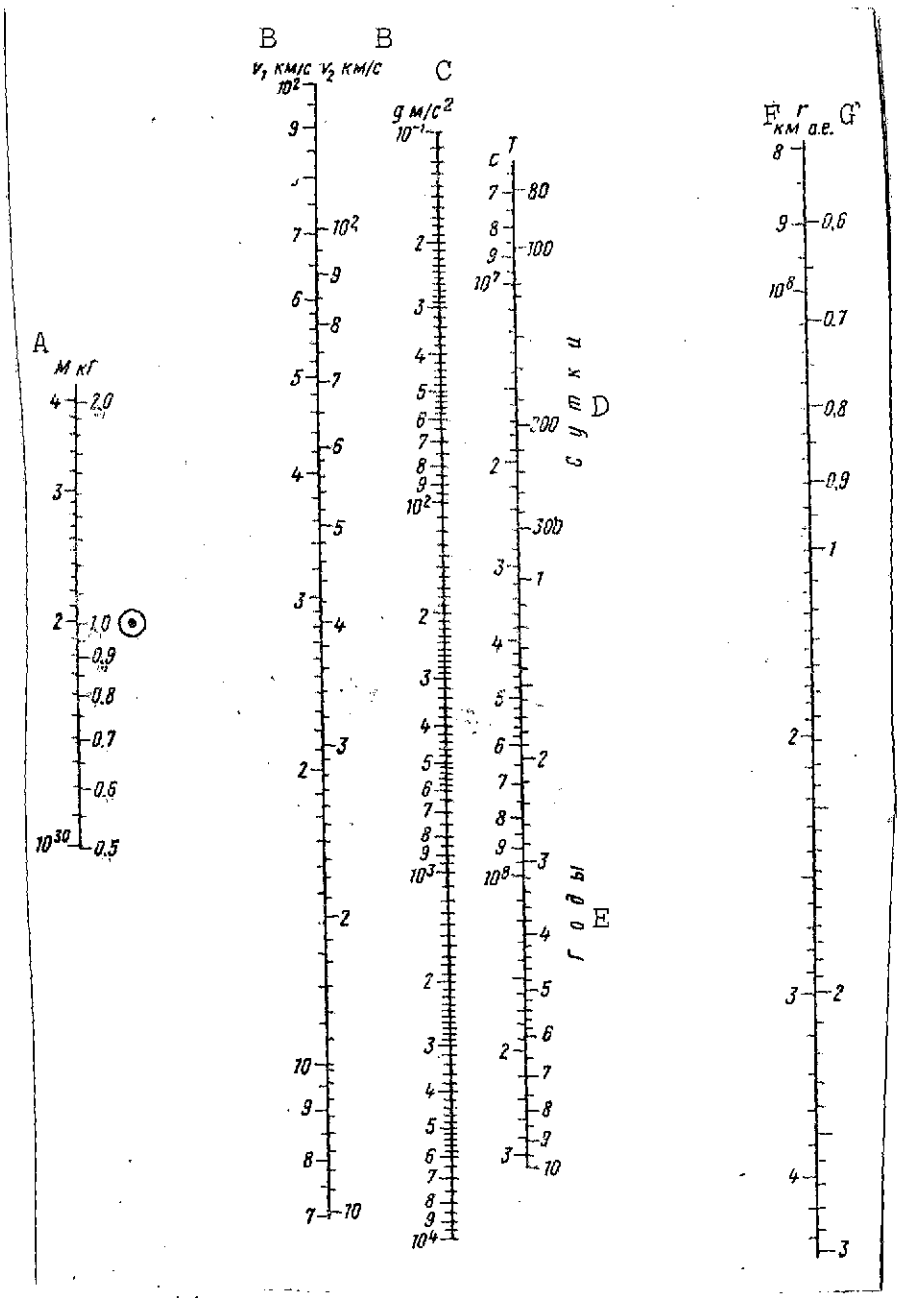

Fig. 44. Nomogram for near-solar orbits

Key:
A. M, kg
B. M/sec
C. M/sec^2
D. Days
E. Years
F. km
G. Astronomical units

ORIGINAL PAGE IS
OF POOR QUALITY

The nomogram for determining the velocity at any point in the orbit was constructed on the basis of the relation

$$\left(\frac{v}{v_{01}}\right)^2=\frac{2}{\frac{r}{r_0}}+e-1. \tag{4.64}$$

Fig. 47 shows the geometrical structure of this nomogram consisting of the following scales: the right scale is the scale of e values (linear scale); the central scale is the scale of v/v_{01} (quadratic scale); and the left scale is the r/r_0 scale (hyperbolic scale). The left scale reflects the law of inverse proportionality, and its ordinates are the reciprocals of the ray lying between 1 and ∞.

Now let us examine how the nomogram gives an insight into the physical meaning of this phenomenon. The first scale consists actually of two scales -- the e scale and the v_0/v_{01} scale. The v_0/v_{01} scale is uniquely related to the e scale by the function /70

$$e=\left(\frac{v_0}{v_{01}}\right)^2-1. \tag{4.65}$$

The coefficient $k_0 = v_0/v_{01}$ multiplied by v_{01} determines the required velocity to attain an orbit with given e. As we can see from Fig. 47, all kinds of orbits from bottom to top are arranged along the e scale and the v_0 in a specific order, as follows: at the right in the orbit of vertical descent: internal ellipses situated within the circular orbit by the orbits of flight to the innermost planets; the circular orbit is the orbit of flight at constant altitude; the external ellipses situated to the exterior of the circular orbit are the orbits of flight to the outermost planets; the parabola is the orbit of the spacecraft departing to infinity, that is, virtually beyond the sphere of action of the central attracting body with zero velocity; and the hyperbola is the orbit of a spacecraft departing to infinity with residual velocity -- the orbit within the sphere of action of the central attracting body. /72 /73

The scale of this nomogram is the scale of radial distances from the attracting center to the spacecraft. On this scale the marker 1 refers to the initial position of the spacecraft.

For all orbits, with the exception of the internal ellipses, this is the pericenter, the orbital point closest to the attracting center. For the internal ellipses, this is the apocenter, that is, the orbital point furthest from the attracting center. Considering that when a spacecraft is moving from the pericenter of all orbits the distance r increases while when moving from the

apocenter it decreases, it is not difficult to understand that the ray of the first scale from the values 1 to ∞ will be used for the entire nomogram (except for the section of internal ellipses on the right scale when e = 0 - -1. The segment of the left scale from values 1 to 0 is used only for the internal ellipses, therefore in constructing the nomograms for practical use it is expedient to divide this nomogram into two parts, assigning one of them as the nomogram for the internal ellipses. The curve ABC constructed in the lower part of the nomogram is the envelope of the calculated positions of the cursor on the section AB for which they intersect the values of the r/r_0 scale corresponding to the positions of the spacecraft at the apocenters for external ellipses and along the section BC -- at the pericenters for the internal ellipses. This envelope can be constructed from the cursor positions, determined by the formula

$$\frac{r_{180^\circ}}{r_0} = \frac{1+e}{1-e},$$

where r_{180° is the radius-vector rotated 180° relative to the position of the initial radius-vector. By assigning a specific value of e or v_0/v_{01} and by drawing the tangent to the curve ABC so that it would pass also through the given value on the corresponding scale, we can obtain at the points of intersection of the two left scales the radius-vector and the velocity in the opposite orbital point -- at the pericenter for internal ellipses, and at the apocenter -- for other orbits.

By examining the geometrical and physical structure of the nomogram, we can readily see that in the form represented in Fig. 47 we cannot attain good accuracy of calculations for the reason that the cursor positions for the internal ellipses in the calculated positions yield always acute angles when the r/r_0 scale and the v/v_{01} scale are intersected. To eliminate this shortcoming, it is best to transform the appearance of the nomogram shown in Fig. 47 by using the mutual displacement of the outermost scales by one level. So in making nomograms for practical use, the nomogram must be divided into two parts as shown in Figs. 48 and 49. /74

For the actual conditions of space flight, it proves to be quite possible to construct nomograms with any prespecified accuracy, but with a restricted range variation in the parameter values. As an example, in Fig. 50 is shown a nomogram for the orbits of spacecraft flight from Earth to Moon, which yields the desired initial velocity coefficient to five decimal places. In this nomogram we can easily inspect the relationship between /76 the required accuracy of the initial velocity, the possible error in the distance, and the accuracy with which the velocity of approach to the Moon is determined. The accuracy of determining the velocity of the approach to the Moon is necessary in determining the conditions of maneuver in the Moon's sphere of action and the conditions of landing on its surface.

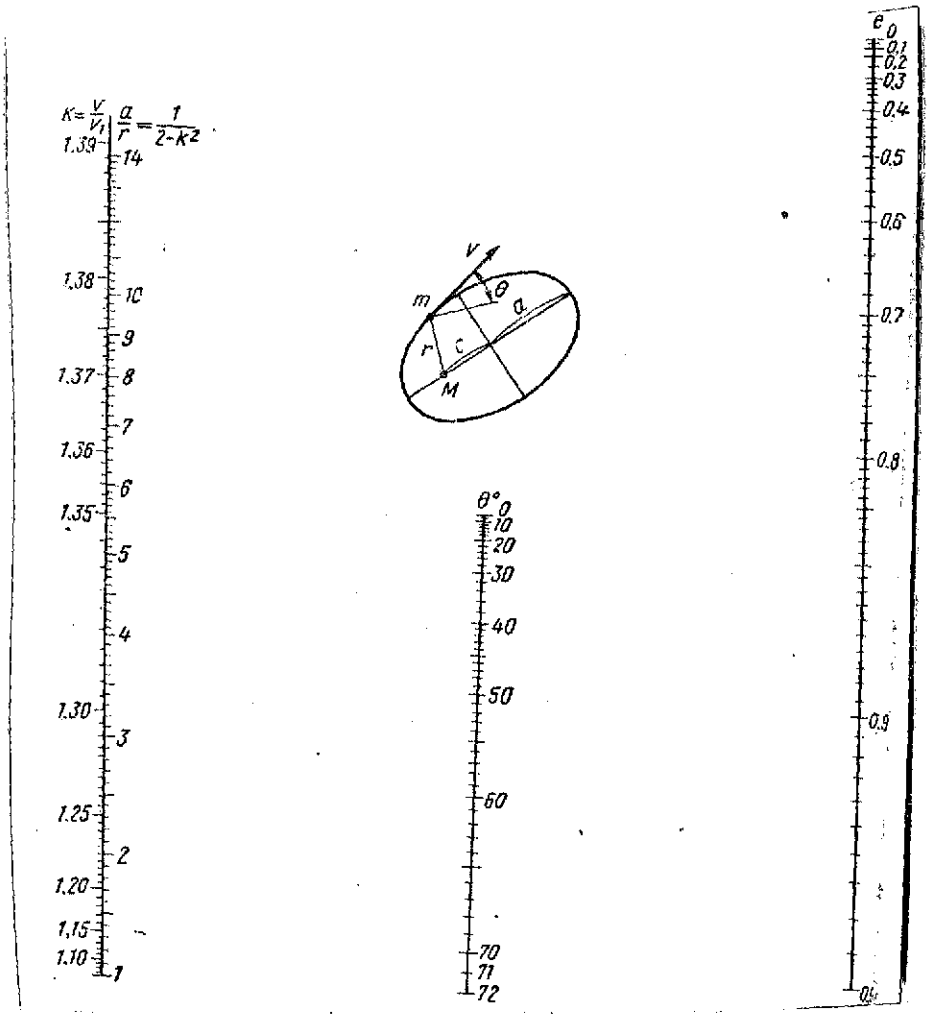

Fig. 45. Nomogram of elliptical orbits

4.9. Disc nomograms

Nomograms described in the section above can be designed so that their scales fit along the arc of a circle. We will call these nomograms of the disc type. To construct this kind of nomogram, lets represent Eq. (4.63) as follows:

$$\frac{2k_1^2 - k_1^4}{\frac{1}{\cos^2\theta}} = \frac{1 - e^2}{1}. \qquad (4.66)$$

ORIGINAL PAGE IS
OF POOR QUALITY

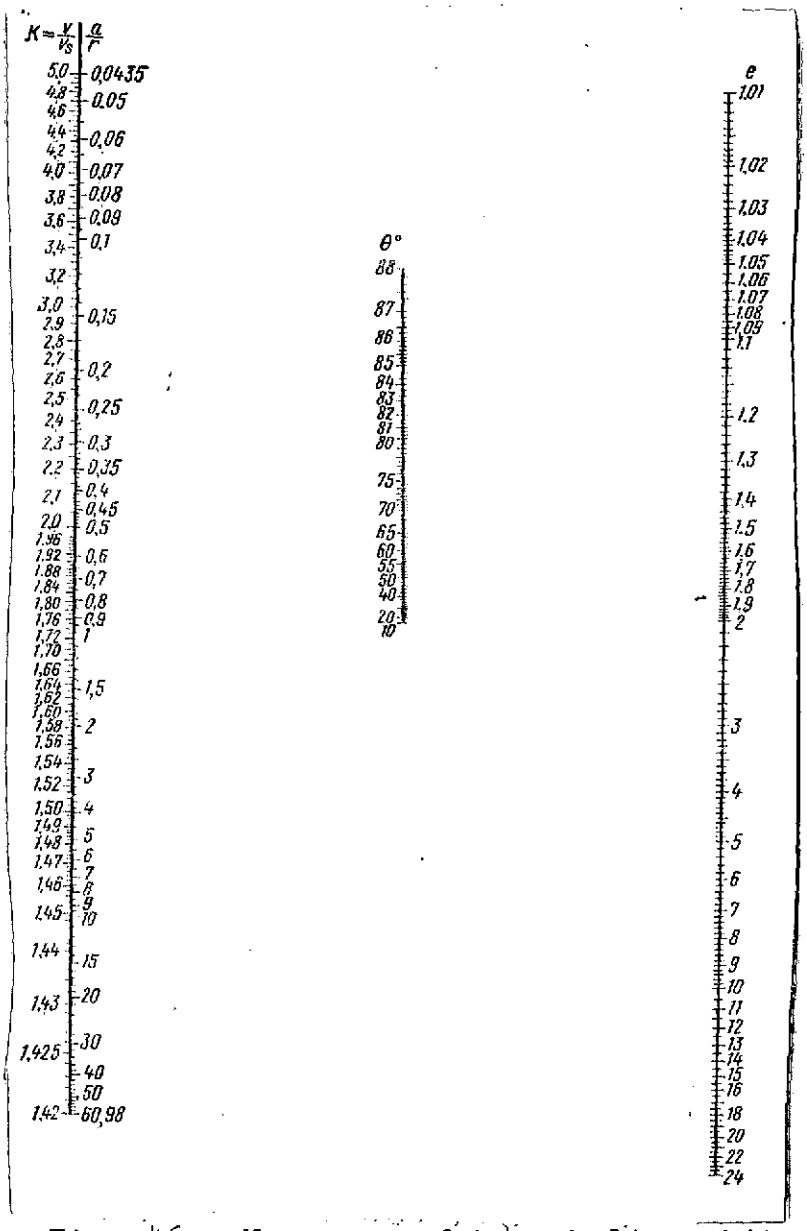

Fig. 46. Nomogram of hyperbolic orbits

The scheme of arranging logarithmic scales for this expression is shown in Fig. 51. When $\sqrt{2} > k_1 > 1$, the quantity $2k_1^2 - k_1^4$ decreases with increase in k_1; therefore, if the direction of the k_1 scale remains unchanged, the θ and e scales must be reversed in direction. Hence the θ and e scales are given a mirror image relative to the vertical line extending through "zero" and the scheme of scale arrangement in the disc nomogram thus constructed will be as shown in Fig. 52. The a/r scale can be constructed as earlier, on the same line as the k_1 scale. We will show the procedure in the use of this nomogram below. Let us assume that we know the orbital eccentricity e. Then, by positioning the internal disc (with the e scale) with a known

ORIGINAL PAGE IS
OF POOR QUALITY

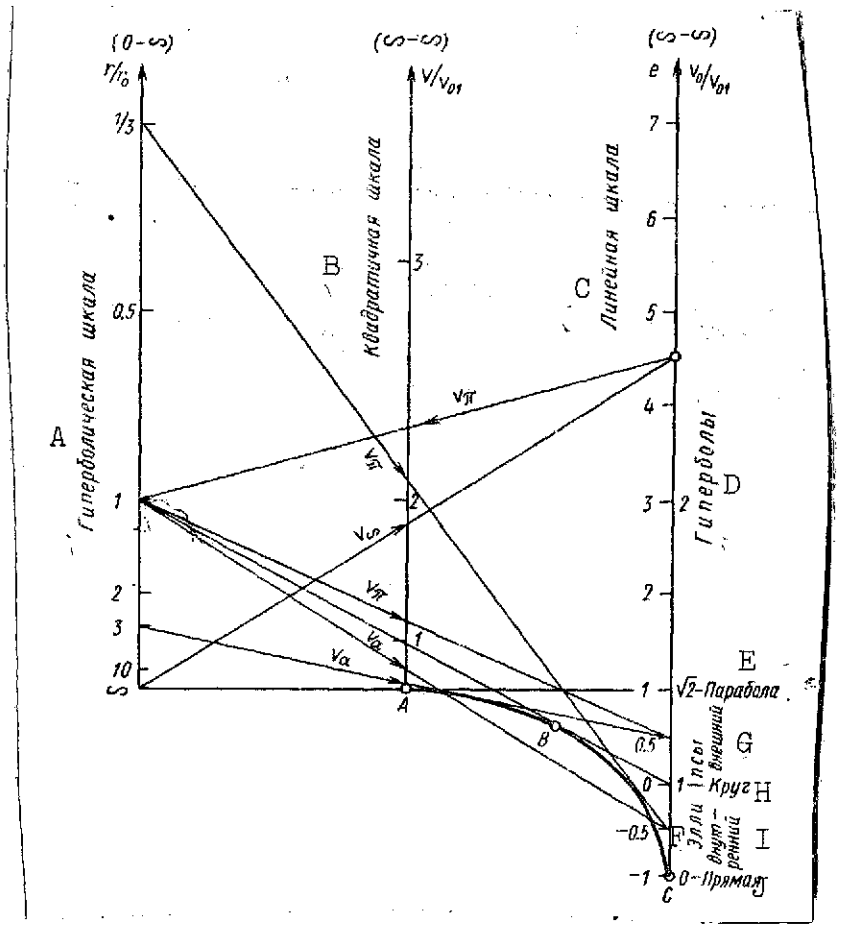

Fig. 47. Nomogram for determining velocity at any point in an orbit:
$v_п$ is the velocity at the pericenter; $v_α$ is the velocity at the apocenter; $v_∞$ is the residual velocity

Key:
A. Hyperbolic scale
B. Quadratic scale
C. Linear scale
D. Hyperbolas
E. Parabola
F. Ellipses
G. Outermost
H. Circle
I. Innermost
J. Straight line

ORIGINAL PAGE IS
OF POOR QUALITY

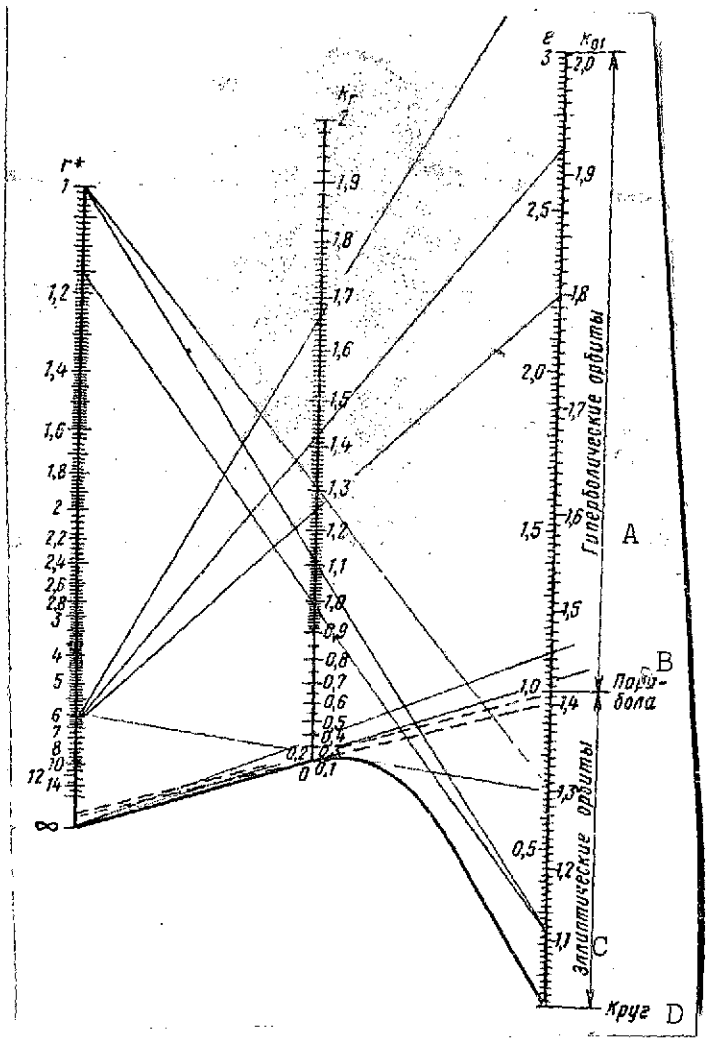

Fig. 48. Nomogram for determining dimensionless velocity coefficient k_r

Key: A. Hyperbolic orbit
B. Parabola
C. Elliptical orbits
D. Circle

value of e opposite the e arrow, we read off opposite any k_1 the value of θ corresponding to it. We can also solve the inverse problem, that is, determine e for given k_1 or θ. /77

The disc nomogram for solving Eq. (4.64) is based on the following form of this equation

$$k^2 - \frac{2}{r/r_0} = -(1-e). \qquad (4.67)$$

ORIGINAL PAGE IS
OF POOR QUALITY

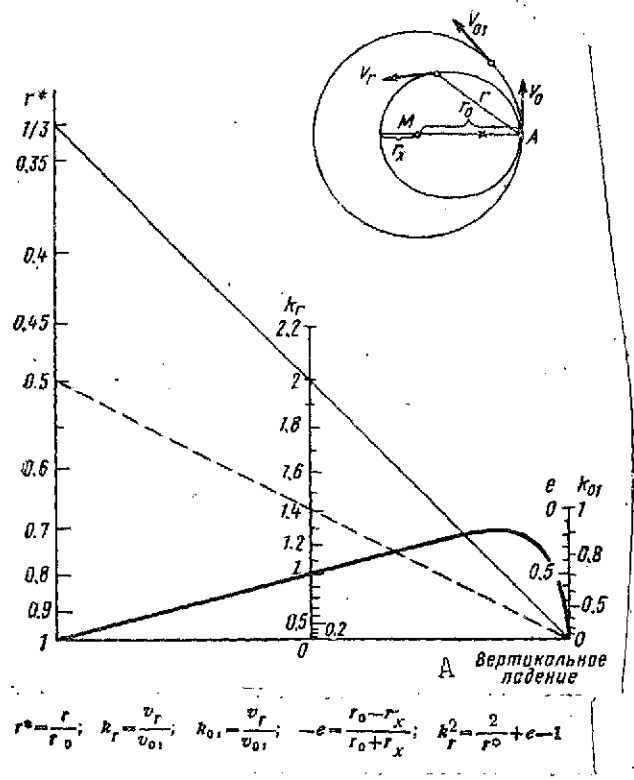

Fig. 49. Nomogram of velocity for internal ellipses

Key: A. Vertical descent

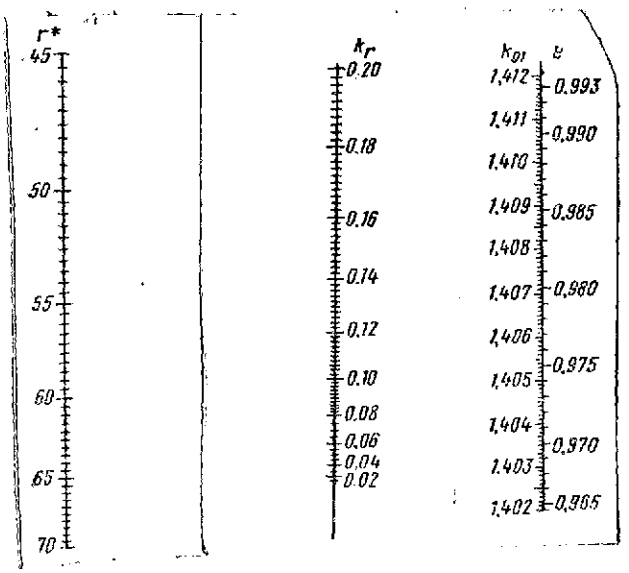

Fig. 50. Nomogram of velocity for near-lunar ellipse

This expression can be interpreted by the nomogram shown in Fig. 53. Let us explain the steps in working with this nomogram. By placing the e arrow opposite the eccentricity, we will have across from each r/r_0 the k corresponding to it, and vice-versa (see scales at the left), in similar fashion we can solve the inverse problem. An additional scale can also be laid out along this nomogram -- the $r_{180°}/r_0$ scale. We must know the $r_{180°}$ values to calculate velocities along the entire orbit so as not to fall in the region of imaginary r values. The $r_{180°}/r_0$ scale in Fig. 53 is placed parallel to the e scale and is constructed according to the relation

$$e = \frac{r_{180°}/r_0 - 1}{r_{180°}/r_0 + 1}. \qquad (4.68)$$

Fig. 54 presents samples of the disc nomograms.

4.10. Nomograms of Kepler's equation.

The relation between the three variables M, E and e appearing in Kepler's equation can be expressed with a nomogram of equated points in the first category. The scheme of this nomogram for the three variables u, v and w a new shown in Fig. 55. For the variables u and v it has rectilinear parallel scales, and for the variable w -- a curvilinear scale. Let us represent the distance between the u and v scales by ℓ and trace the steps in constructing the nomogram. Let us bring the Y axis of the Cartesian coordinate system into alignment with the direction of the u scale. Let us align the origin of the

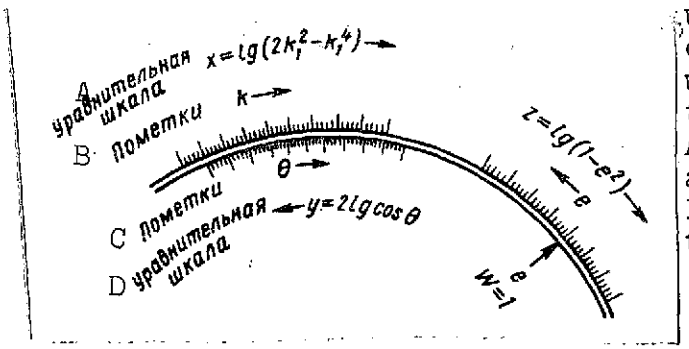

Fig. 51. Scheme of disc nomogram (variant)

Key: A. Equation scale
B. k values
C. θ values
D. Equation scale

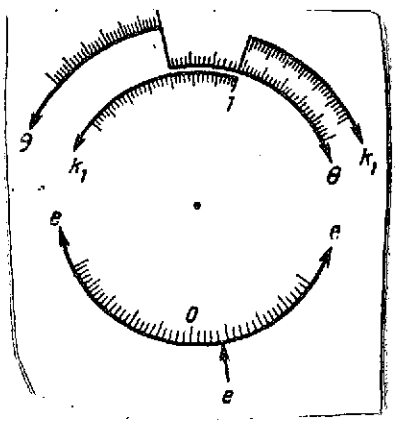

Fig. 52. Scheme of disc nomogram (variant)

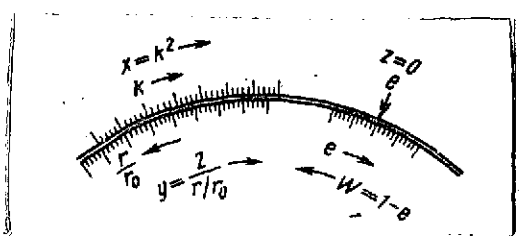

Fig. 53. Scheme of disc nomogram (variant)

coordinate system "O" with the initial point on the scale. We will take as the starting point of the v scale the point at which it intersects the X axis -- the point "C'." Then if the points $A(0;y_1)$, $B(x_3;y_3)$ and $C(l;y_2)$ are the points lying on the same line, from the congruence of the triangles it follows that /79

$$\frac{y_3-y_1}{y_2-y_1}=\frac{x_3}{l}, \tag{4.69}$$

or

$$(l-x_3)y_1+x_3y_2-ly_3=0. \tag{4.70}$$

The equations of the u and v scales are of the form

$$\left.\begin{aligned} y_1&=n_1f_1(u);\\ y_2&=n_2f_2(v), \end{aligned}\right\} \tag{4.71}$$

where n_1 and n_2 are the scale coefficients, or the scale moduli. By transforming Eqs. (4.71) and (4.70) we get

$$n_1(l-x_3)f_1(u)+n_2x_3f_2(v)-ly_3=0. \tag{4.72}$$

The quantities $(l - x_3)$; n_2x_3 and ly_3 depend only on the variable w, therefore

$$\left.\begin{aligned} n_1(l-x_3)&=f_3(w);\\ n_2x_3&=\varphi_3(w);\\ -ly_3&=\psi_3(w). \end{aligned}\right\} \tag{4.73}$$

By substituting the functions (4.73) into (4.72) we get the form of the equation being subjected to nomography:

$$f_1(u)f_3(w)+f_2(v)\varphi_3(w)+\psi_3(w)=0. \tag{4.74}$$

ORIGINAL PAGE IS
OF POOR QUALITY

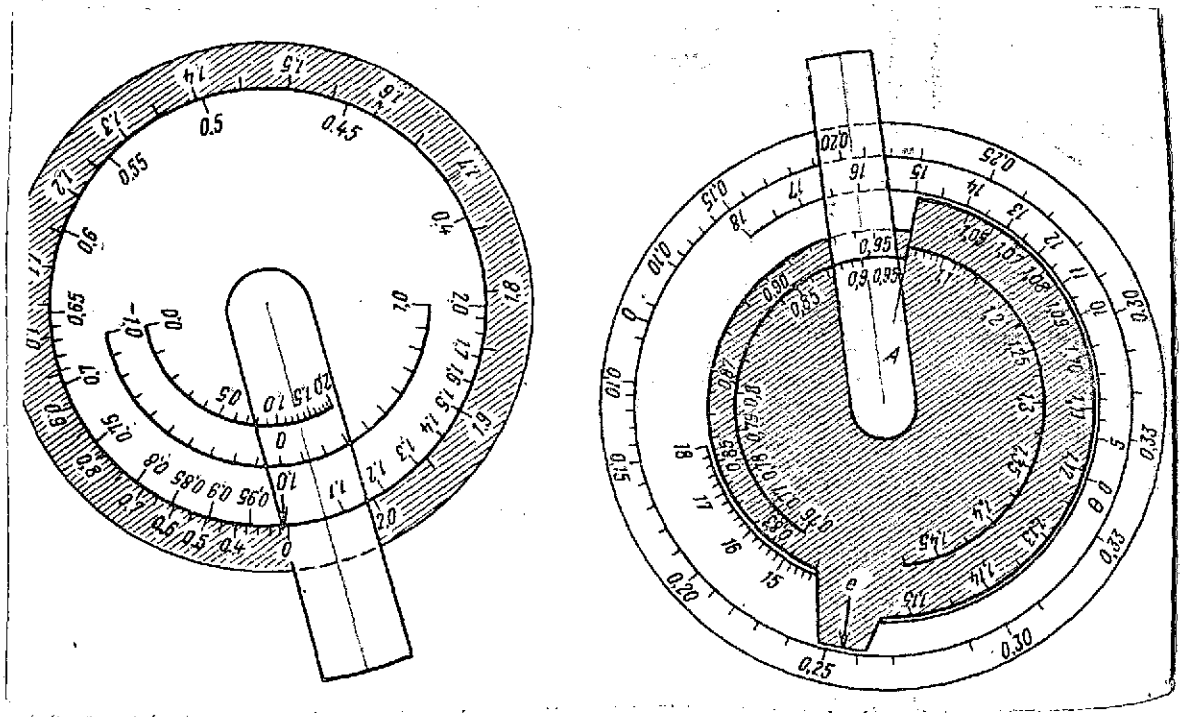

Fig. 54. Disc nomograms

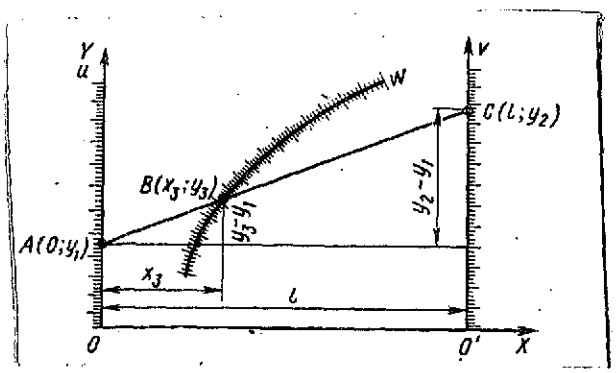

Fig. 55. Scheme of nomogram for the variables u, v, and w.

By dividing the first equation of the function (4.73) by the second, and the second by the third, we get these two equations: /80

$$\frac{n_1(l-x_3)}{\varphi_3}=\frac{n_2x_3}{\varphi_3};\quad \frac{n_2x_3}{\varphi_3}=\frac{ly_3}{\psi_3}.$$

Now by solving them for x_3 and y_3, we find

$$x_3=\frac{ln_1\varphi_3}{n_1\varphi_3(w)+n_2f_3(w)};$$

$$y_3=\frac{n_1n_2\psi_3(w)}{n_1\varphi_3(w)+n_2f_3(w)} \qquad (4.75)$$

ORIGINAL PAGE IS
OF POOR QUALITY

These functions are the equations of the w scale. By comparing Eq. (4.74) with Kepler's equation

$$M = E - e \sin E,$$

where M = 2πt/T is the mean anomaly (the angle described for uniform motion along the circle during the time of motion from pericenter t during the same period of revolution T)

E is the eccentric anomaly, and

e is eccentricity

and by representing it in the form

$$M + e \sin E - E = 0, \tag{4.76}$$

we get

$$f_1(u) = M;\ f_2(v) = e;\ f_3(w) = 1;\ \varphi_3(w) = \sin E;\ \psi_3(w) = -E. \tag{4.77}$$

When $n_1 = n_2 = n$, the scale equations for variable E become

$$x_3 = \frac{l \sin E}{\sin E + 1};\quad y_3 = \frac{nE}{\sin E + 1}. \tag{4.78}$$

The nomogram shown in Fig. 56 is constructed on the basis of these equations. In Fig. 57 the same nomogram is reduced to a symmetric form[1].

4.11. Network nomograms

Using the above-described methods, graphs can be constructed with a large information content or restricted to specific regions in space -- network nomograms. Fig. 58 shows an example of this kind of nomogram intended for the calculation and analysis of spacecraft motion in near-lunar orbits. For practical purposes, nomograms of two types are expedient:

a) synoptic nomograms of small scale, but with large limits of change in variables; and

b) nomograms for relatively exact calculations with restricted/82 limits of variation in variables.

[1] The transformation of this nomogram to the symmetric form was proposed and carried out by engineer G. S. Zolotarenko.

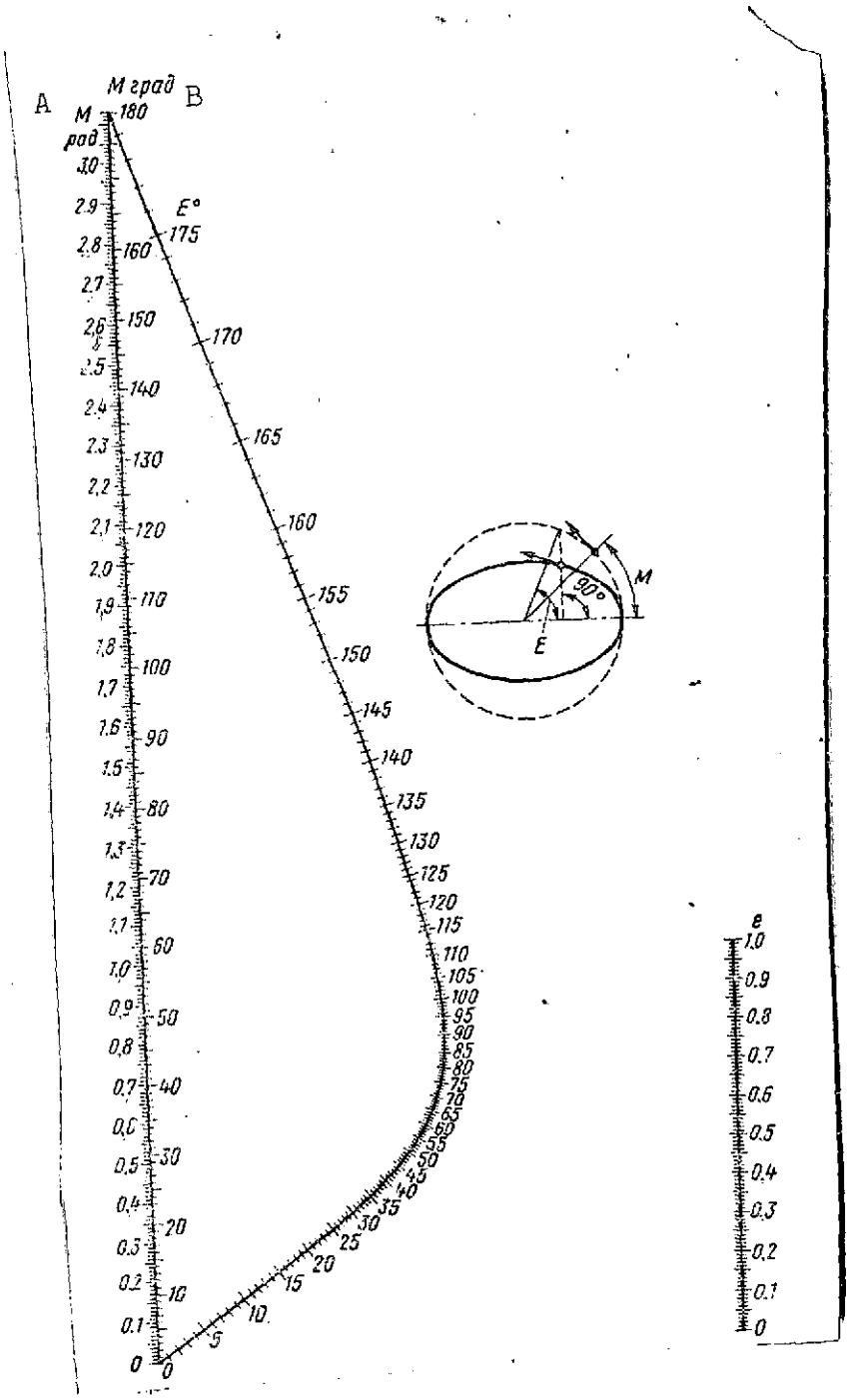

Fig. 56. Nomogram of Kepler's equation

Key: A. M, rad
B. M, deg

ORIGINAL PAGE IS
OF POOR QUALITY

The graphical construction of orbits and isochrones is conveniently carried out in the coordinate grid of two distances r_1 and r_2, respectively, from two foci F_1 and F_2. In this coordinate system the equations of the conic sections take on this form:

$$\left.\begin{array}{ll} \text{for ellipses} & r_1+r_2=2a; \\ \text{for hyperbolas} & r_1-r_2=2a. \end{array}\right\} \qquad (4.79)$$

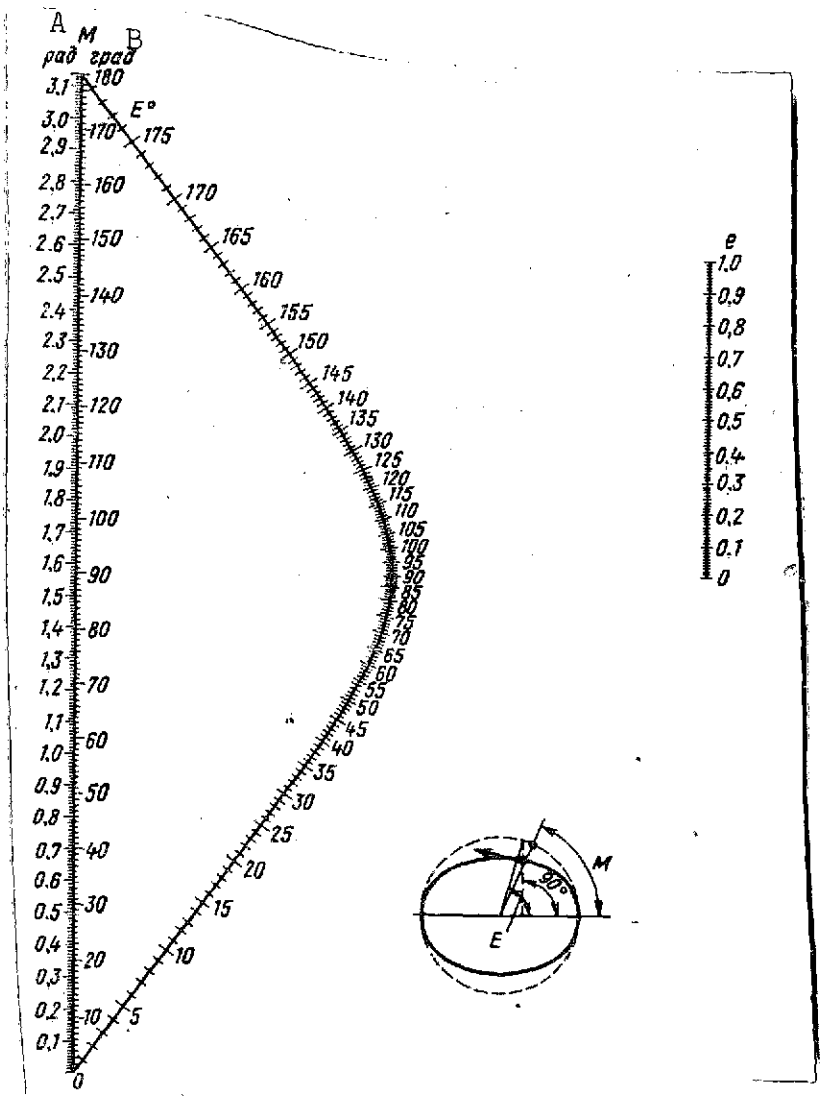

ORIGINAL PAGE IS
OF POOR QUALITY

Fig. 57. Symmetric nomogram of Kepler's equation

Key: A. Rad
B. Deg

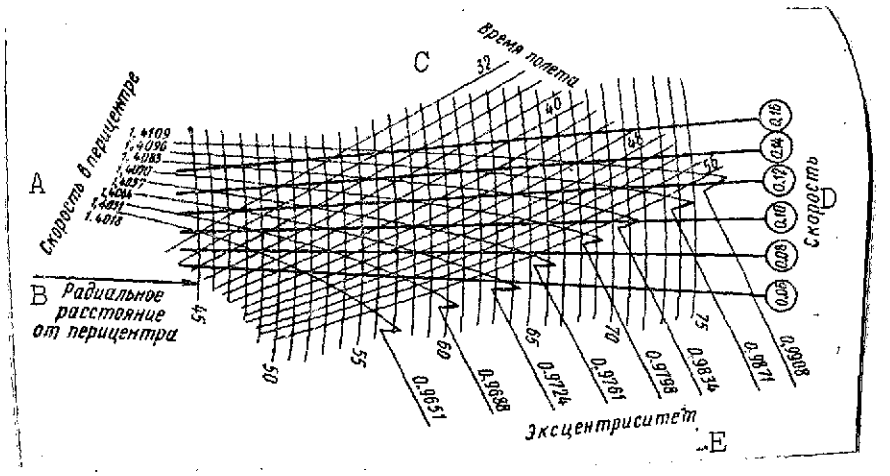

Fig. 58. Network nomogram of near-lunar orbits

Key: A. Velocity at pericenter
B. Radial distance from pericenter
C. Time of flight
D. Velocity
E. Excentricity

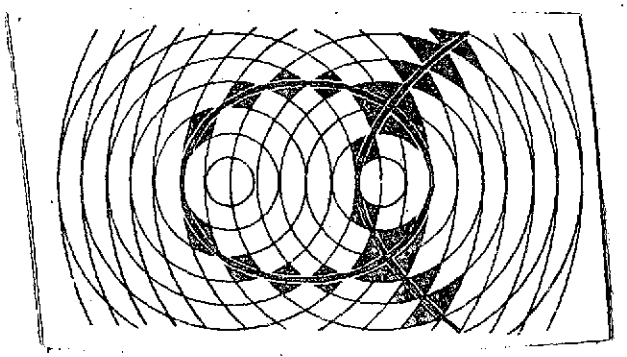

Fig. 59. Construction of elliptical and hyperbolic orbits

To determine the scale, the following formula is used. It expresses the difference between the foci 2C as a function of e: /83

$$\frac{2C}{r_0}=2\frac{e}{1-e}. \qquad (4.80)$$

Fig. 59 gives an example of the construction of elliptical and hyperbolic orbits. For parabolic trajectories, the family of circles with center at the infinitely distant point faces the family of parallel lines, as shown in Fig. 60.

The isochrones for determining the flight time when problems in orbital mechanics are solved graphically can be constructed by a method similar to the method of determining the position in navigation by means of position lines. Actually, for assigned

ORIGINAL PAGE IS
OF POOR QUALITY

orbital parameters, finding in the orbit the point corresponding /84 to the given time geometrically reduces to searching for the point at which the orbit is intersected by another position line, since the orbit of the spacecraft itself is one of the two position lines. Here it should be noted that in astronomy the segments of the circle of equal elevations of a celestial body above the horizon are called the position lines. The second position line can be any of the two coordinate functions expressed in terms of t with constant given value of the latter.

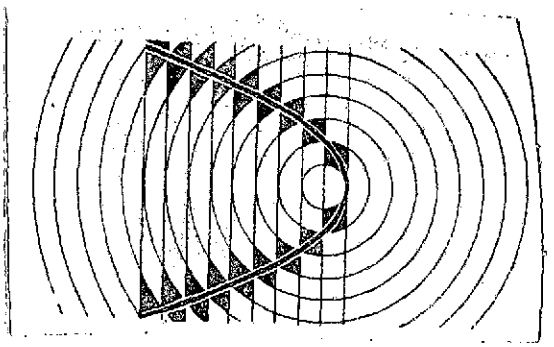

Fig. 60. Construction of parabolic orbit

The geometrical difference berween the elliptical and hyperbolic orbits requires that we use also different methods of constructing the second position line. For example, it is convenient in the case of elliptical orbits to use the value of the true anomaly or the eccentric anomaly defined by Kepler's equation, while for hyperbolic orbits -- the radius-vector, obtaining it by means of Lambert's theorem. For hyperbolic orbits, it is inexpedient to construct the second position line using the angular coordinates, since this leads to acute angles at the points of intersection of the position lines.

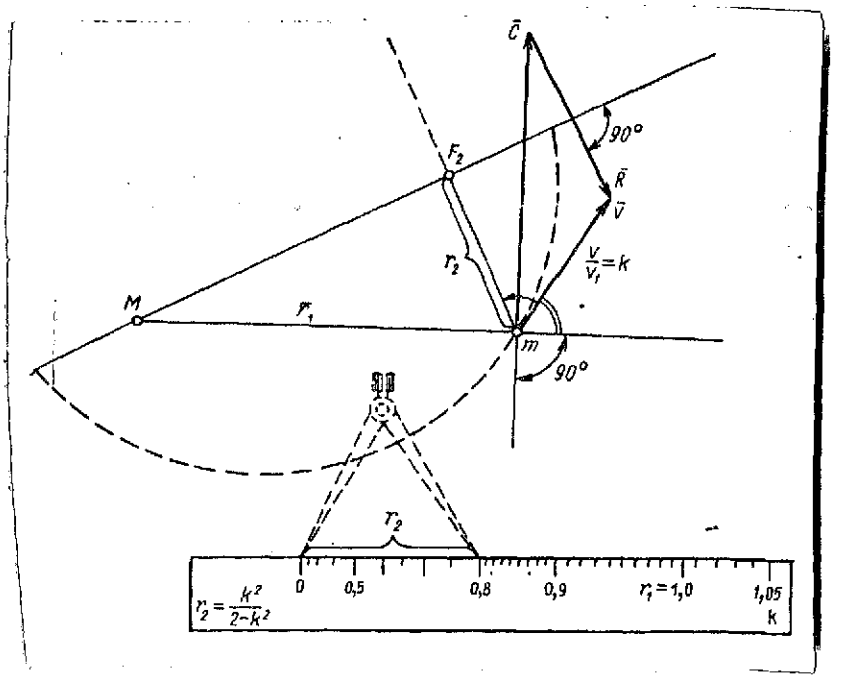

Fig. 61. Constructing orbits and velocity vectors using compass and rule

K=0,79; ϑ = 31,5°

Concluding our examination of the methods of constructing orbits and determining orbital velocities at any points, we present a graphical method that makes use of the second focus of the conic section. This focus is remarkable in that it permits finding the direction of the velocity vector at any orbital point since the bisector of the angle formed by the position vectors are $\bar{r}_1$ and $\bar{r}_2$ is the tangent to the curve of the conic section at the given point. By representing the orbital equation as the function (4.79) and by solving it together with the semimajor axis (see function (4.21)), we get a simple formula for the determination of r_2:

$$r_2 = \frac{r_1 k^2}{2 - k^2}. \qquad (4.81)$$

Constructing the orbit on an assigned velocity vector and its position relative to the center of attraction M is shown in Fig. 61. By constructing the angle between the velocity vector $\bar{v}$ and position vector $\bar{r}_1$ we get a ray in which we must find the second focus F_2 at some point. Further, let us lay out in the direction of the ray a segment with magnitude r_2 from the point m and let us find F_2 at its endpoint. Let us draw from the end of vector $\bar{v}$ normal to the semimajor axis of the orbit -- the segment MF_2, and from the point m -- a normal to the vector $\bar{r}_1$ until they intersect. The point of intersection will define the end of the vector $\bar{C}$ and the head of the vector $\bar{r}$. These invariant vectors enable us at any point of an orbit to construct the orbital velocity vector. /85

CHAPTER 5

/86

SPACE NAVIGATION

Symbols

a	semi-major axis of orbit
a^*	semi-major axis of lunar orbit
b	semi-minor axis of orbit
f	gravitational constant
c	distance from orbit to orbital center
h_{min}	minimum altitude of spacecraft flight above surface of Moon on the condition that flight safety is provided
e	orbital eccentricity
h	instantaneous flight altitude of spacecraft above lunar surface
i_1, i_2	inclinations of first and second orbits, respectively, to the ecliptic i
i_t	inclination of transit orbit to ecliptic
i	inclination of orbit of target planet
k, k_{01}, k_t	velocity coefficients

$$k=\frac{v}{v_{01}};\quad k_0=\frac{v_0}{v_{01}};\quad k_t=\frac{v_t}{v_{01}}.$$

$k_1 = \frac{v_{II}}{v_I}$	coefficient of the orbital escape velocity -- the ratio of the velocity at which the spacecraft enters the planet's sphere of action to the magnitude of the first escape velocity at the boundary of this sphere of action
$k_{1\mathbb{C}}=\frac{v_{\mathbb{C}}}{v_1}$	coefficient of the orbital escape velocity for the Moon
$M_{\mathbb{C}}$	mass of the Moon
M	mass of the principal central celestial body
m	mean solar time
$m_\odot$	true solar time
R	mean radius of the orbit, equal to the semi-major axis of the ellipse (R = a) /87
R_A	mean radius of the orbit of the departure planet
R_B	mean radius of the orbit of the target planet
R_t	mean radius of the transit orbit
$\bar{R}_\varphi$	mean Sun-Venus distance
$\bar{R}_\sigma$	mean Sun-Mars distance
$\bar{r}$	instantaneous radius-vector of the transit orbit

$\bar{r}_0$	initial radius-vector of the transit orbit at the launch point, equal to the radius-vector of the orbit of the departure planet at the instant of launch
$\bar{r}_A$	radius-vector of the orbit of the departure planet
$\bar{r}_t$	radius-vector of the perihelion of the transit orbit
$\bar{r}_\alpha$	radius-vector of the aphelion of the transit orbit
$\bar{r}_B$	radius-vector of the orbit of the point of encounter, equal to the radius-vector of the orbit of the target planet at the moment of encounter
$r_{(\alpha)} = \frac{r_\alpha}{r_0}$	relative magnitude of the radius-vector of the aphelion of the transit orbit
$r_{\mathbb{C}}\|_{av}$	mean radius of the Moon $\approx$ 1740 km
$r_{\mathbb{C}}=h+r_{\mathbb{C}}\|_{av}$	radial distance of spacecraft relative to lunar center
s	sidereal time
T_0	period of revolution in a circular orbit with radius r_0
T_1, T_2	periods of revolution in an orbit relative to the departure planet and the target planet
T_t	period of revolution in the transit orbit
$T^*_t = \frac{T_t}{T_0}$	generalized parameter of the period of revolution
t	instantaneous time of flight
$t^* = \frac{t}{T_0}$	generalized parameter of instantaneous time
t_t	transit time
v	instantaneous velocity in the transit orbit
v_1	first escape velocity at the boundary of the sphere of action
v_0	initial velocity in the transit orbit
v_{01}	first circular escape velocity at the boundary of the sphere of action
$v_{d.p.}$	velocity of the departure planet at the instant of launch
$v_{t.p}$	velocity of the target planet at the instant of encounter
$v_{(1)}$, $v_{(2)}$	spacecraft velocities at the transfer point before and after the impulse Δv has been applied, respectively
$\bar{v}_I$	vector of the heliocentric spacecraft velocity
$\bar{v}_{III}$, $\bar{v}_{II}$	heliocentric velocity vector when the spacecraft is leaving the planetary sphere of action, and when the spacecraft is entering the planetary sphere of action, respectively /88

v_h, v_v	horizontal and vertical velocity components of the spacecraft relative to the Earth
$v_{\mathbb{C}}$	total spacecraft velocity relative to the Moon
v_∞	orbital hyperbolic velocity of the spacecraft
$v_{\oplus()}$	orbital velocity of the Earth (for flight from Earth $v_\oplus = v_{d.p}$)
Δv	magnitude of the velocity impulse of the spacecraft -- the energy characteristic of the transit orbit; $\overline{v} = \overline{v}_0 - \overline{v}_{d.p}$
$\Delta\overline{v}$	vector of the spacecraft velocity impulse
Δv_{min}	optimal velocity impulse of the spacecraft
α	displacement angle of the transit-orbit aphelion relative to the initial radius
β	angle swept out by the target planet in the transit time
γ	angle of rotation of the planetocentric velocity
β_d, β_a	angular distance of the arrival point from the descending node and from the ascending node of the target planet orbit, respectively
$\vartheta_{1,2}$	angle of inclination of velocity vector $\overline{v}$ to the Ox axis of the launch coordinate system, or the so-called trajectory angle
ϑ_{opt}	optimal trajectory angle
$(\vartheta_1, \vartheta_2)$	true anomaly
λ	heliocentric longitude -- the longitude which is measured from the direction toward the point of vernal equinox to the direction at the given point measured counterclockwise if one is looking from the side of the North Pole
λ_A, λ_B	heliocentric longitudes of the departure planet and the target planet, respectively
λ_ℓ	necessary heliocentric longitude of the target planet on the launch date
$\lambda_{t.p.}$	heliocentric longitude of the target planet
$\Delta\lambda$	difference between the heliocentric longitudes of the departure planet and the target planet on the launch date
$\Delta\lambda_0$	necessary initial difference between the heliocentric longitudes to ensure spacecraft encounter with the planet
$\Delta\lambda_{inn}$, $\Delta\lambda_{out}$	difference between the heliocentric longitudes, respectively, for transit flight to the innermost planets and the outermost planets /89
$\lambda_\oplus$	heliocentric longitude of the Earth
$\Delta\lambda_{\oplus-\varphi}$	difference between the heliocentric longitudes of the Earth and Venus

$\Delta\lambda_{\oplus\to\sigma'}$	difference between the heliocentric longitudes of the Earth and Mars
$\Delta\lambda_{act}$	difference in the heliocentric longitudes from astronomical almanac data for the corresponding year; $act = {}_{\oplus} - t.p$
ϕ_B	heliocentric latitude of the encounter point
ψ	angular range of the spacecraft flight
Ω_1, Ω_2	longitudes of the ascending nodes of the orbits
ω_1, ω_2	angular distances of the orbital pericenter from the ascending node
Υ	point of vernal equinox -- the point at which the celestial equator intersects the ecliptic, where the Sun passes from the southern hemisphere to the northern.

5.1. Universal computational tool

In the previous chapters we outlined methods of solving problems in space orientation using a stereographic projection and methods of determining orbital flight parameters employing velocity nomograms and hodographs. The solution of practical problems in space navigation leading to a combination of various analytical-graphical methods opened up an approach to building a universal computational tool in which calculation rationalization is combined with graphical clarity of the calculations. The function of the universal computational tool is to perform analytical-graphical calculations both in spherical astronomy and in celestial mechanics. This device developed with reference to procedures in analytical-graphical calculations in space navigation made it possible to perform a single computational complex, which will be discussed below.

The universal computational tool consists of a base and several assembly elements, whose set permits solving a series of problems associated with spherical coordinates. They include numerous problems of orientation, determination of visibility conditions, determination of the conditions and selection of methods of navigation, determining initial angles and times of spacecraft launch, determining characteristics of optimal transit orbits and so on. The elements comprising the computation tool represent a modification of transparent nomograms, with the only difference that additional constructions are required to perform calculations /90 by means of these nomograms. Owing to the limited space in this book, the description of the procedures in using the universal computational tool is illustrated only by individual model problems.

ORIGINAL PAGE IS
OF POOR QUALITY

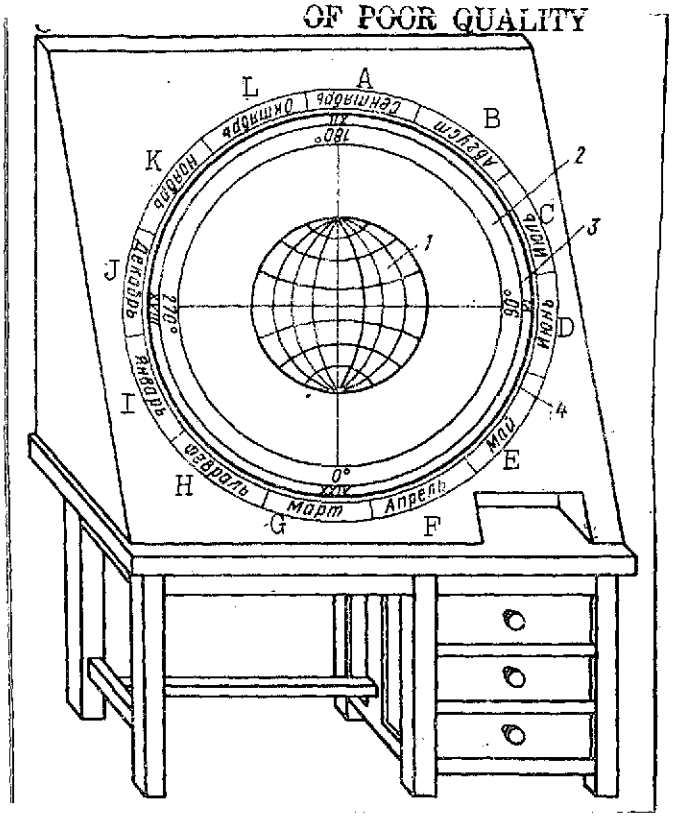

Fig. 62. General view of base of computational device: 1. stereographic grid; 2. degree scale; 3. scale of right ascensions and hour angles; 4. date scale.

Key: A. September; B. August; C. July, D. June; E. May; F. April; G. March; H. February; I. January; J. December; K. November; L. October

The base of the device (Fig. 62) is a fixed plane on which the following elements are constructed, oriented relative to the common center: Wulf's grid (shown in the center); degree scale; scale of time of day (Figs. 63 and 64); date scale; and scale of day number from 0 to 365.

In order to read off the heliocentric longitudes, right ascensions, and hour angles using the computational tool, all the scales except for the last are oriented relative to their direction toward the vernal equinox point. Thus, the central meridian (axis of Wulf's grid) in the device intersects the date scale at the mark 22 March, and the day number scale -- at /91 the mark 81, which will correspond to the values equal to zero on the remaining scales. The date scale corresponds to the right ascensions of the mean equatorial Sun, and, therefore, when it is used Wulf's stereographic grid is a heliocentric coordinate system with its pole at the grid center, and its principal meridian maps the celestial equator.

The individual assembly elements can be secured with fasteners in the center of the device's base. Thus, it becomes possible to mutually rotate the elements one relative to the other and to rotate them about a common center. The element set includes the following:

-- transparent radial rule with scale of "grid equator /92 angles," which corresponds to the latitude scale in the polar stereographic projection (see Fig. 62);

-- map of stellar sky (see Fig. 64) with ecliptic superimposed on it in the polar stereographic projection. This element is

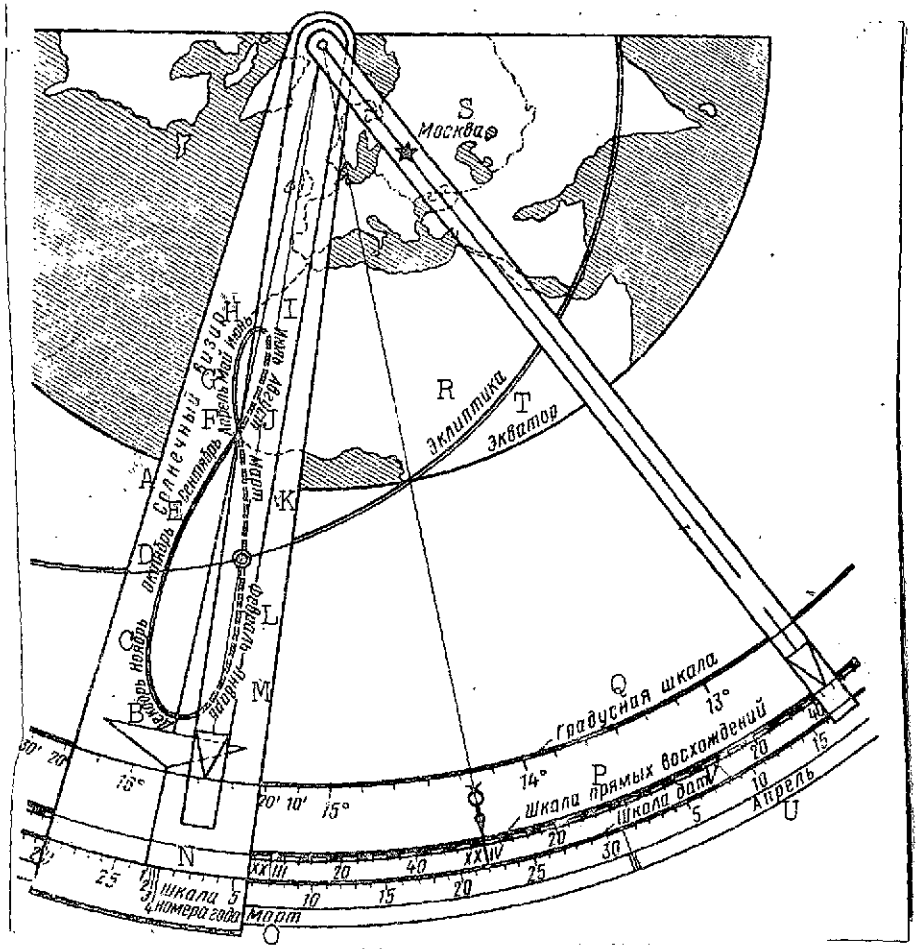

Fig. 63. Solar cursor.

Key: A. Solar cursor; B. December; C. November; D. October; E. September; F. April; G. May; H. June; I. July; J. August; K. March; L. February; M. January; N. Scale of year number; O. March; P. Scale of right ascensions; Q. Degree scale; R. Ecliptic; S. Moscow; T. Equator; U. April; V. Date scale

fixed to the base of the device in the position determined by the direction toward the point of vernal equinox;

-- map of terrestrial hemisphere (Fig. 65) in the polar stereographic projection with a circle of hour angles;

-- solar cursor (see Fig. 63) -- a transparent sector with the curve of the equation of time noting on the ecliptic the position of the true Sun, and with a year positioning scale. The year positioning scale is necessary to allow for fluctuations in

in 4 year

ORIGINAL PAGE IS
OF POOR QUALITY

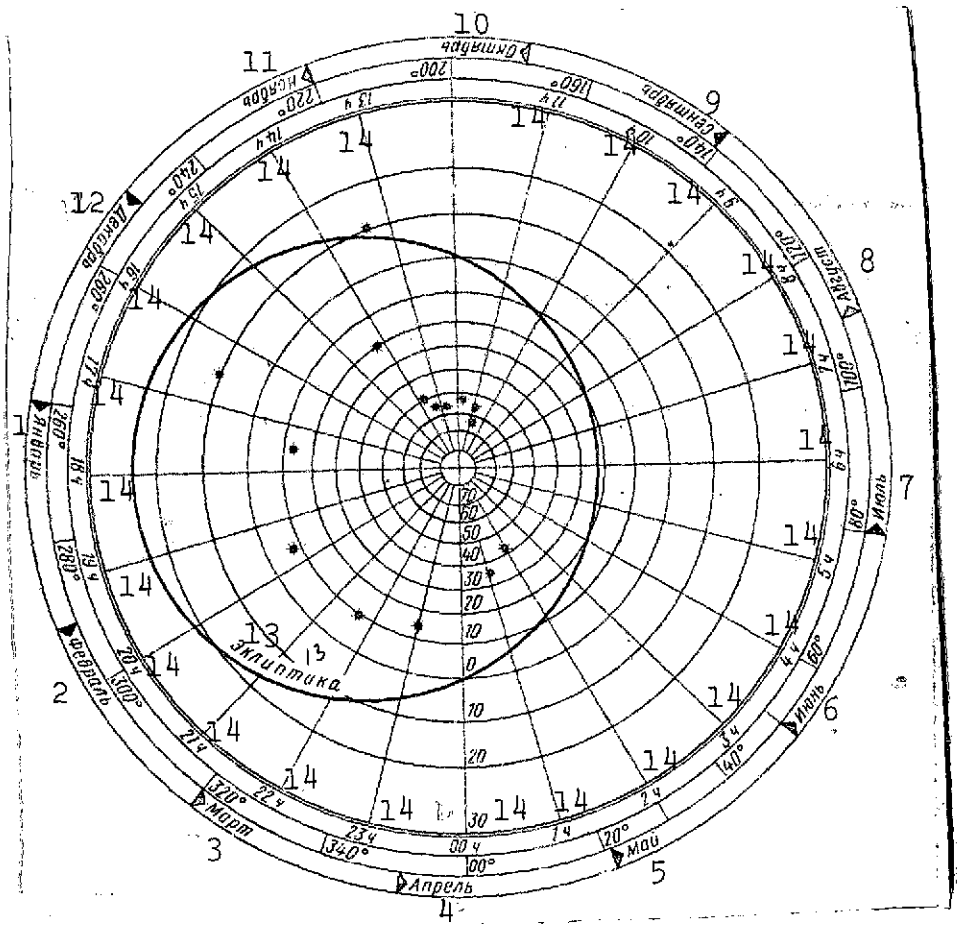

Fig. 64. Map of stellar sky.

Key: 1. January; 2. February; 3. March; 4. April; 5. May; 6. June; 7. July; 8. August; 9. September; 10. October; 11. November; 12. December; 13. Ecliptic; 14. hours

the date scale values relative to the vernal equinox, whose period is 4 years. The cursor includes a mean solar time indicator; /93

-- transparent cursors with a single line extending through the pole. They bear indicators for reading off the true solar time and the sidereal time;

-- "orbital grid" on a transparent disk (Fig. 66) -- the grid of transit orbits with isochrones for a common aphelion and with different energy levels. The "orbital grid" must always be placed over the plan of the mutual disk position of the spacecraft in the departure planet orbits on the launch day and on the target planet orbits on the arrival day;

ORIGINAL PAGE IS
OF POOR QUALITY

Fig. 65. Map of northern hemisphere of the Earth in the polar stereographic projection and hour angle scale for Moscow time.

-- circular or spiral scales of heliocentric longitudes of different planets (Fig. 67 shows the scale for Mars). Each scale is an element of a movable "heliocentric longitude nomogram," since the planetary positions are determined by their heliocentric longitudes. /94

The number of individual elements of the universal computational tool can grow without limit with further development in the use of analytical-graphical methods of space navigation. Moreover, among replaceable elements are the clear circular disks made of transparent material used for corresponding projections in the course of solving a particular problem. Now let us turn to a more detailed examination of the designs of elements and their functions.

A radial scale rule in conjunction with the stereographic grid (Fig. 68) already constitutes a movable nomogram combining the equatorial and the polar projections of spherical coordinates, since the "grid equator" scale for the polar projection is a scale

ORIGINAL PAGE IS
OF POOR QUALITY

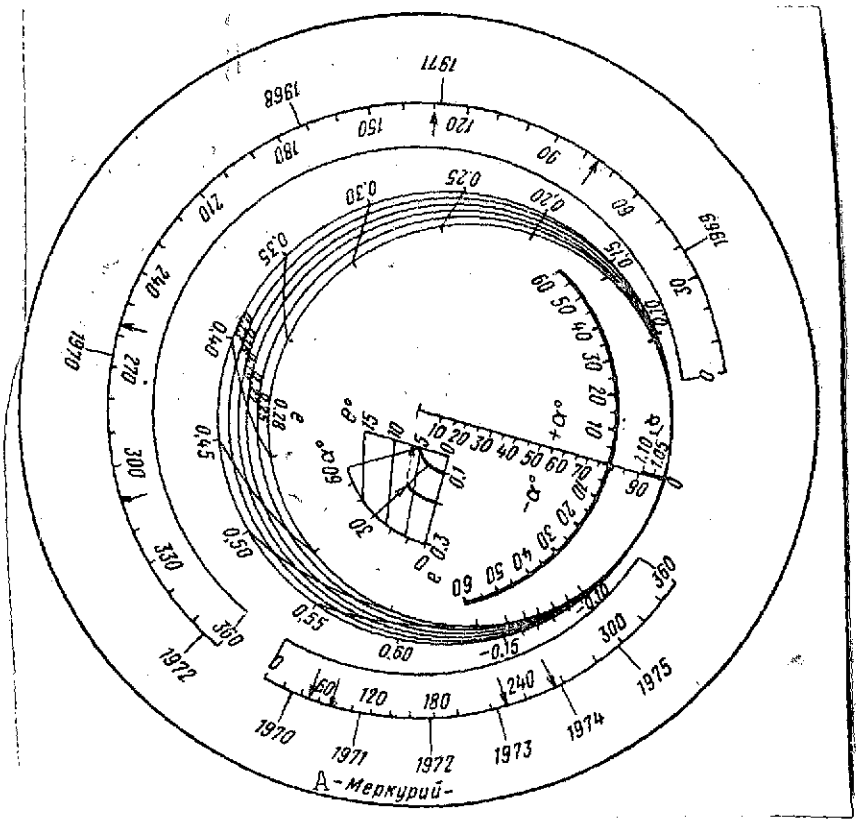

Fig. 66. Orbital grid and nomogram of heliocentric longitudes.

Key: A. Mercury

of latitudes. As an example of the use of this nomogram, let us look at the determination of i_t [t = transit] from given values of ψ and ϕ_B. By inspecting the heliocentric sphere, we will assume /95 the principal meridian of the grid to be the projection of the Earth's orbit. The Earth occupies a position at the point A at the launch instant, the planet position at the instant of encounter with the spacecraft will be determined by point B, which can be found by rotating the radial scale rule from the "grid equator" by the angle at which the mark ϕ_B belonging to the scale of the "grid equator" angles will intersect the corresponding value ψ of the grid "parallel." The meridian of the grid AB extending through point B will be the orbital projection, and its inclination to the ecliptic i_t will be determined by the meridian of point B, whose value can be read off from the "grid equator" scale.

It is not without interest to trace in Fig. 69 how i_t -- the inclination of the transit orbit, gradually approaching 90° -- increases with increase in the angular flight range to 180°, even for the smallest inclination of the target planet orbit. For a /96

ORIGINAL PAGE IS
OF POOR QUALITY

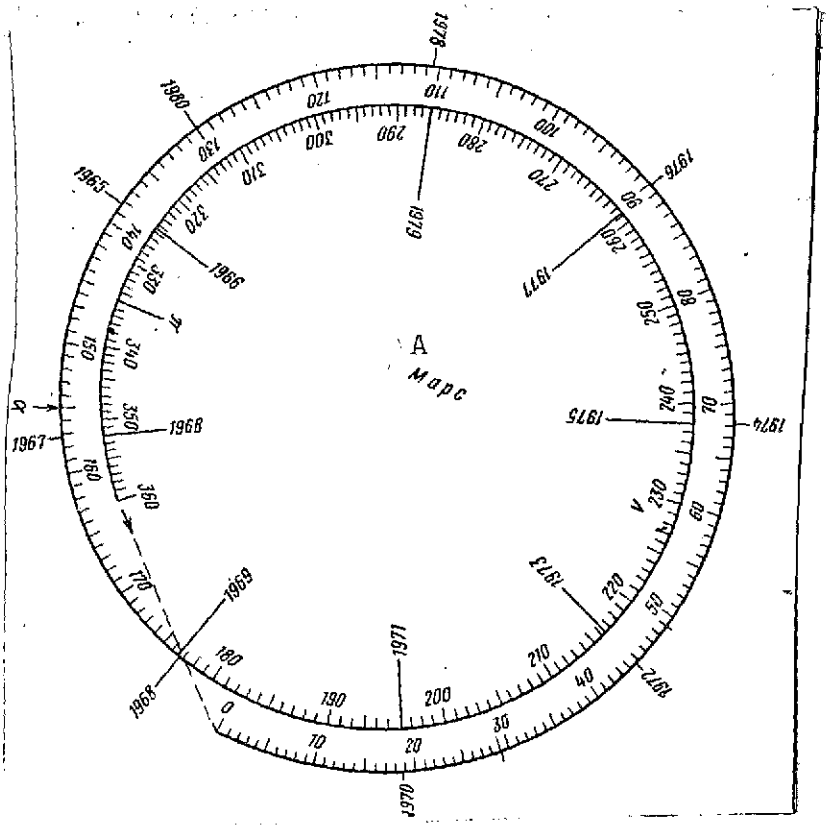

Fig. 67. Scale of heliocentric longitudes for Mars (the year marker corresponds to 0 January).

Key: A. Mars

more exact determination of it, in Fig. 69 is given a nomogram mapping the function

$$\sin i_t = \frac{\sin \phi_B}{\sin \psi} . \qquad (5.1)$$

The map of the stellar sky (see Fig. 64) in the polar stereographic projection with the ecliptic superimposed on it maps the so-called sphere of fixed stars. This element is made of a transparent material, although generally it will be secured in its working position on the axis beneath the base of the device. But it may be necessary in these calculation instances for performing constructions on the map of the stellar sky and then it is placed on the base axis above Wulf's grid. But if Wulf's grid interferes with the calculation, it can be blocked off with a clear white disk. In this case, the marker of the direction toward the vernal equinox is used for the correct orientation of the stellar map.

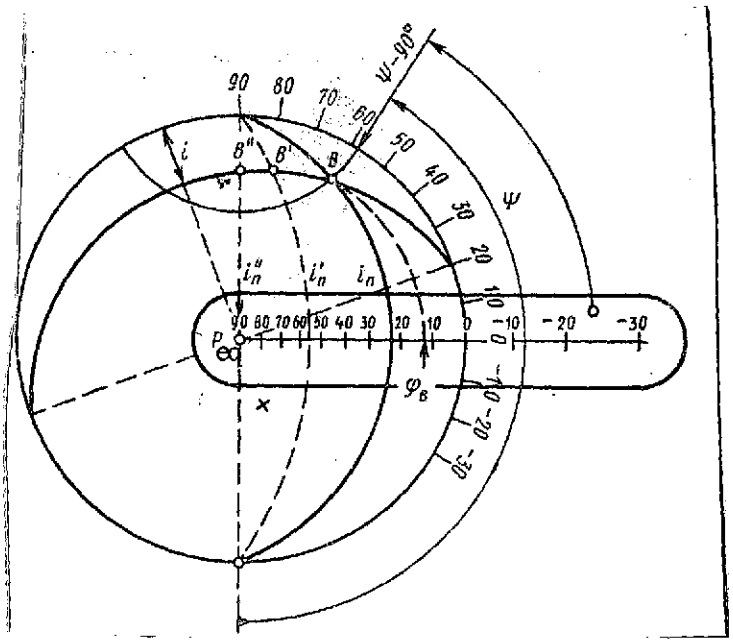

Fig. 68. Determination of inclination of transit orbit.

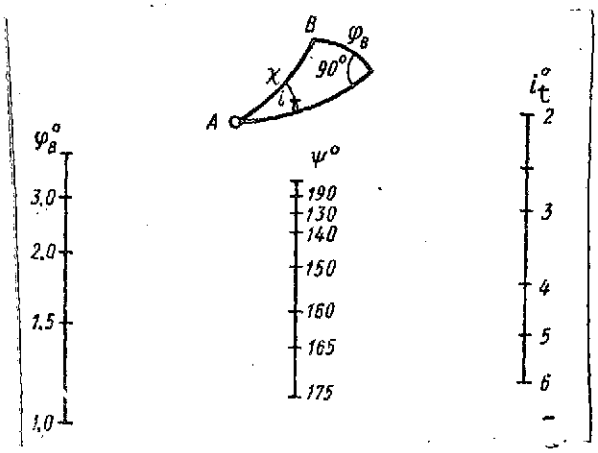

Fig. 69. Nomogram of angle of inclination of transit orbit.

The sphere of fixed stars is a system of geocentric fixed equatorial spherical coordinates associated with inertial space. For the purposes of stellar astronavigation, on the stellar map we can construct a network of circles of equal zenith distances from each navigation star. However, there is no particular need for this since in each specific instance the circles of equal zenith distances can be readily constructed by a method described above (see Section 3.2). /97

The scale of hour angles in the map of the terrestrial hemisphere is constructed for Moscow time, since it is oriented by Moscow time at the mean Moscow noonday -- 12 hours 30 min in the Moscow meridian. One can easily construct on this map for any point a network of azimuths and zenith distances as a horizontal (oblique) stereographic projection using the method described in Section 3.2.

The year scale of the solar cursor allowing for fluctuations in the values on the date scale relative to the point of vernal equinox thus serves to increase the accuracy with which the mean solar time is read and the accuracy of obtaining the date 29 February in a leap year. The year scale divisions are set at the given date thusly: for a leap year with 29 February inclusively, the scale is set at division 1, and up to 29 February -- at division 4; for the remaining years the scale is positioned according to the ordinal number of the year, reckoning from the first leap year. The maximum error in determining the time with this scale is ±30 sec, while an ordinary fixed scale gives an error of 4 min.

Hence this device will always ensure the guaranteed minute error in time determination. The accuracy can be increased by replacing the discrete year scale with which it is convenient to interpolate. However, this is inexpedient since the constant curve of the equation of time introduced into the device produces an unavoidable /98 instrumental error of ±10 sec.

Clear cursors with a single line are used in reading off the true solar and sidereal times. The mark $m_\odot$, when the sighting line is placed at the true Sun -- the point of intersection of the ecliptic with the curve of the equation of time -- indicates the true solar time, while the mark s, when the sighting line is placed at the local meridian, shows the sidereal time.

The plan of the mutual disposition of the spacecraft in the orbits of the departure planet at the launch date and the target planet at the arrival date determine the orbital projections onto the plane of the ecliptic. And since the plan and the "orbital grid" are made on different sheets, their scales must correspond to each other. The "orbital grid" consists of a family of elliptical orbits with a common aphelion. The value of its eccentricity is indicated for each orbit. The isochrone lines intersecting the orbits have their relative time of flight from the aphelion, whose value is indicated for each isochrone. And the time of the total revolution in the circular orbit emanating from the initial point is taken as the unit of this time. On the same element of the computational tool are two additional scales: one serves for reading off α, and the other -- for determining the scale of r_0.

The sliding heliocentric longitude nomogram for different planets is made up of two scales: a fixed date scale, which belongs to the device base, and a circular or spiral heliocentric longitude scale placed over it. The longitude scale has marks for scale orientation at 0 January of each year. The scale of heliocentric longitudes, owing to the influence of the orbital eccentricity, is nonuniform, but periodic and can be constructed from available data in any astronomical almanac without calculation based on Kepler's equation. To determine the heliocentric longitude of a planet on any day of the year the longitude scale must be placed with the corresponding year opposite 0 January of the date scale and the reading made opposite the given date. Here, it should be remembered that if on the date scale section from 0 January to the given date there is a discontinuity in the scale from 360 to 0°, it must be advanced by this interval, that is, the 0° must be placed opposite the 360°.

Below we present several examples of the use of the universal computational device. The scheme of the corresponding assembly of elements in shown in Fig. 63, illustrating the procedures in solution when converting time from one system to another and when determining the position of the Sun in the celestial sphere. Here

there are three device elements rotating relative to each other:

-- the map of the terrestrial hemisphere combined with the hour angle circle so that the local meridian passes through the local time at mean solar noonday ($m^h = 12^h\ 30^m$ for Moscow time); /99

-- the solar cursor with the curve of the equation of time and the year scale; and

-- the circle of right ascensions with the date scale and with the ecliptic (the stellar sky map can be used).

The following steps in solving this problem are recommended. By rotation of the solar cursor we bring the mark of the corresponding year number beneath the given date. By rotating the map of the terrestrial hemisphere to the value of the given sidereal time, we get the Sun's position in the celestial sphere and the desired mean time opposite the arrow bearing the m. The solar position is determined by the point at which the curve of the equation of time intersects the ecliptic. The set of universal computational device elements examined in this example well illustrates the astronomical determination of time reckoning systems.

Let us trace the functioning of the device with the example of determining sidereal time and true solar time for Moscow on 27 February 1969, at 15^h50^m Moscow time:

1. Let us rotate the hour circle relative to the terrestrial hemisphere map until the value 12^h30^m is opposite the Moscow meridian, that is, let us set Moscow time at mean noonday.

2. Let us position the solar cursor with marker 2 (the year positioning scale) opposite the date 27 February and, by rotating the map of the terrestrial hemisphere together with the hour circle, let us place the axial line of the solar cursor opposite the value of the given Moscow time 15^h50^m.

3. By aligning the cursor with one line with the Moscow meridian, we get opposite the arrow bearing s the sidereal time 1^h45^m, and by passing the cursor with one line across the position of the true Sun -- the intersection of the ecliptic with the curve of the equation of time, we can read off the true solar time on the hour circle.

5.2. Transfer to other orbits

As our first model problem, let us examine the transfer of a spacecraft from one orbit to another in a central gravity field. Fig. 70 shows the flow chart for solving this problem. Its entire

algorithm is divided into three interrelated stages. In the flow chart the input and output parameters are determined for the case when two orbits are specified as the initial data with their positions given in space, by the position of the pericenter of the first orbit, by the eccentricity of the second orbit, and by the radius-vector at the transfer point, and Δv and its direction in the inertial (sidereal) coordinate system is the unknown.

The operations proceed as follows. From the quantities i_1, i_2, Ω_1, and Ω_2 the orbital projections are constructed onto the celestial sphere and the position of the projection of the transfer point N* is found as the result of their intersection (see construction I). From ω_1 in this same construction one finds $|\theta_1|$ of the transfer point. From the r values for the transfer point N, $|\theta_1|$, and e_2, using the polar diagram (see construction II), one determines θ_2, θ_1, $\theta(2)$, $v(2)$, and $v(1)$ at the transfer point N (corresponding to the application of [velocity impulse] Δv after and before the transfer point). The position of the pericenter projection π^*_2 is found from the value of $|\theta_2|$ (in construction I) and, therefore, its angular distance to the ascending node ω_2. /100

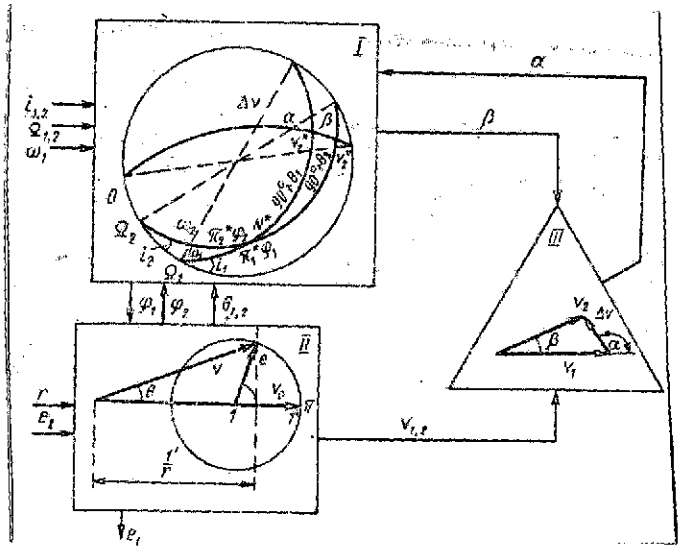

Fig. 70. Flow chart for solving problems of transit flight to other orbits: I. space orientation of orbits and velocity vectors in stereoscopic [sic] projection; II. diagram of orbital velocity and orbital parameters; III. velocity triangle.

By laying off from the point N* the angles $90° - \theta_1$ and $90° - \theta_2$ along the corresponding arcs of the great circles -- the orbital projections, we seek the positions of the points v^*_1 and v^*_2 giving the directions of the velocity vectors $v_{(1)}$ and $v(2)$ at point N for the old and new orbits, respectively. Next, the arc of the circle is drawn through points v^*_1 and v^*_2 and the angle β between the vectors $v(1)$ and $v(2)$ is determined. Knowing the magnitude of the vectors $v(1)$, $v(2)$, and β, from the velocity triangle (see construction III) we find the vector $\Delta\bar{v}$ and α -- the angle that is used for constructing the orientation of $\Delta\bar{v}$ relative to the stars in the celestial sphere (see construction I).

ORIGINAL PAGE IS
OF POOR QUALITY

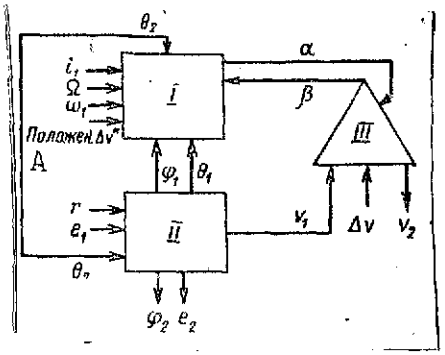

Fig. 71. Flow chart of solution of inverse problems of transit flight to other orbits.

Key: A. Position of Δv*

Similarly, problems of this type /101 are solved also for other combinations of given and unknown parameters, with the only difference that the transfer from one stage of the calculation to the other is carried out in a different sequence. As an example, in Fig. 71 is given a scheme for solving the inverse problem -- finding the parameters of a new orbit if $\Delta\bar{v}$ is given.

In conclusion, let us look at the calculation of a gravitational maneuver. A gravitational maneuver of a spacecraft is effected in the period during which the spacecraft is passing through the planetary sphere of action, as a result of which the vector of the spacecraft's heliocentric velocity changes (Fig. 72 a). If upon entering the planetary sphere of action the spacecraft has a heliocentric velocity v_I, then its planetocentric velocity at this point is determined by adding to $\bar{v}_I$ the vector $\bar{v}_t$ [t = = transit] with the opposite sign. Thus, the velocity v_{II} of entry into the planetary sphere of action is determined.

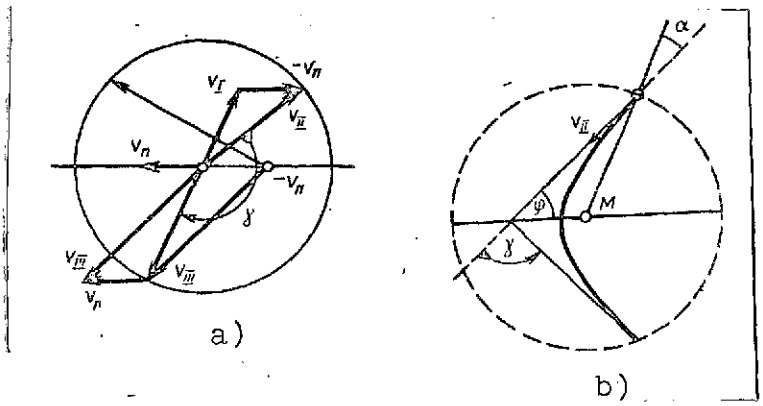

Fig. 72. Vector diagrams of gravitational maneuver: a. vectors; b. scheme of motion of spacecraft in planetary sphere of action.

If the value of v_{II} exceeds the second escape velocity for this point in the planetary gravity field, then by circumventing the planet in a hyperbola, the spacecraft begins to leave the planetary sphere of action with the same magnitude of the planetocentric velocity, but directed otherwise (see Fig. 72 b). We assume that the direction of the planetocentric velocity changed by the angle γ; then upon /102 leaving the planetary sphere of action the new heliocentric velocity v_{III} will be equal to the sum of the vector $\bar{v}_{II}$ rotated by the angle γ and the vector $\bar{v}_t$.

From Fig. 73 it is clear that a circle with radius v_{II} will be the locus of the ends of the resultant vector if its head is placed

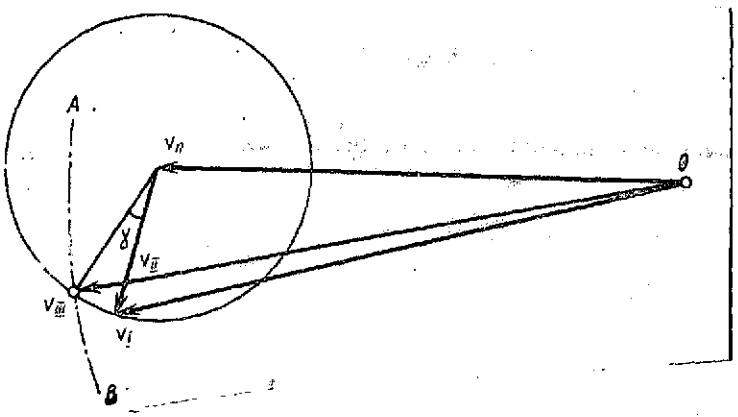

Fig. 73. Circular hodograph of velocity.

at the end of vector $\bar{v}_t$ rotated in the opposite direction. The angle γ depends on the mass of the planet and the "miss" distance. Depending on this angle, either the velocity v_I is increased or reduced by an amount equal in the limiting case to double the orbital velocity of the planet.

Fig. 74 gives the flow diagram for the calculation of the gravitational maneuver. Let us trace in it the procedure in calculating the gravitational maneuver to ensure an escape velocity required in a flight to another planet. Knowing the heliocentric velocity v_I of spacecraft approach to the planetary sphere of action from the calculation of the terminal velocity of the transit orbit, we can determine the required angle γ by seeking the points of intersection of the circular vector diagram by the line of the hodograph of the required escape velocities, which are calculated by using the orbital grid. From γ one determines the e of the hyperbolic orbit, obtaining the function $e = \frac{1}{\cos\frac{180^\circ - \gamma}{2}}$. Knowing e and $k_I = \frac{v_{II}}{v_I}$, from the nomogram shown in Fig. 75 we can find the angle α at which the spacecraft must enter the planetary sphere of action in order to effect the required gravitational maneuver. /103

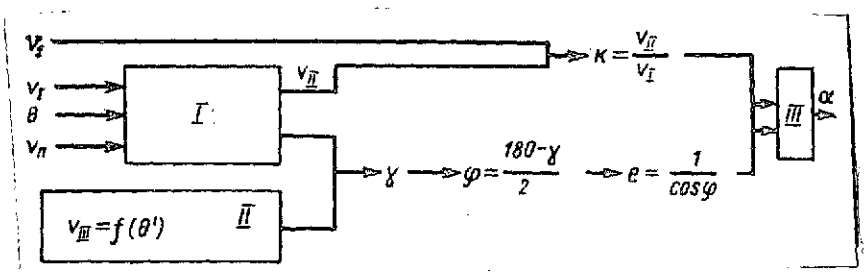

Fig. 74. Flow chart for solving problems of gravitational maneuver: I. construction of circular vector diagram; II. construction of hodograph of required velocity; III. construction of nomogram of functions k, α, and e.

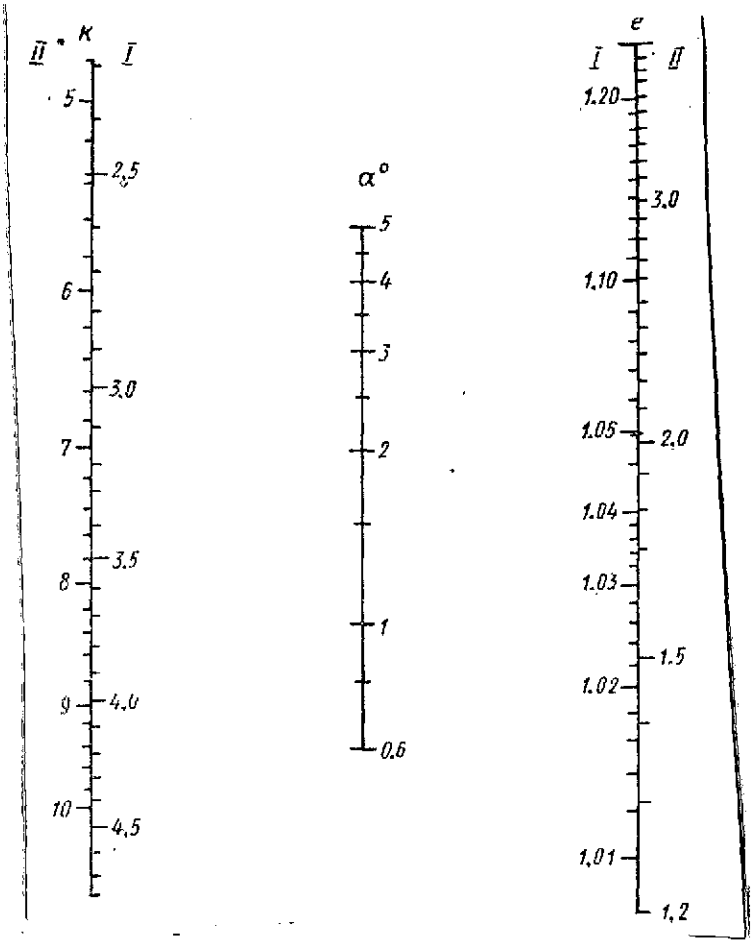

Fig. 75. Nomogram of gravitational maneuver.

Let us note, finally, that the nomogram shown in Fig. 75 essentially is a modification of the nomogram shown in Fig. 46.

5.3. Determination of optimal transit orbits and launch date

/104

A passive flight in a central gravity field is executed in the so-called Keplerian orbits, which are the conic sections examined above. The initial condition for determining orbital elements must be the velocity at the initial trajectory point which, on the other hand, is the terminal velocity for the powered trajectory section where the jet engine is firing. In view of the relatively small extent of the powered trajectory sections compared to the duration of the space voyages, in the scale of our sketches the powered trajectory sections are shown as points where there is a discontinuous velocity change by the given amount Δv.

The transit orbit calculation consists in determining the parameters of the orbit that is optimal with respect to minimum velocity impulse, where the parameters are needed for constructing the orbital plan [planform] in the plane of the transit with the spacecraft position marked at specific instants of time. Selection of the orbit initially is considered for the case of a transit from an outermost planet to an innermost, or, as is sometimes expressed, from an "upper" planet to a "lower", if the "lower" planet is regarded as closer to the Sun.

/105

The conversion to dimensionless magnitudes of the distances, velocities, and times is carried out with respect to the outermost [outermost as defined in the explanations in Fig. 76] orbit. Then the following are taken as the units: the initial radius at

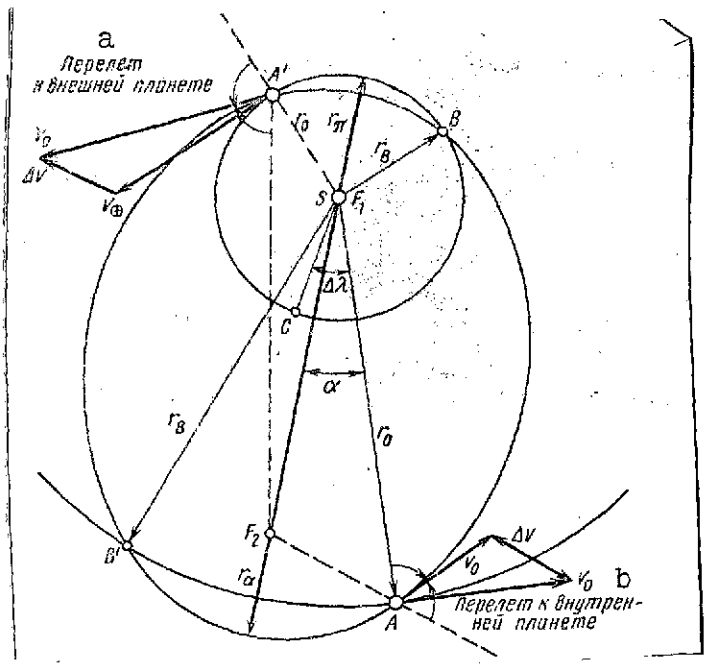

Fig. 76. Transit scheme.

Key: a. Transit to outermost planet [planets farther removed from the Sun than the Earth]; b. Transit to innermost planet [planet closer to the Sun than is the Earth].

the launch point, the first escape velocity at the launch point, and the period of revolution in the circular orbit constructed for the launch point. The scheme in Fig. 76 explains the calculation procedures; the characteristic points are denoted as follows: A is the launch point (the initial point on the transit orbit) -- the position of the departure planet at the launch instant; B is the encounter point -- the position of the target planet at the instant of encounter; and C is the position of the target planet at the instant of launch. Hence it is clear that the position of point A is uniquely associated with the launch date. The basic criterion for selecting the launch date ensuring that the spacecraft will enter the sphere of action of the target planet is the required difference $\Delta\lambda$ of the heliocentric longitudes of the departure planet and of the target planet on the launch date.

For a preliminary orientation, let us consider the simplest idealized case when $\psi = 180°$ and the orbits are concentric circles. For a transit flight to the innermost planets we have

$$\Delta\lambda = \frac{360°}{T_2}\,\frac{T_t}{2} - 180° = 180°\left(\frac{T_t}{T_2} - 1\right).$$

Considering that

$$T_t = \frac{2\pi}{\sqrt{fM}} R_t^{3/2};\quad T_2 = \frac{2\pi}{\sqrt{fM}} R_B^{3/2};$$

$$\frac{T_t}{T_2} = \left(\frac{R_t}{R_B}\right)^{3/2} \text{ and } R_t = \frac{R_A + R_B}{2},$$

ORIGINAL PAGE IS
OF POOR QUALITY

we finally get

$$\Delta\lambda_{inn} = 180^\circ\left[\left(\frac{R_A + R_B}{2R_B}\right)^{3/2} - 1\right]. \tag{5.2}$$

Similarly, for a transit flight to the outermost planets we get

$$\Delta\lambda_{out} = 180^\circ\left[1 - \left(\frac{R_A - R_B}{2R_B}\right)^{3/2}\right]. \tag{5.3}$$

Taking R_φ = 0.723 astronomical unit and R_σ = 1.523 astronomical unit, let us determine based on Eqs, (5.1) and (5.2) the differences of the heliocentric longitudes for Earth-Venus and Earth-Mars flights:

$$\Delta\lambda_{\oplus-\varphi} \cong 55^\circ \quad \text{and} \quad \Delta\lambda_{\oplus-\sigma} \cong 44^\circ.$$

The optimal orbit for a transit flight to a given point -- the node of the orbit of the target planet -- is used as an example to clarify the method of using the orbital grid. To determine the angle β, we must know the transit flight time t_t, which is a function of ψ and r_∞. From the bundle of orbits corresponding to different values of the energy level, that is, to different Δv (or e values), only one passes through both points A and B (Fig. 77) for the one r_∞ corresponding to it. The optimal orbits are determined by use of two elements of the universal computational device: a) the orbital plane in the plane of the ecliptic in which the position of the points A and B are entered for given r_∞ and ψ in a scale such that the segment AS = 1; and b) the orbital grid (see Fig. 66). On the isochrones of the orbital grid is shown the relative flight time from aphelion in fractions of the period of revolution in a circular orbit of the aphelion radius r_∞. For convenience in performing the constructions, this element gives the radial unit scale of the distances SA for a given r_∞. /106

The computational operations are carried out in this order. By rotating the second element, both points A and B are brought onto the trajectory of the same orbit. In this position, it is not difficult for given ψ and r_∞ to determine the following orbital parameters: α (from the position of the segment AS on the α scale), e (from the chosen grid curve), and $t_t = t_1 - t_2$ (based on t_1, which is read off from the isochrone grid at point B, and from t_2, which is read off on the isochrone grid at point A). By varying r_α with ψ held constant, we find the optimal orbit for the minimum energetics. Here the optimal angle α is determined. /107

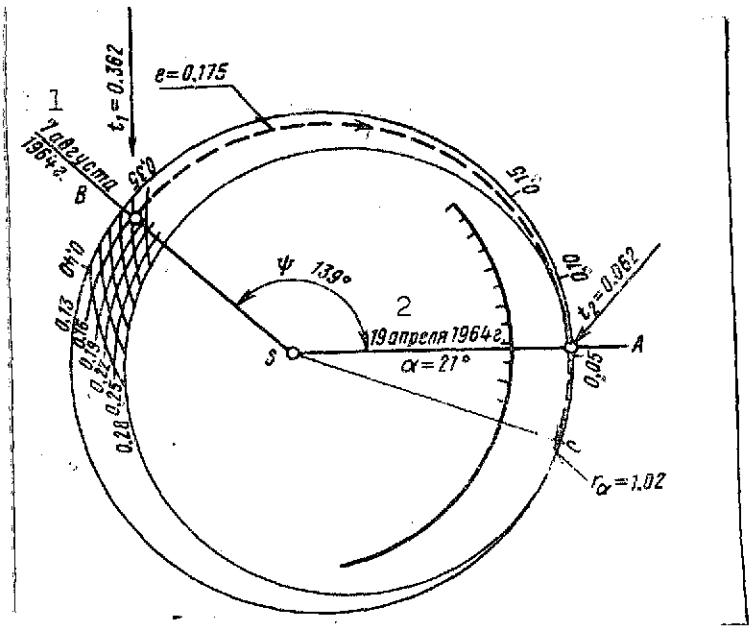

Fig. 77. Example of solving a problem by using the orbital grid.

Key: 1. 7 August 1964; 2. 19 April 1964

Fig. 78 shows the flow chart for solving the problem of spacecraft transit flight to an innermost planet along the Earth-Venus or Earth-Mercury path when the point of encounter B is given. Let us assumed, for example, that there are three r_α values individually for each preselected ψ. Let us assume that there will also be three ψ values -- in practice this is sufficient. Let us construct the position of points A and B in the orbital plan. The values of r_A are determined by the selected values of r_α, while those of r_B are determined by the ratio r_B/r_A. The special radial scale on the orbital grid -- the scale of r_α values -- is used for plotting the position of points A as a function of r_α. By positioning the orbital grid onto the orbital plan and by rotating it about the common center up to the position when the points A and B lie on the trajectory of the same orbit (already shown or interpolated), one can readily obtain the corresponding orbital parameters. After performing these operations several times, the resulting data must be systematized as in Table 6.

TABLE 6

ψ_1									ψ_2									ψ_3								
$r_{\alpha 1}$			$r_{\alpha 2}$			$r_{\alpha 3}$			$r_{\alpha 1}$			$r_{\alpha 2}$			$r_{\alpha 3}$			$r_{\alpha 1}$			$r_{\alpha 2}$			$r_{\alpha 3}$		
a	e	t_t	a	e	t_t	a	e	t_t	a	e	t_t	a	e	t_t	a	e	t_t	a	e	t_t	a	e	t_t	a	e	t_t

ORIGINAL PAGE IS
OF POOR QUALITY

Further, using the program shown in Fig. 79, from α and e let us determine θ, and from e and r_α, using the nomogram shown in Fig. 80, let us find Δv. Based on the values θ and Δv found for different r_α, but for the same ψ, let us construct the velocity hodograph as shown in Fig. 81. The optimal velocity impulse Δv_{min} and the optimal trajectory angle θ_{opt} are found by dropping a perpendicular from the point O onto the hodograph curve. The optimal values of the remaining parameters are determined based on Δv_{min} or θ_{opt} by using the graph of these quantities as a function of the angle θ.

/108

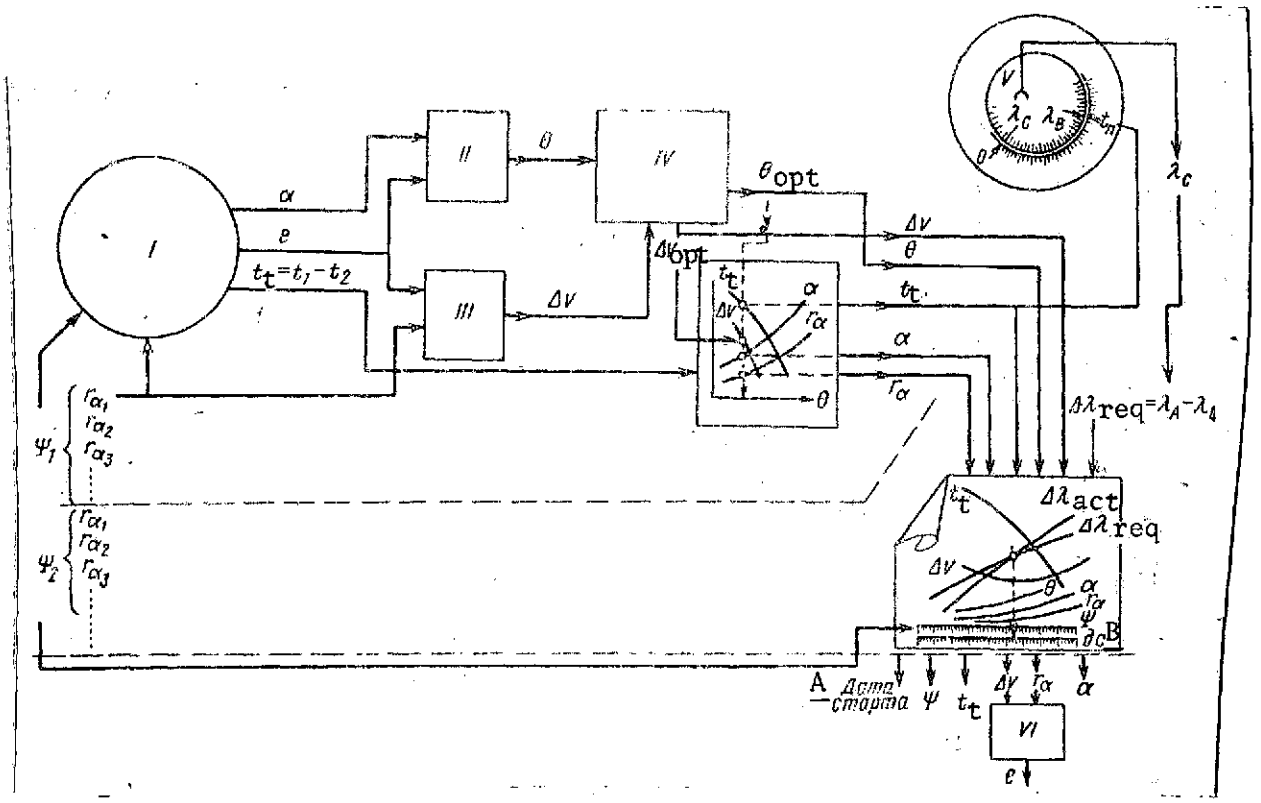

Fig. 78. Flow chart of solution of problem of spacecraft transit flight to innermost planet: I. orbital grid; II. nomogram of functions α, θ, and e; III. Nomogram of functions e, Δv, and r_α; IV. construction of velocity hodograph; V. Nomogram of functions λ_C, λ_B, and t_t; VI. Nomogram of functions e, Δv, and r_α.

Key: A. Launch date
B. Launch date scale

ORIGINAL PAGE IS
OF POOR QUALITY

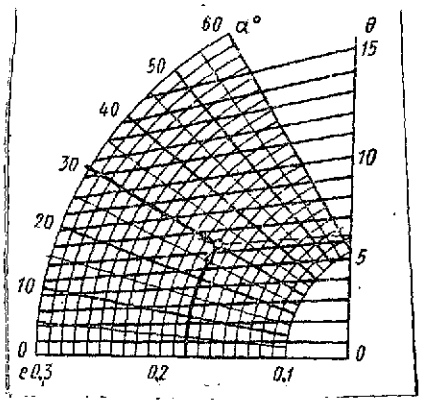

Fig. 79. Nomogram of function α, e, and θ.

By performing similar operations for /110
ψ_2 and ψ_3, let us construct the main calculation graph suitable for any year (see Fig. 78). Along the X-axis on this graph we must lay out the value of ψ, which at a given point B is uniquely associated with a launch date. Therefore, the date scale is also laid out along the X-axis.

The curve of the required initial difference of heliocentric longitudes in order to ensure that the spacecraft encounters the planet is plotted on the principal calculation graph. For this purpose, we must first calculate the required heliocentric longitudes of the target planet on the launch date. It is

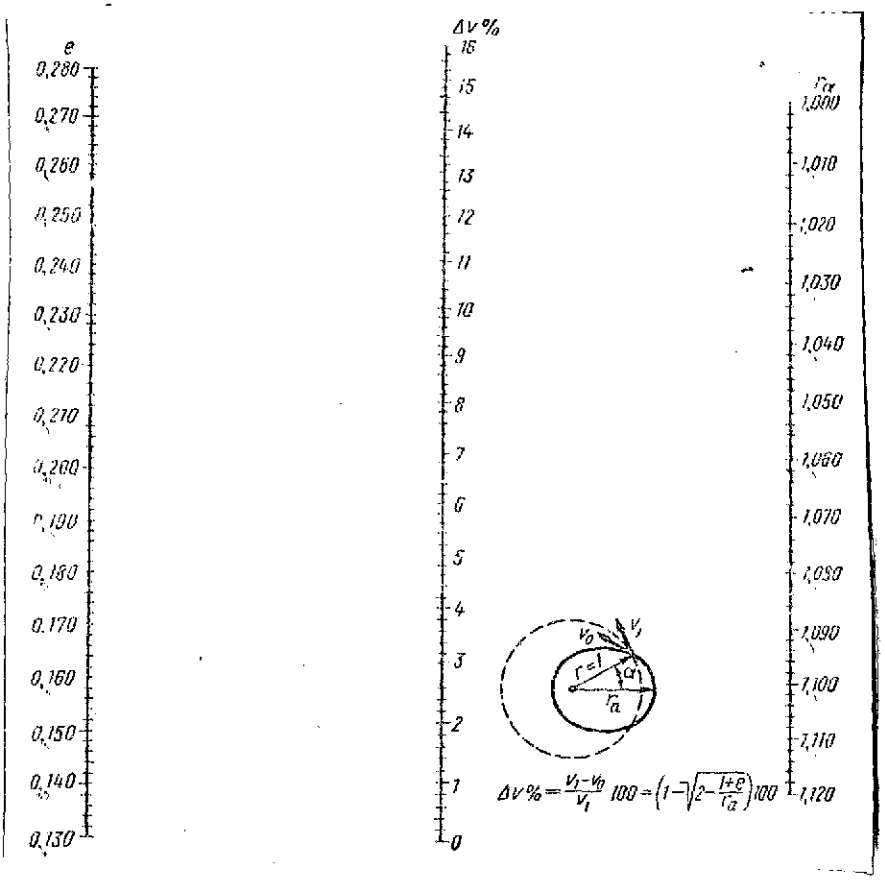

Fig. 80. Nomogram of functions e, r_α, and ΔV:

$$\Delta v\% = \frac{v_1 - v_0}{v_1} = \left(1 - \sqrt{2 - \frac{1+e}{r_\alpha}}\right) 100$$

ORIGINAL PAGE IS
OF POOR QUALITY

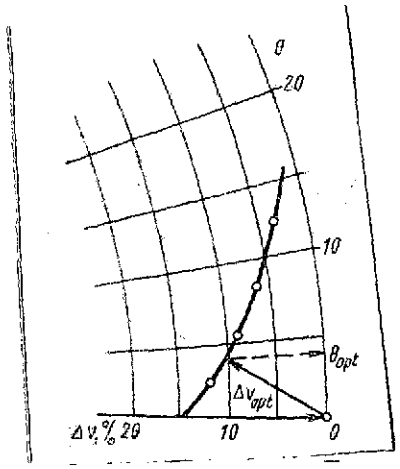

Fig. 81. Velocity hodography.

convenient to do this calculation using the nomogram of heliocentric longitudes (see Section 5.1).

By solving this problem, one must not orient the element of the circular or spiral scales of the heliocentric longitudes at 0 January. In our case the value λ_B is aligned with T_t on the day number scale and opposite the mark 0 on the day scale is found the desired λ_C. The launch date is determined from the intersection of the curves $\Delta\lambda_0 = \lambda_A - \lambda_C$ and $\Delta\lambda_{act} = \lambda_\Theta - \lambda_{t.p}$ for the given year. And the latter curve is plotted on the graph based on data of the astronomical almanac for the required year or from the heliocentric longitude nomogram.

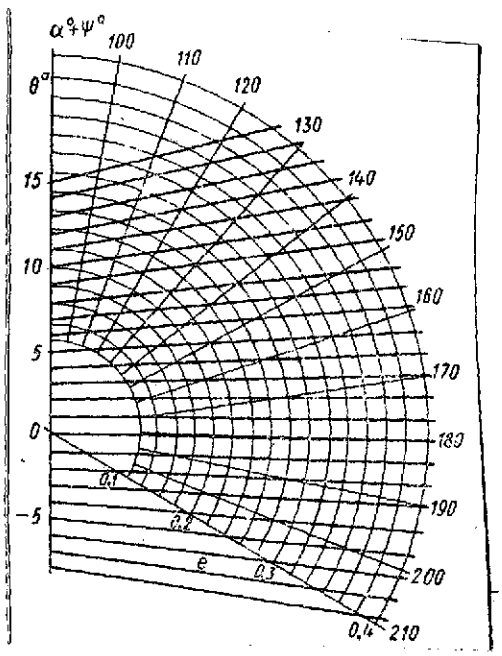

Fig. 82. Nomogram of functions α, e, and θ.

Calculations of flight to outermost planets can be done by using the orbital grid in similar fashion. Converting to dimensionless distances, velocities, and times is carried out with respect to the outermost orbit, which in this case is the orbit of the target planet. Here the nomogram shown in Figs. 79 and 80 must be replaced by the nomograms shown in Figs. 82 and 83, and the orbital grid must be rotated toward the other side.

In the general case the flight of a spacecraft to the point of a planetary orbit when $\psi \neq 180°$ is not optimal, since the small trajectory drift from the projected point with increase in ψ can be a cause of a reduction in Δv. Let us examine below how this circumstance can be allowed for.

Total optimization of the calculation of the transit orbit requires examination of cases when the arrival point of the spacecraft does not coincide with the trajectory of the target planet orbit. By converting from the idealized case -- circular coplanar orbits -- to actual orbits, two factors are taken into account: the eccentricity of the orbits and the inclination of the transit orbit. The orbital eccentricity leads to $\Delta\lambda$ becoming a variable and changing during the year within certain limits. As for the /101

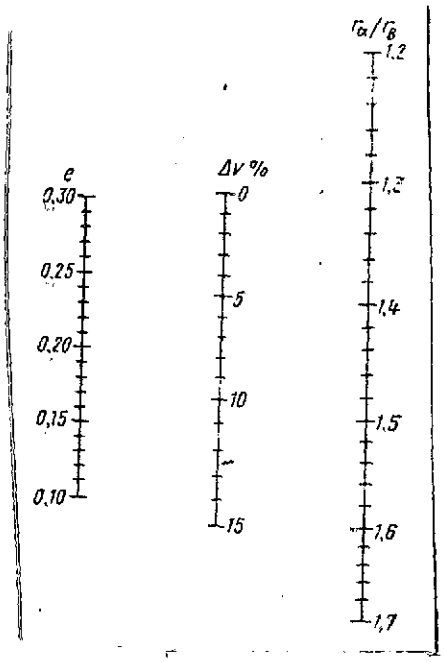

Fig. 83. Nomograms of functions e, r_α, and Δv:

$$\Delta v\% = \left(\sqrt{2 - \frac{1-e}{r_a/r_B}} - 1\right) 100$$

energy level, the quantity Δv expressing it also acquires a more complicated dependence on the mutual disposition of the launch and arrival points.

The inclination of the transit orbit is absent only for a flight to the point of the target planet orbit. When the arrival point is increasingly distant from the point of the target planet orbit, the angle of inclination of the transit orbit forms, which becomes 90° if the angular range is close to 180°, but more properly, close to 180° -- Δ, or $\Delta < i$ (see Fig. 69). The method of determining the angle of transit orbital inclination is outlined in Section 5.1. With greater accuracy this angle can be found using the nomogram shown in Fig. 70.

In the idealized case the value of Δv as ψ is reduced must increase, which leads to the well-known fact of increase in Δv if the flight time is shortened. On the other hand, in actual cases when the inclination of the transit orbit has an effect, as the arrival point is increasingly distant from the point of the target planet orbit, rotating the plane of the transit orbit entails an increase in the required Δv. As the result of the addition of the influences of these two factors, the characteristic curves of variation in Δv as a function of /112 ψ are obtained (Fig. 84). Here are given the results of calculation for the case of two circular planetary orbits with a 1.5:1 ratio of their radii and with the angle between them i = 10°. The orbital radii are assumed to be close to the initial radii of the planets in possible cases of transit of a spacecraft along the Earth-Venus and Earth-Mars paths. The overstated magnitude of the angle i is selected for greater clarity of the figures.

Although overall this example of calculation is an ideal case, it still quite clearly illustrates the physical meaning of the actual case. The dashed curve in Fig. 84 shows how Δv varies for coplanar orbits when the minimum of Δv occurs at the value ψ = 180° (the parameter of a Hohmann orbit). The influence of the inclination of the transit orbit was analyzed with the example of a calculation in which the angular position of the launch point was 112° from the ascending node of the target planet orbit. The curve $\Delta v = f(\psi)$ determines the well-defined minimum that has an optimal angular range for a given launch date.

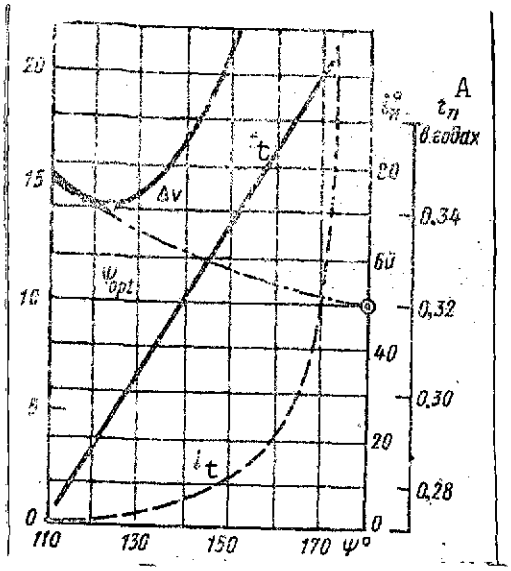

Fig. 84. Nomogram of the function $\Delta v = f(\psi)$.

Key: A. t_t, in years

The orbital eccentricity was excluded from this example. If then the eccentricity is also allowed for, it becomes necessary to find the optimal orbit for each pair of launch and arrival points by varying one of the parameters. The method of determining the optimal transit orbit for a given point of arrival presented in Section 5.3 uses variation in r_α. For the final selection of the optimal orbit we must investigate by this method the regions of minimum Δv (see Fig. 84), by suitably varying the transit point B.

Fig. 85 well illustrates the geometrical meaning of the trajectory angle θ.

In the actual practice of preselection of the optimal orbits for a transit flight from the Earth to other planets, use is made of graphs that are lines of constant energy levels for the transit trajectories between the planetary spheres of influence. These /113
graphs are constructed in the system of the launch date coordinates and the flight duration, or else in a system of coordinates of the launch date and the arrival date. A comparison of these graphs requires numerous calculations on a computer for each year of possible launches. The transit orbits are selected from these graphs in the region of the energy minimum for each launch year. The analytical-graphical approach to solving this problem provides a method of predetermining the energetically optimum trajectories and the launch dates corresponding to them, without requiring calculations for each year, by use of the so-called invariant nomographic scale. The required difference between the heliocentric longitudes of the departure planet and of the destination planet at the launch instant is the principal starting parameter under the methods.

5.4. Invariant nomographic scale /114

The invariant nomographic scale of energy levels for optimal orbits -- the Δv scale -- is constructed in a system of launch date coordinates and the necessary difference between heliocentric longitudes or, which amounts to the same thing, in the system of the coordinates of launch date [LD] and $\Delta\lambda$. The invariance is a consequence of the fact that the launch dates are uniquely

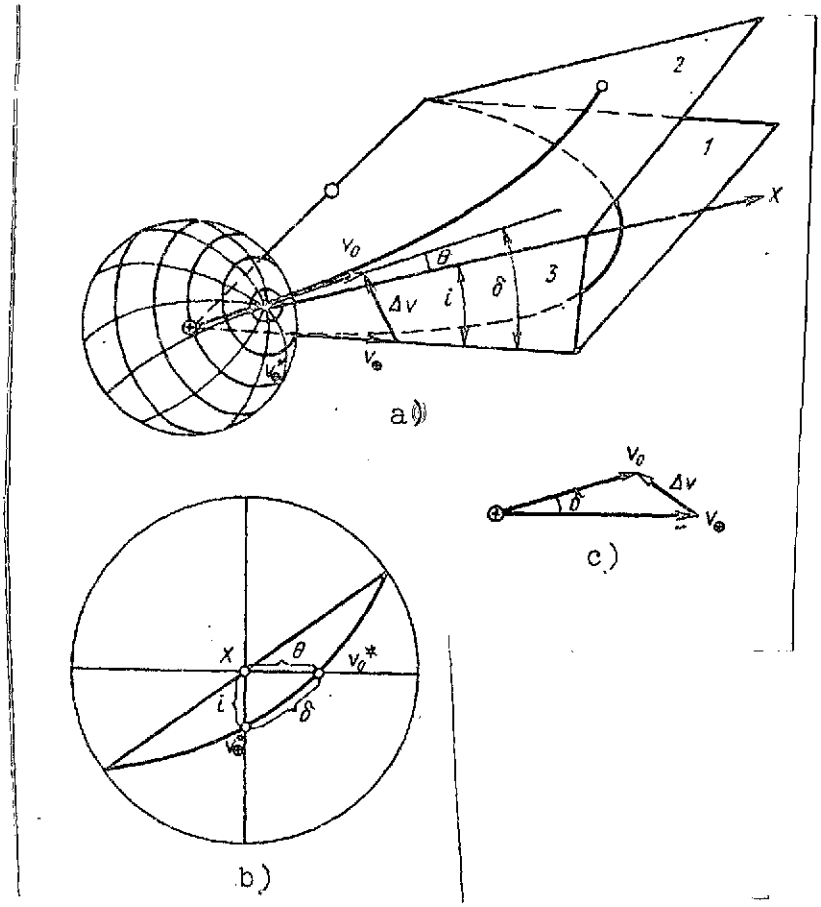

Fig. 85. Geometrical meaning of trajector angle: a) calculated planes; b) construction based on Wulf's grid for determining the angle δ; c) determination of the velocity vector $\overline{\Delta v}$; 1. plane of Earth orbit; 2. plane of transit orbit; 3. plane perpendicular to the Earth-Sun line.

associated by a function with the position of the Earth in its orbit and $\Delta\lambda_0$ is determined only by the orbital geometry and the laws of motion along them regardless of where the target planet is at the given moment if one neglects the secular changes in the orbital parameters of the planets and their perturbations.

Construction of the invariant nomographic scale begins by varying the angular ranges of the flight and one of the parameters of the transit heliocentric ellipses. Here the ellipticity of the planetary orbits and their inclination to the plane of the ecliptic are taken into account. Further, one seeks the energetically optimal transit orbit for a given heliocentric longitude of the departure planet. The parameters of the optimal transit orbit and the required heliocentric longitude of the target planet at the moment of arrival are placed in memory. The heliocentric longitude of the target planet at the launch instant and the difference between the heliocentric longitudes of the departure planet and the target planet at the instatn of launch are calculated.

Similar calculations are performed also for other launch instants throughout one revolution of the departure planet. As a result of these calculations, one finds the plot of the variation in the necessary differences between the heliocentric longitudes of the departure planet and those of the destination planet at the instant of launch based on launch dates. The graph is invariant for any launch year according to the assumptions made. Each point on the graph reflects the energetically optimal transit trajectory

from the fixed position of the departure planet to the orbit of the target planet.

The energy levels of the orbits are characterized by Δv -- velocity increments in the sphere of action. If we enter the points with specific Δv in the resulting graph, an invariant nomographic Δv scale is formed in the system of the coordinates LD and $\Delta\lambda$. The lines of effective differences between the heliocentric longitudes for specific years are plotted in the same coordinates. The intersections of these lines with the invariant nomographic scale results in points determining on the X-axis the optimal launch dates, and on the ordinate scale -- the energy level of the optimal transit orbits. To determine the other optimal orbital parameters, graphs are constructed based on the launch dates for these functions: i_t, t_t, e, ψ, α, β, and β'.

As an example of the application of the method, Figs. 86, 87, and 88 examine optimal transits from Earth to Mars. Here it was taken into account that the sphere of action of the planet Mars will be reached by the spacecraft during the first half-orbit of its heliocentric ellipse, and the energetically optimal orbits will be selected on the basis of a minimum boost velocity impulse. In Fig. 86 is plotted the invariant nomographic Δv scale and the lengths of the change in the effective values $\Delta\lambda$ for a series of years (1971-1996). Figs. 87 and 88 give the plots of the remaining parameters and the curve of variation of Δv. /115

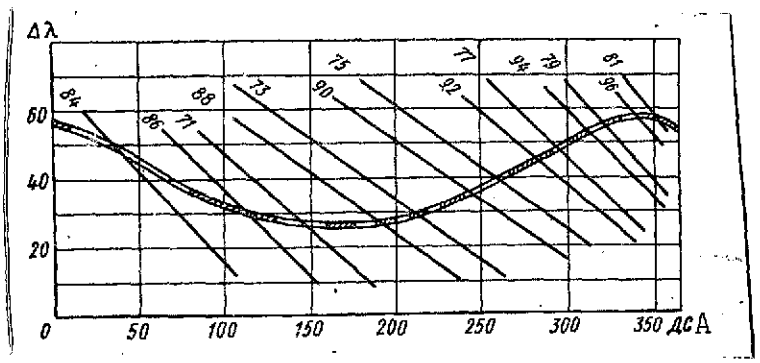

Fig. 86. Invariant nomographic scale.

Key: A. LD [launch date]

Not precluded is the possibility that the energetically optimal transit orbit of a spacecraft to the orbit of Mars at a given date obtained from the invariant nomographic scale can prove to be "worse" than the energetically nonoptimal transit orbit on another date. But this situation does not detract from the significance of the proposed method of calculation for the following considerations, which concern the character of the physical functions of the nomograms and other criteria for selecting the launch date. As the result of constructing the family of lines of equal energy levels Δv in the system of the coordinates $\Delta\lambda$ and Ld, concentric closed contours greatly elongated along the invariant scale are obtained, because the gradient Δv in the direction of the /116

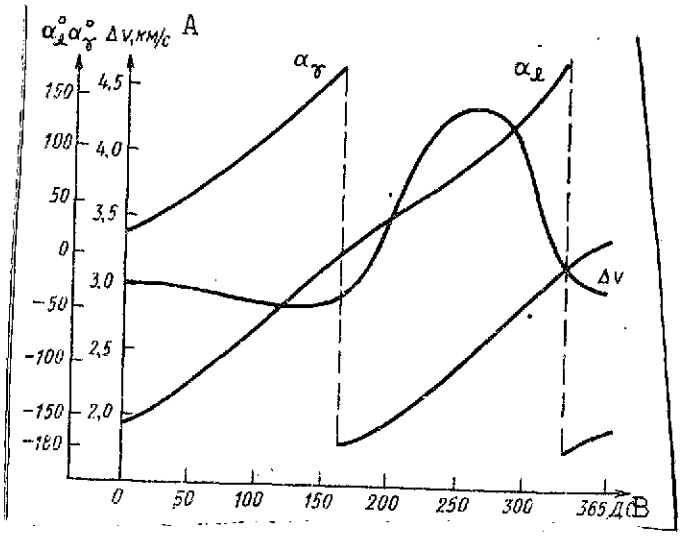

Fig. 87. Plots of orbital parameters.

Key: A. km/sec; B. LD [launch date]

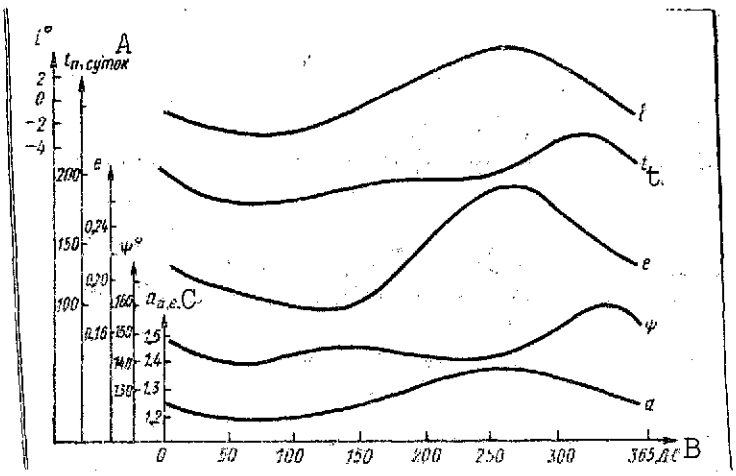

Fig. 88. Graphs of orbital parameters.

Key: A. t_t, days; B. LD; C. α, astronomical units

Δλ axis is much larger than the gradient Δv in the direction of the LD axis. The centers of these contours are found on the invariant scale. The optimal launch dates for a given year must be determined by the points at which the lines of actual Δλ values are tangent to the Δv lines. Owing to the great elongation of the contours of the Δv = const line, the displacement of the LD values proves to be slight and the change in the energy level Δv also proves to be slight. To this it must be added that the actual value of LD is expressed in an integer, so that the launch time in the course of a day is determined from other considerations, which will be outlined in detail below.

5.5. Determination of space orientation of transit orbit and launch time

Usually, a circular orbit is the intermediate orbit for extended space flights of a spacecraft. Departure from the circular orbit into the transit orbit is effected by short firing of the booster engine, increasing the velocity by the required amount by the end of the firing period.

What then is the fundamental difference between a flight to the Moon and a flight to planets of the solar system? /117

In the first case, after leaving the circular orbit the spacecraft flight occurs within the sphere of action of the Earth and for some additional time it does not actually attain the sphere of

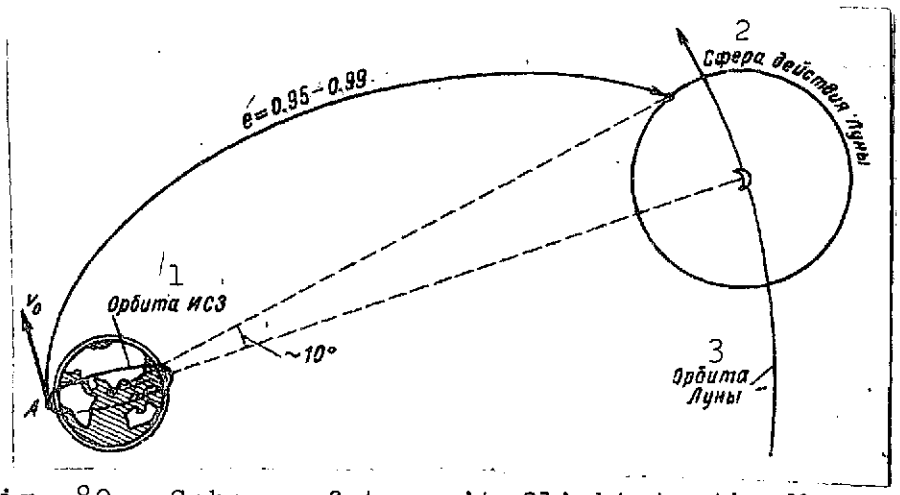

Fig. 89. Scheme of transit flight to the Moon.

Key: 1. Orbit of AES [artificial Earth satellite]
2. Moon's sphere of action
3. Orbit of Moon

action of the Moon (the radius of the Moon's sphere of action $\approx$ $\approx 66 \cdot 10^3$ km). The spacecraft moves along an orbit whose center of attraction is the center of the Earth, that is, along the so-called geocentric orbit. The scheme of the flight to the Moon's sphere of action is shown in Fig. 89.

In the second case the transit is effected along heliocentric orbits, for which the point of departure from the Earth's sphere of action is taken as the starting point. Here it must be recalled that on the cosmic scale the Earth's sphere of action for flights to other planets is in practice converted into a point. The radius of the Earth's sphere of action is approximately $9 \cdot 10^5$ km, while the radius of the Earth's orbit is $150 \cdot 10^6$ km. So the spacecraft velocity at the boundary of the Earth's sphere of action must reach a value whose vector sum when added to the Earth's velocity $v_\oplus$ yields a resultant velocity v_0 that is the initial velocity of the transit orbit. This increment to the velocity $V_\oplus$ must ensure that the spacecraft transfers to the elliptical geocentric orbit with large eccentricity equal to approximately unity. This orbit is near-parabolic.

During a flight to planets of the solar system, to acquire the required initial velocity, in practice it is necessary at the boundary of the Earth's sphere of action, the distance to which can be taken as infinity for geocentric hyperbolic orbits, to have a residual hyperbolic velocity v_∞ equal to the required increment /118
Δv to the velocity $v_\oplus$ (Fig. 90). The points of departure from the circular orbit in the case of a flight to the Moon are determined by the position of the perigee of the transit orbit, while in the

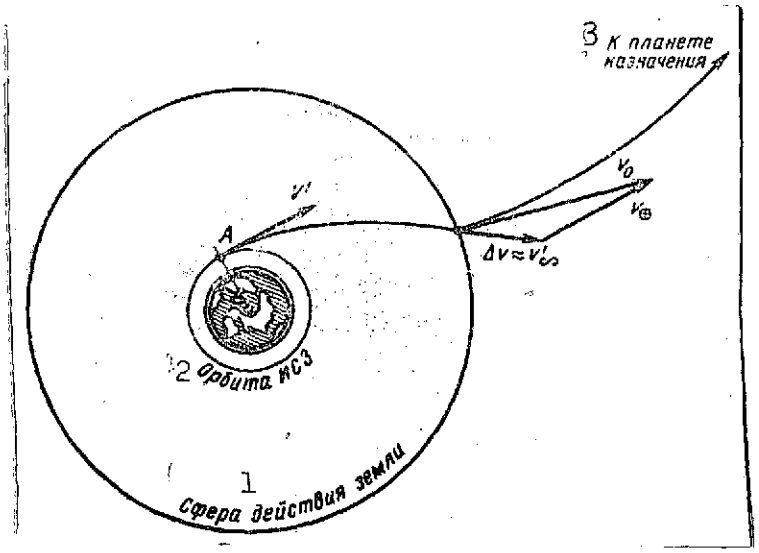

Fig. 90. Scheme of transit flight to planet.

Key: 1. Earth's sphere of action; 2. Orbit of AES; 3. To target planet

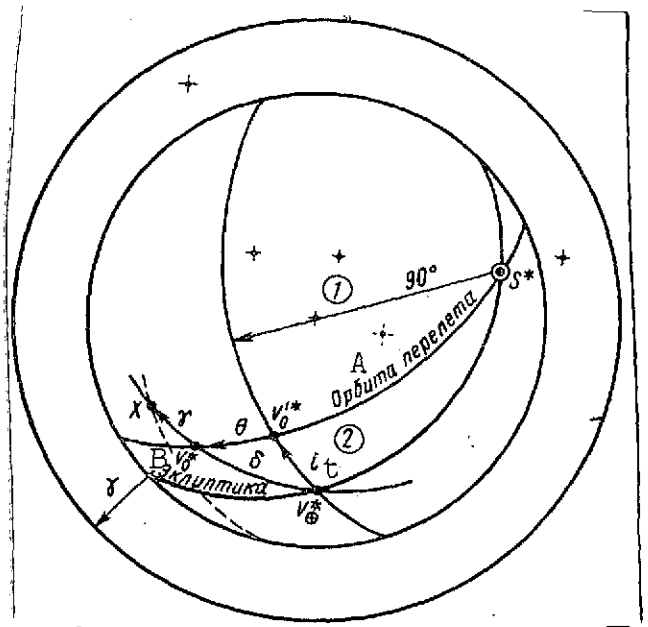

Fig. 91. Scheme of construction for determining the launch time (for clarity of the scheme, the angles i_t and θ are considerably increased).

Key: A. Transit orbit; B. Ecliptic

case of a flight to planets of the solar system -- by the position of the perigee of the hyperbolic orbit bringing the spacecraft from the Earth's sphere of action at the point at which the transit orbit begins. A determination of the point of origin of the transit orbit is presented below.

In examining the problem of a launch time, let us start from the idea that when a spacecraft is launched from Earth, the Earth is a kind of moving launch pad with diurnal rotation about the terrestrial axis. The position of the plane of the circular orbit will be determined by the launch azimuth and instant. A launch azimuth relates the circular orbit to the Earth at the instant the spacecraft is inserted into this orbit. The launch time, more exactly, the time of insertion of the spacecraft into the circular orbit, is defined by the instant when the path of the circular orbit or the projection of the orbit onto the surface of the Earth at the instant of insertion into orbit coincides with the plane of the transit orbit. The second determining instant of time is the time of departure from the circular orbit.

Let us examine the general case of a transit flight to a planet to the orbital point not coinciding

ORIGINAL PAGE IS
OF POOR QUALITY

with its node. The order of the constructions carried out on a transparent sheet of paper (Fig. 91) in the geocentric equatorial coordinate system is as follows:

1. The position of the Sun on the ecliptic is determined by point S^* on the launch date and a great circle 90° from the Sun is drawn. The intersection of the ecliptic with this circle yields the point $v^*_\oplus$ defining the direction of the orbital velocity of the Earth. /119

2. The angle i_t is measured off from the resulting point and the position of the transit orbit is found as the arc of the great circle passing through the points v'^*_0 and S^* found.

3. Along the arc of the transit orbit is measured off the angle θ found when determining the parameters of the optimal transit orbit and, thus, the point on the sphere v^*_0 toward which the vector $\bar{v}_0$ is directed is determined.

4. By connecting the points $v^*_\oplus$ and v^*_0 with a great-circle arc, one determines the angle δ between the vectors $\bar{v}_0$ and $\bar{v}_\oplus$ (see Fig. 91).

5. From the values, v_0, $v_\oplus$, and δ based on the velocity triangle one finds the revised Δv with reference to the inclination of the transit orbit and the angle required for further construction (Fig. 92).

6. From point $v^*_\oplus$ in the direction of the arc of $\overset{\frown}{v^*_\oplus v^*_0}$ the angle γ is measured off, determining the position of the start of the transit orbit (see point X in Fig. 91), that is, the orbit whose position on the geocentric sphere shows the direction of the correcting impulse. /120

7. After the completed constructions, the following set of elements of the universal computational tool are assembled: the device base -- the map of the Earth with the circular orbit superimposed on it; the geocentric sphere with constructions completed earlier; and the solar cursor.

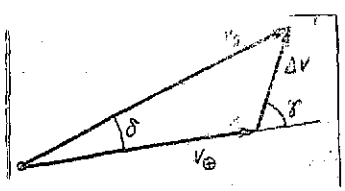

Fig. 92. Velocity triangle.

Here we must add the revision that the geocentric sphere with constructions is fixed to the axis of the device relative to the base at some position γ_1, which is entered onto the map of the Earth and onto the geocentric sphere. The operations involving the computational tool are as follows: the year mark is brought opposite the launch date; by rotating the map of the Earth one finds the position at which the circular orbit of the spacecraft falls at point X. Next, one determines the launch /121

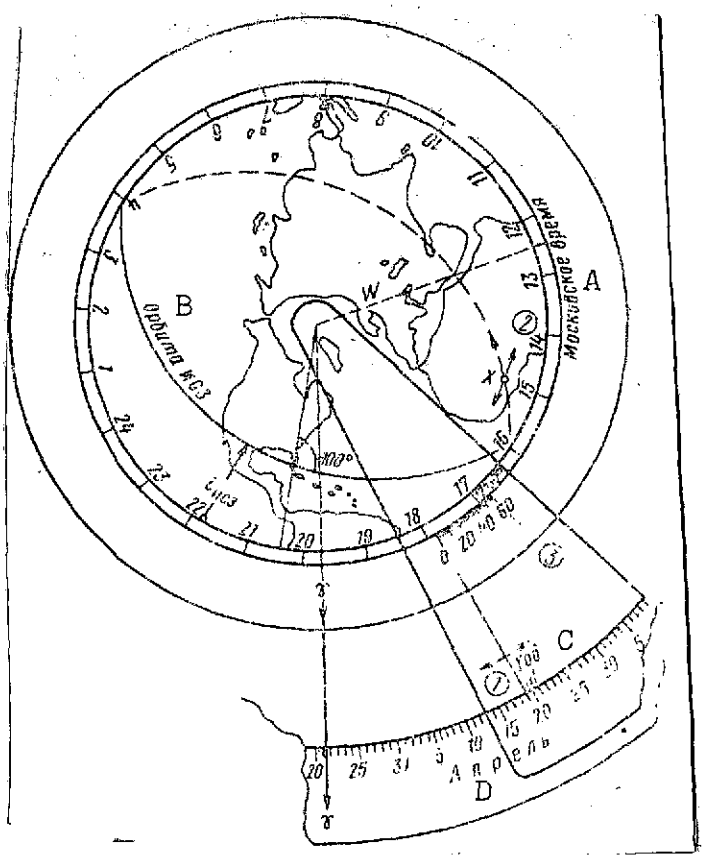

Fig. 93. Example of calculation of flight of craft to Venus.

Key: A. Moscow time; B. orbit of AES; C. Year; D. April

time in the hour circle, or, to be more exact, the time of day for the moment of spacecraft insertion into the circular orbit. An example of this kind of calculation is shown in Fig. 93 for a flight to Venus from Cape Canaveral (United States) on 19 April 1964 when the launch azimuth was 100° (see [2]).

5.6. Example of construction of operational device in space navigation

Astronautics offers nomography broad possibilities for its use not only in the design bureaus but also in space flight conditions where the time for reasoning is at a minimum. In spite of the fact that some kinds of maneuver in space and the solution of all kinds of encounter problems even in unforeseen cases of space flight obviously will require in the future the transfer of flight control to a computer, these navigational problems must periodically fall within human control. Therefore it is extremely important to be able to use this analytical-graphical apparatus that permits an evaluation of problems under study. Nomograms with sliding scales will doubtless find further development and broad use in the future.

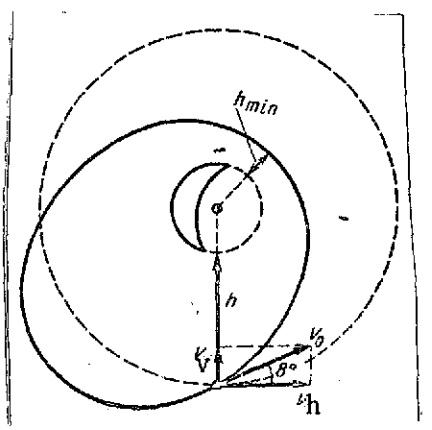

Fig. 94. Flight past the Moon.

As an example, let us show how we can carry out the necessary calculations of flight problems near the surface of the Moon using a small computational device. First it is of interest to calc

ORIGINAL PAGE IS
OF POOR QUALITY

calculate h_{min}, associated with spacecraft flight safety (Fig. 94). From the readings of the measuring equipment we must know h, v_h, and v_v. These nomograms enable us to predict the flight trajectory when the engine is off, from the instantaneous velocity and altitude. If it is required to change orbit, then by using the nomograms, the initial velocity for the new orbit can be determined. The vector difference between the required and effective velocities gives the required velocity impulse that must be imparted to the spacecraft for orbit correction. /122

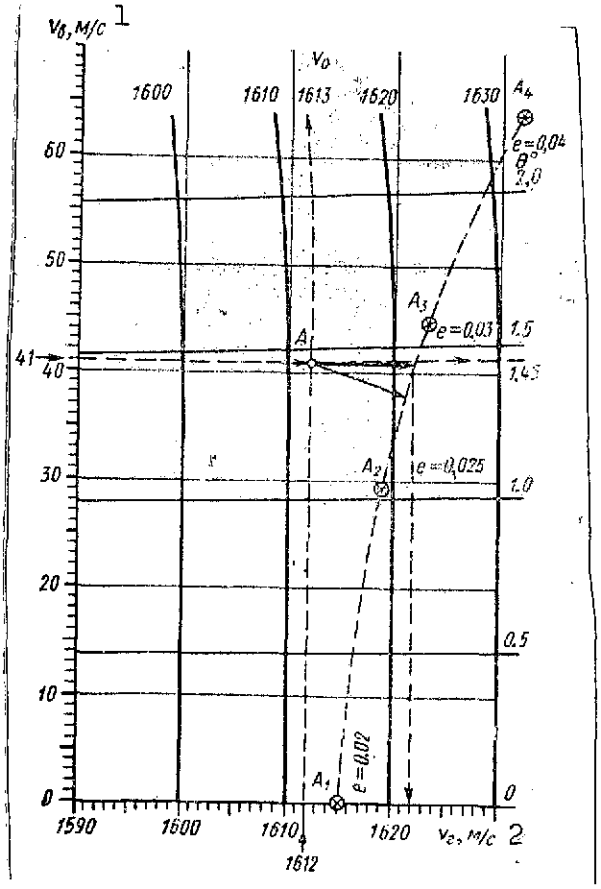

Fig. 95. Velocity hodograph.

Key: 1. v_v, m/sec; 2. v_h, m/sec

The proposed computational tool can solve problems in space navigation using these quantities: h, h_{min}, $r_{ц\,av}$, $r_{ц}$, α, α^*, c, e, $v_{ц}$, v_v, v_h, v_l, $k_{1ц}$, and θ. The entire computational tool consists of three sets of nomograms, in whose construction these relations were used:

$$a^* = \frac{1}{2-k_{1ц}}; \quad k_{1ц} = \frac{v_ц \sqrt{r_ц}}{\sqrt{fM_ц}};$$
$$r_{min} = a(1-e); \quad e^2 = 1 - \cos^2\theta\left(2k_{1ц}^2 - k_{1ц}^4\right),$$

where the gravitational parameter of the Moon $f_{M_ц}$ = = 4.890 kg^3/sec^2.

The first nomogram (Fig. 95) consists of a polar and a rectangular grid laid out on the same element. It is used in determining $v_ц$ and θ from known v_v and v_h. Using this ame nomogram, one finds the velocity impulse for orbit correction, as the difference between the vectors of the required and effective velocities. Then A in the network nomogram maps the end of the resultant vector, and the line connecting the ends of several resultant vectors A_1, A_2, A_3, and A_4 is the velocity hodograph. /123

The second nomogram (Fig. 96) consists of three sliding elements, 1, 2, and 3, pivoting at a [common] center. It determines the relationship between flight velocity and altitude. The

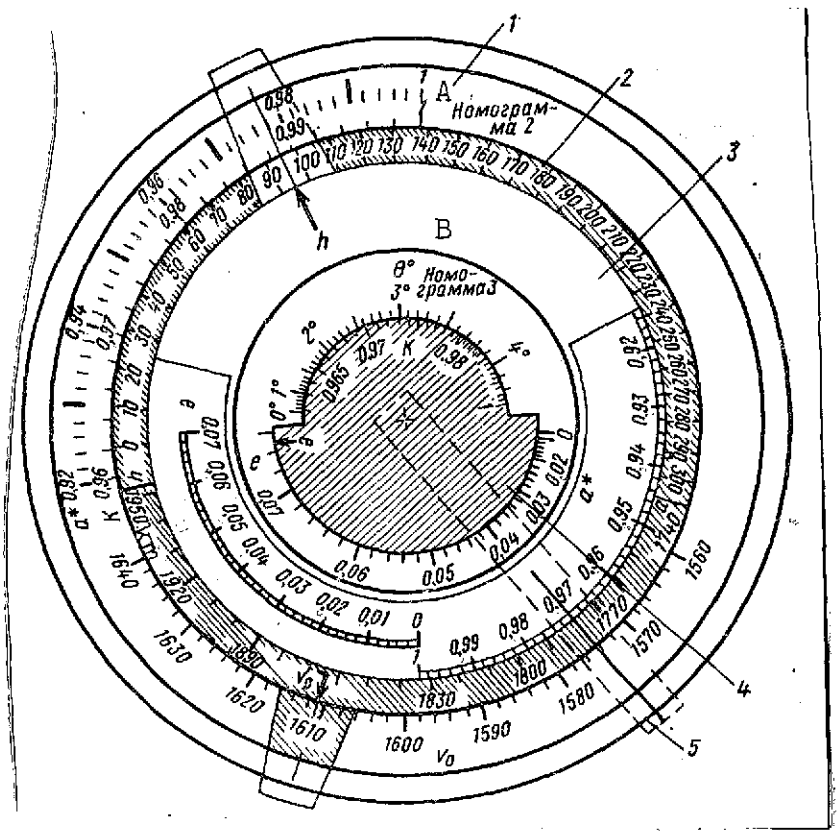

Fig. 96. Space navigation calculation device.

Key: A. Nomogram 2; B. Nomogram 3

dimensional quantity v_{1c}, m/sec, in this program, can be expressed in terms of k_{1c}, e, and α. The third nomogram, consisting of two sliding elements 4 and 5 (see Fig. 96), is used for calculating e from the values of k_{1c} and θ, and vice versa -- for calculating θ from the value of k_{1c} and e.

Let us show the procedure of operations with the nomograms in the example of the determination of h_{min}. We will assume that the following starting data are given: h = 90 km, v_h = 1612 m/sec, and v_v = 41 m/sec. Using nomogram 1 /124 (see Fig. 95), based on v_h and v_v the point A is determined, which gives the following readings by its position: v_{1c} = 1613 m/sec and θ = 1.45°. By rotating element 2 of nomogram 2 (see Fig. 96), one positions the arrow denoted by "v_0" opposite 1613 on the corresponding scale of element 1. Opposite h = 90 km, which is on the scale of element 2, one reads off the values k_{1c} and α* on the scale of element 1: k_{1c} = 0.989 and α* = 0.978. Further, by rotating element 3 one places the cursor bearing the arrow "h" opposite the value 90 km which is on the scale of element 2. The value α* = 0.978 is found on the α* scale of element 3, and the sliding cursor 5 is placed opposite 0.978. Using nomogram 3 and elements 3 and 4, one determines e based on k_{1c} = 9.89. For this purpose, the value 0.989 is placed opposite the value 1.45°, and one reads e = 0.034 across from the "e" arrow. By rotating element 3 with cursor 5 kept fixed, one brings the value 0.034 thus found beneath the cursor 5, then opposite the "h" arrow one seeks the unknown h_{min}.

It turns out that h_{min} = -5 km. Therefore, one cannot continue motion along this orbit since the spacecraft will collide with the surface of the Moon. Orbit correction is required. The

ORIGINAL PAGE IS
OF POOR QUALITY

correction problem is an inverse of the problem solved above. It must be solved by assuming h_{min}. Here the following are assumed: the height of the lunar mountains, terrain irregularity, and deviation of the actual shape of the Moon from a sphere. Let us assume that with consideration of all of the foregoing, h_{min} = = 20 km. The most immediate goal of the calculation is formulated: to find the required initial velocity. But before solving the inverse problem, let us show how all of the above described operations can be graphically and simply represented as the calculation flow chart presented below (Table 7). This chart not only graphically reproduces the calculations, but also permits determining the procedures of the operations for calculation in any other direction, since it reflects the relationship among all the calculation quantities. The procedure in solving the inverse problem is also shown in Table 7.

Let us clarify the steps of the operation. Thus, by assuming h_{min} = 20 km, we must also know the value of e. Here it is necessary to clearly imagine several physical features of the variation in the orbital parameters when there is variation in the velocity vector in magnitude and direction. To do this let us turn to Fig. 30.

The smallest orbital eccentricity must always be obtained in the case when horizontal velocity is introduced. Introducing a vertical velocity component (in our case, it is directed toward the center of the Moon) increases the eccentricity, therefore to obtain the same descent altitude the initial velocity must be increased. From the energy point of view it is profitable to assume an eccentricity in order for the velocity increment impulse to be at a minimum. This problem can be solved by dropping a perpendicular from point A (see Fig. 95) on the velocity hodograph /126
A_1A_4 obtained in advance from the results of several special calculations. These calculations were carried out for different e values within the limits of its variation from e_{min} to the e of the initial orbit in the direct problem.

It is sufficient to assume only two or three values of e. But the value of e_{min} can be obtained by using nomogram 2. Let us show how this is done. Place the "h" arrow at the division of the corresponding scale denoting the value 90 km, and place the cursor at the e scale marker 0. Next, the "h" arrow is shifted by the amount h = 20 km and from the e scale is read the quantity e = 0.04. Since the desired value for small e is virtually half as large, we get e = 0.02. Thus, we obtain the following limits of variation in e values: from 0.02 to 0.034. A hodograph constructed based on four e values is shown in Fig. 95 for this example.

It is not difficult to arrive at the following practical conclusion. There is a very small difference between the optimal

TABLE 7

FLOW CHART OF SOLUTION OF PROBLEM ON OPERATIONAL SPACE NAVIGATION DEVICE

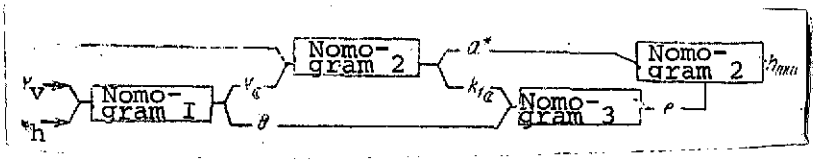

TABLE FOR DETERMINING hmin BASED ON GIVEN $v_{\mathbb{C}}$, h AND θ

Operation number	Number of nomogram used	Setting on device	Resulting values after operation
1	2	$v_{\mathbb{C}} = 1613$, $h = 90$	$a^* = 0.978$ $k_{1\mathbb{C}} = 0.9895$
2	3	$k_{1\mathbb{C}} = 0.9895$ Place opposite $\theta = 1.45°$	$e = 0.034$
3	2	Place cursor at $a^* = 0,978$ Place $e = 0,034$ on cursor	$h \approx 5$ km

TABLE FOR DETERMINATION OF $v_{\mathbb{C}}$ AND θ BASED ON GIVEN h_{min}, h AND e

Operation number	Number of nomogram used	Setting on device	Resulting values after operation
1	2	$h_{min} = 20$	$a^* = 0.99$
2	2	Set cursor at $e = 0,03$, $h = 90$	
3	2	$a^* = 0,99$, $h = 90$	$v_{\mathbb{C}} = 1.622$ $k_{1\mathbb{C}} = 0.995$
4	3	$e = 0.03$	Opposite the value $k_{1\mathbb{C}} = 0.995$ $\theta = 1.6°$ is read off

ORIGINAL PAGE IS
OF POOR QUALITY

velocity increment (we have in mind the increment equal to the segment of the perpendicular) and the velocity increment in the horizontal direction. Therefore, considering the great convenience in making the spacecraft correction by imparting an impulse to it only in the horizontal direction, let us assume the value $e = 0.03$. As we can see from the nomogram (see Fig. 95), the correcting horizontal velocity impulse for the calculation example we have considered must be 1622 m/sec - 1613 m/sec = 9 m/sec.

These examples of the use of the universal computational tool and the construction of an operational instrument confirm the broad possibilities of analytical-graphical methods in space navigation.

REFERENCES

1. Al'tman, S.P., "Theory of hodographs in Newtonian mechanics," /127 in: Sovremennoye sostoyaniye mekhaniki kosmicheskogo poleta [Present Status of Space Flight Mechanics], Moscow, "Nauka" Press, 1969, pp. 40-92.

2. Bettin, R., Navedeniye v kosmose [Guidance in Space], translated from the English, Moscow, "Mashinostroyeniye" Press, 1966, 448 pp.

3. Wulf [Vul'f], G.V., Sposob graficheskogo resheniya zadach po kosmografii i matematicheskoy geografii [Methods of Graphical Solution of Problems in Cosmography and Mathematical Geography], Nizhniy-Novgorod, 1909, 240 pp.

4. Gavr, D.L., Osnovy nomografii [Fundamentals of Nomography], Leningrad, "Kubuch" Press, 1934, 17 pp.

5. Mantirov et al., Tolkovyy slovar' matematicheskikh terminov [Explanatory Dictionary of Mathematical Terms], Moscow, "Prosveshcheniye" Press, 1965, 89 pp.

6. Nevskiy, B.A., Spravochnaya kniga po nomografii [Handbook on Nomography], Moscow-Leningrad, "Tekhizdat" Press, 1951, 256 pp.

7. Osnovy teorii poleta kosmicheskikh apparatov [Fundamentals of Spacecraft Flight Theory], edited by G.S. Narimanov, Moscow, "Mashinostroyeniye" Press, 1972, 606 pp.

8. Feodos'yev, V.I. and Sinyarev, G.B., Vvedeniye v raketnuyu tekhniku [Introduction to Rocket Technology], Moscow, "Obornogiz" Press, 1961, 507 pp.

9. Vertregt, M., Osnovy kosmonavtiki [Principles of Astronautics], translated from the English, Moscow, "Prosveshcheniye" Press, 1969, 301 pp.

10. Hickock, F.A., Grafiki kosmicheskogo poleta [Graphics of Space Flight], translated from the English, Moscow, "Mashinostroyeniye" Press, 1968, 132 pp.

11. Anderson, J.D., "A simple method of plotting the track of Earth satellites," Journal of the British Interplanetary Society 16, 355-361 (Mar-Apr 1958).

12. Vertregt, M., "A method of calculating the mass ratio in step-rockets," Journal of the British Interplanetary Society, 95-97 (Mar.-Apr. 1956).

13. Wallace, R.E., "Graphic solution of some Earth satellite problems by use of the stereographic net," Journal of the British Interplanetary Society 17, 120-123 (Sept.-Oct. 1959).